

FOR OFFICIAL USE ONLY

JPRS L/10126

19 November 1981

# Translation

ANTIRADAR CAMOUFLAGE

By

Yu. G. Stepanov



FOREIGN BROADCAST INFORMATION SERVICE

FOR OFFICIAL USE ONLY

NOTE

JPRS publications contain information primarily from foreign newspapers, periodicals and books, but also from news agency transmissions and broadcasts. Materials from foreign-language sources are translated; those from English-language sources are transcribed or reprinted, with the original phrasing and other characteristics retained.

Headlines, editorial reports, and material enclosed in brackets [ ] are supplied by JPRS. Processing indicators such as [Text] or [Excerpt] in the first line of each item, or following the last line of a brief, indicate how the original information was processed. Where no processing indicator is given, the information was summarized or extracted.

Unfamiliar names rendered phonetically or transliterated are enclosed in parentheses. Words or names preceded by a question mark and enclosed in parentheses were not clear in the original but have been supplied as appropriate in context. Other unattributed parenthetical notes within the body of an item originate with the source. Times within items are as given by source.

The contents of this publication in no way represent the policies, views or attitudes of the U.S. Government.

COPYRIGHT LAWS AND REGULATIONS GOVERNING OWNERSHIP OF MATERIALS REPRODUCED HEREIN REQUIRE THAT DISSEMINATION OF THIS PUBLICATION BE RESTRICTED FOR OFFICIAL USE ONLY.

FOR OFFICIAL USE ONLY

JPRS L/10126

19 November 1981

## ANTIRADAR CAMOUFLAGE

Moscow PROTIVORADIOLOKATSIONNAYA MASKIROVKA in Russian 1968 (signed to press 26 Apr 68) pp 2-144

[Book by Yuriy Grigor'yevich Stepanov, Izdatel'stvo "Sovetskoye Radio", Moscow, 12,200 copies, 144 pages, UDC 623.68]

### CONTENTS

Annotation	1
Introduction	2
Chapter 1. The Reflective Properties of Radar Targets	4
1. The effective back-scatter cross-section	4
2. Amplitude fluctuations of returns and the radar cross-sections of targets	8
3. Phase front fluctuations of a return	15
4. The polarization characteristics of a return	17
5. The effective target cross-section in the case of diversity (bistatic) radars	18
6. The average values of the effective radar scatter cross-section of real targets	22
Chapter 2. Experimental Studies of Effective Target Back-Scatter Cross-Sections	23
1. Methods of experimentally studying the effective radar cross-section	23
2. Specific features of electromagnetic simulation	24
3. Measurement systems for the study of effective radar cross-sections with models	27
4. The RAT SCAT facility for the measurement of the effective radar cross-sections of various objects	32

- a -

[II - USSR - FOUO]  
[III - USSR - 4 FOUO]

FOR OFFICIAL USE ONLY

FOR OFFICIAL USE ONLY

Chapter 3. The Reduction of the Effective Back-Scatter Cross-Sections of Objects by Using Poorly Reflecting Shapes and Radio-Absorbent Materials	35
1. The use of poorly reflecting shapes	35
2. General information on radio absorbent materials	38
3. Some theoretical questions	40
4. Narrow band interference coatings	43
5. Broadband radio absorbent coatings and materials	46
6. Measuring the characteristics of radio absorbent materials	51
Chapter 4. The Camouflage Properties of Terrain and Hydrometeors	53
1. The effective back-scatter cross-section of surface distributed targets	53
2. The reflective properties of the earth's surface	55
3. The masking properties of returns from a sea surface	58
4. The masking action of hydrometeors	63
Chapter 5. Artificial Radar Reflectors and Their Applications	67
1. General information	67
2. Dipole reflectors	69
3. Corner reflectors	77
4. Luneberg lenses	92
5. Passive antenna arrays	96
6. Guided missiles - decoy targets	104
7. Antiradar camouflage for ballistic missiles	107
Bibliography	113

- b -

FOR OFFICIAL USE ONLY

FOR OFFICIAL USE ONLY

Annotation

[Text] Basic information is given on the techniques and tools of antiradar camouflage for military and industrial facilities. The reflective properties of radar targets are treated as well as ways of reducing the radar visibility of various objects, the camouflage properties of terrain and hydrometeors, and distracting and masking false targets. Experimental methods of determining effective back-scatter cross-sections are described.

Along with theoretical questions, considerable space is devoted in the book to the description of specific samples of foreign camouflage hardware and the ways it is used. The methods and means of solving the major problems of antiradar camouflage are consistently set forth.

The book is intended for engineering and technical workers in the radio engineering specialty, as well as for military readers interested in questions of radio camouflage.

Some 5 tables, 87 figures and 45 bibliographic citations.

Table of Contents

Introduction	[4]
Chapter 1. The Reflective Properties of Radar Targets	[7]
1. The effective back-scatter cross-section	[7]
2. Amplitude fluctuations of returns and the radar cross-sections of targets	[12]
3. Phase front fluctuations of a return	[20]
4. The polarization characteristics of a return	[22]
5. The effective target cross-section in the case of diversity (bistatic) radars	[24]

FOR OFFICIAL USE ONLY

6. The average values of the effective radar scatter cross-section of real targets	[28]
Chapter 2. Experimental Studies of Effective Target Back-Scatter Cross-Sections	[29]
1. Methods of experimentally studying the effective radar cross-section	[29]
2. Specific features of electromagnetic simulation	[31]
3. Measurement systems for the study of effective radar cross-sections with models	[34]
4. The RATSCAT facility for the measurement of the effective radar cross-sections of various objects	[41]
Chapter 3. The Reduction of the Effective Back-Scatter Cross-Sections of Objects by Using Poorly Reflecting Shapes and Radio-Absorbent Materials	[44]
1. The use of poorly reflecting shapes	[44]
2. General information on radio absorbent materials	[48]
3. Some theoretical questions	[50]
4. Narrow band interference coatings	[55]
5. Broadband radio absorbent coatings and materials	[59]
6. Measuring the characteristics of radio absorbent materials	[65]
Chapter 4. The Camouflage Properties of Terrain and Hydrometeors	[68]
1. The effective back-scatter cross-section of surface distributed targets	[68]
2. The reflective properties of the earth's surface	[71]
3. The masking properties of returns from a sea surface	[75]
4. The masking action of hydrometeors	[80]
Chapter 5. Artificial Radar Reflectors and Their Applications	[85]
1. General information	[85]
2. Dipole reflectors	[87]
3. Corner reflectors	[97]
4. Luneberg lenses	[115]
5. Passive antenna arrays	[121]
6. Guided missiles - decoy targets	[131]
7. Antiradar camouflage for ballistic missiles	[136]
Bibliography	[143]

Introduction

The rapid development of radio engineering and radio electronics has necessitated a transition in military affairs to fundamentally new techniques of weapons utilization and reconnaissance in enemy territory. One of the major means of target detection and recognition, as well as for the guidance of ones own weapons

FOR OFFICIAL USE ONLY

on the target is radar. Radars and radar systems make it possible to determine the coordinates of military, industrial and defense installations of an enemy at long range, regardless of the visibility conditions.

Almost from the very first days when radar appeared and in the course of its further development during the Second World War, means of countering the effect of enemy radars were also being developed. A new special field of radio engineering appeared: electronic countermeasures. At the present time, the goal of electronic countermeasures is not only the suppression or reduction of the effectiveness of the means of radio communications, radio navigation and radar, but also fire control facilities, primarily missile guidance systems. Under modern conditions, where radio electronics is the major means of combat equipment and troop guidance, skillfully set up electronic countermeasures can in the final analysis significantly reduce the combat capability of the enemy and boost the effectiveness of one's own forces and equipment.

Antiradar camouflage is one of the major methods of reducing the effectiveness of enemy radar facilities in the overall set of electronic countermeasures. Its basic function is to render difficult or to completely preclude the possibility of detection of military, defense or industrial facilities by means of radar equipment.

In refining their means of attack, the military specialists of the imperialist states take into account the fact that the Soviet Union possesses everything necessary to deal a shattering blow in reply. For this reason, they also devote great attention to the design of new equipment and the refinement of techniques for antiradar camouflage. This attention is explained not only by the necessity of concealing their own military and industrial installations from an answering strike, but also by the striving to assure the suddenness of the use of weapons of mass destruction.

The considerable increase in the detection ranges of various targets, the improvement in the precision of the determination of their coordinates, the automation of the processes of obtaining and processing the information as well as the increase in the noise immunity and operational reliability of modern radar equipment have made it a considerably more complex matter to realize antiradar camouflage and have expanded its areas of application.

An especially large amount of work is underway abroad in the field of antiradar camouflage for the means of air attack, primarily ballistic missiles. Thus for example, a draft budget of the U.S. Department of Defense in 1966 provided for allocations amount to 168 million dollars for the development of means to facilitate the penetration of ballistic missiles through an anti-ballistic missile system (ABM) of an enemy. The basis of such hardware is antiradar camouflage.

An attempt is made in this book to generalize and systematize information on the means and methods of antiradar camouflage based on data from the foreign press. Along with the analysis of the operational principle and design of individual means of camouflage as well as the principles of their utilization, specific samples of foreign antiradar camouflage hardware are described.

## FOR OFFICIAL USE ONLY

The methods and means of solving the major problems of antiradar camouflage are logically presented in the book; these consist in reducing the radar contrast of the object being camouflaged down to the level of the ambient background; creating an artificial masking false target of considerable extent on the radar screens, having a return intensity much greater than the returns from the target being camouflaged; disorienting an observation and fire control radar system by means of false distracting targets.

The book is intended for engineering and technical workers in the radio engineering speciality. Some of the chapters of the book which contain descriptive material and examples can be of interest to a wide circle of readers.

The author would like to express his gratitude to lecturer and candidate of the technical sciences, V.T. Borovik, candidate of the technical sciences, I.S. Luk'yashchenko and A.D. Trofimovich for assisting in the work on the book.

## CHAPTER I. THE REFLECTIVE PROPERTIES OF RADAR TARGETS

## 1. The Effective Back-Scatter Cross-Section

One of the constant (though still insufficient) conditions for providing effective antiradar camouflage for protected objects is the presence of the most complete information on the quantitative and qualitative characteristics of the reflection of electromagnetic energy from various targets.

When electromagnetic energy impinges on any object (a target), electrical currents appear at its surface, if the target is a conductor, or electrical charges, if the target is a dielectric. In this case, the target itself becomes a source of electromagnetic emissions. The energy of an electromagnetic wave incident to a target is scattered in all directions. The portion of the energy reflected from a target, which arrives at the input to a radar receiver, forms a target marker on the radar screen. The level of the signal reflected from the target depends on the radar parameters, the electromagnetic propagation conditions and the nature of the target: dimensions, configuration, irradiation angle and electrical properties of the target material.

A conventional quantity is used to quantitatively evaluate the reflective properties of any radar target:  $\sigma_t$  - the effective target back-scatter cross-section (EPR).

As is well known, the secondary emission power,  $P_2$  (the energy scattered by a target when an electromagnetic wave impinges on it), is directly proportional to the flux density of the energy,  $\Pi_1$ , irradiating the target, i.e.:

$$P_2 = \sigma_t \Pi_1 \quad (1.1)$$

The proportionality factor  $\sigma_t$  in formula (1.1) is called the effective back-scatter cross-section. Since the majority of radar targets have the property of directional secondary emission, taking into account the directionality factor of the reflecting object,  $D$ , which characterizes the degree of concentration of the scattered power



## FOR OFFICIAL USE ONLY

in the direction to the radar, the expression for  $\sigma_t$  can be written in the following form [2]:

$$\sigma_t = (P_2/\pi_1)D \quad (1.2)$$

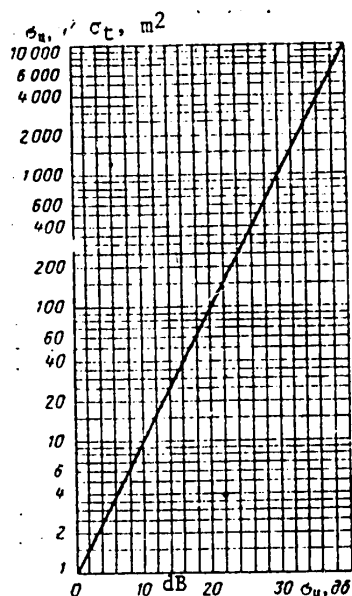


Figure 1.1. Graph for the conversion of effective back-scatter cross-section measurement units.

The effective back-scatter cross-section can be expressed in units of area ( $m^2$ ) or in decibels (dB), where  $\sigma_t [dB] = 10 \log \sigma_t [m^2]$ , i.e., a level of zero decibels corresponds to a value of  $\sigma_t$  of  $1 m^2$  (Figure 1.1).

It can be seen from formula (1.2), that to determine the effective back-scatter cross-section of a target, it is necessary to know the energy flux densities at the points where the target and the radar antenna are located. The derivation of theoretical data on the field of the reflected wave, and consequently, on the effective target cross-section reduces in practice to the solution of Maxwell's equations with the appropriate boundary conditions. The methods of solving such equations which exist at the present time allow only for the calculation of the effective back-scatter cross-section of bodies with a simple geometric shape (Table 1.1).

Objects with a simple geometric shape are encountered rather rarely under actual radar detection conditions. As a rule, they have a complex configuration and consist of a large number of elementary reflectors. Examples of single targets with a complex configuration



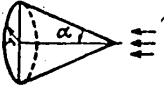
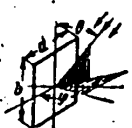
ships, aircrafts, missiles, various ground structures, etc. Several individual objects, located within the bounds of the reflecting volume (Figure 1.2) at relatively large ranges as compared to the radar wavelength, form a group target.

It can be seen from Figure 1.2 that the dimensions of the reflecting volume with respect to range are governed by the quantity  $(c\tau/2)$  ( $c$  is the propagation velocity of the electromagnetic energy and  $\tau$  is the radar pulse width), and with respect to the angular coordinates by the linear dimensions of the beam of the radar antenna at the 0.5 power level ( $\theta_{az}\theta_{elev}$ ).

An overall set of reflecting elements, arranged relatively close together and occupying a comparatively large region of space, forms a so-called volume distributed target. Hydrometeors, a cloud of dipole reflectors, etc. can be numbered among such targets.

## FOR OFFICIAL USE ONLY

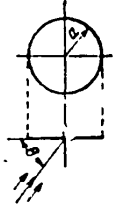
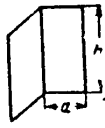
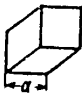
TABLE 1.1. Formulas for Calculating the Effective Back-Scatter Cross-Section of Geometric Bodies

	<p>Шар Sphere</p> <p>For a wavelength of: При длине волны <math>\lambda \ll a</math>:</p> <p><math>\sigma_n = \pi a^2</math>.</p> <p>For a wavelength of: При длине волны <math>\lambda \gg a</math>:</p> $\sigma_t = \sigma_n = \frac{144\pi^2 a^6}{\lambda^4}.$
	<p>Круглый цилиндр Circular Cylinder</p> $\sigma_n = k L^2 \sin^2 \theta \left[ \frac{\sin(kL \cos \theta)}{kL \cos \theta} \right]^2;$ $\sigma_n = k L^2 \text{ при } \theta = \frac{\pi}{2};$ $k = \frac{2\pi}{\lambda} \text{ — волновое число.}$ <p>is the wave number.</p>
	<p>Конус Cone</p> $\sigma_n = \pi r^2 \lg^2 \alpha.$ <p>Направление облучения совпадает с осью конуса (1)</p>
	<p>Прямоугольная пластина Rectangular plate</p> $\sigma_n = \left[ \frac{kab}{V\pi} \sin \theta \frac{\sin(ka \sin \theta \cos \varphi)}{ka \sin \theta \cos \varphi} \right] \times$ $\times \left[ \frac{\sin(kb \cos \theta)}{kb \cos \theta} \right]^2.$ <p>(2)</p> <p>При нормальном падении к плоскости пластины:</p> $\sigma_n = 4\pi \frac{a^2 b^2}{\lambda^4}$

FOR OFFICIAL USE ONLY

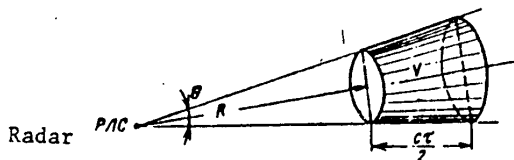
## FOR OFFICIAL USE ONLY

[Table 1.1, continued]:

	<p>Flat Disc Плоский диск</p> $\sigma_n = \pi k^2 a^4 \sin^2 \theta \left[ \frac{J_1(2ka \cos \theta)}{ka \cos \theta} \right]^2,$ <p>где <math>J_1</math> — функция Бесселя 1-го порядка. (3) При нормальном падении к плоскости диска:</p> $\sigma_n = \frac{4\pi^2 a^4}{\lambda^2}$
	<p>Dihedral Corner Reflector Двугранный уголкового отражатель</p> $\sigma_n = \frac{8\pi (ah)^2}{\lambda^2}$ <p>в максимуме диаграммы рассеяния at the back-scatter pattern maximum</p>
	<p>Trihedral Corner Reflector Трёхгранный уголкового отражателя</p> $\sigma_n = \frac{12\pi a^4}{\lambda^2}$ <p>в максимуме диаграммы рассеяния at the back-scatter pattern maximum</p>

Key to Table 1.1.:

1. The direction of irradiation coincides with the axis of the cone;
2. In the case of normal incidence to the plane of the plate;
3. Where  $J_1$  is a first order Bessel function. In the case of normal incidence to the plane of the disc:.

Figure 1.2. The reflecting volume  $V = (\pi/4)R^2\theta(c\tau/2)$ .

If the individual reflecting elements merge into one comparatively thin layer, then they form a surface distributed target. Such targets can be encountered in the radar scanning of a ground or sea surface. The reflective properties of volume and surface distributed targets are treated in Chapter 4.

FOR OFFICIAL USE ONLY

FOR OFFICIAL USE ONLY

The calculation of the effective target cross-section of actual targets with a complex configuration presents great theoretical difficulties. Computers find widespread application in the analytical determination of the effective back-scatter cross-section of actual objects.

At the present time, the effective cross-section of reflecting objects with a complex shape is studied primarily experimentally, using special equipment and hardware.

The following are included among the new trends in the study of radar returns:

- The study of electromagnetic energy scattering by space bodies and vehicles, as well as by plasma formations;
- The synthesis of objects with specified secondary emission characteristics;
- The determination of the effective cross-section of objects in the case of broadband system operation with a high resolution;
- Finding the scattering characteristics at millimeter and optical band wavelengths;
- Determining the effective cross-section of distributed objects for the purpose of recognizing them.

## 2. Amplitude Fluctuations in Returns and the Effective Back-Scatter Cross-Sections of Targets

A complex target can be treated as the aggregate of a large number of elements which scatter the electromagnetic energy in various directions. Such elements can be: the convex portions of the target which are characteristic "shining" spots; flat areas, which produce a mirror or diffuse reflection. The individual structural components of a target, the dimensions of which are commensurate with the wavelength, will produce intense secondary emission because of resonance phenomena. The overall amplitude of the reflected signal will be governed by the relative phases and amplitudes of the signals reflected from the elementary secondary radiators. The amplitudes of the individual signals which have different phases at the reception point either add together, thereby providing for a large total return, or have such ratios that the signal is either partially or completely suppressed. As a rule, the spacing between the individual reflecting elements considerably exceeds the radar wavelength. In this case, the phase of the signals at the receive point will change with a change in the position of the target relative to the direction to the radar, something which in turn will cause additional fluctuations in the return and the effective cross-section of the target.

In order to ascertain the mechanism for reflection from a complex target, we shall initially consider a target consisting of two equal isotropic reflecting elements, spaced a distance  $l$  from each other (Figure 1.3), where:

$$l < c\tau/2 ,$$

## FOR OFFICIAL USE ONLY

where  $c$  is the speed of light;  $\tau$  is the radar pulse width.

The overall voltage of the signal reflected from such a target will be equal to the following at the input to the radar receiver [2]:

$$u_{in} = u_{rx} = U_{m1} \cos(\omega t - \varphi_1) + U_{m2} \cos(\omega t - \varphi_2).$$

Here,  $U_{m1}$  and  $U_{m2}$  are the amplitudes of the voltages of the reflected signal from the first and second targets;  $\phi_1$  and  $\phi_2$  are the phase delays of these voltages, equal to:

$$\varphi_1 = \frac{4\pi R_1}{\lambda} + \varphi_{01}; \quad \varphi_2 = \frac{4\pi R_2}{\lambda} + \varphi_{02},$$

where  $\phi_{01}$  and  $\phi_{02}$  are the phase changes with reflection.

If the effective radar cross-sections of the first and second targets are equal, then  $U_{m1} = U_{m2}$  and consequently,

$$u_{in} = u_{rx} = 2U_{m1} \cos \frac{\varphi_p}{2} \cos \left( \omega t - \frac{\varphi_c}{2} \right),$$

where  $\phi_p$  and  $\phi_c$  are the difference and sum of the phases of the voltages  $U_1$  and  $U_2$ .

If  $\phi_{01} = \phi_{02}$ , then:

$$\varphi_1 = 2(R_1 - R_2) \frac{2\pi}{\lambda} = \frac{4\pi l}{\lambda} \cos \theta.$$

Then the amplitude of the reflected signal voltages will be equal to:

$$U_m = 2U_{m1} \cos \left( \frac{2\pi l}{\lambda} \cos \theta \right).$$

Or, by converting to the total reflected signal power, we obtain:

$$P_{rx} = 4P_1 \cos^2 \left( \frac{2\pi l}{\lambda} \cos \theta \right),$$

where  $P_1$  is the reflected signal power from one isotropic radiator.

Since the power of the return and the effective radar cross-section are related by a linear function, one can write that for two elementary targets, the effective radar cross-section will be:

$$\sigma_2 = 4\sigma_1 \cos^2 \left( \frac{2\pi l}{\lambda} \cos \theta \right). \quad (1.3)$$

where  $\sigma_1$  is the effective cross-section of one isotropic radiator.

## FOR OFFICIAL USE ONLY

It can be seen from expression (1.3) that with a change in the wavelength  $\lambda$  and the angle  $\theta$ , the quantity  $\sigma_2$  can take on any value from zero to the maximum, which is four times greater than  $\sigma_1$  (Figure 1.4).

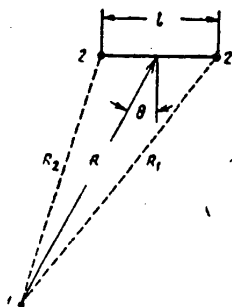


Figure 1.3. A complex target consisting of two scattering elements with a spherical shape.

Key: 1. Radar;  
2. Scattering elements.

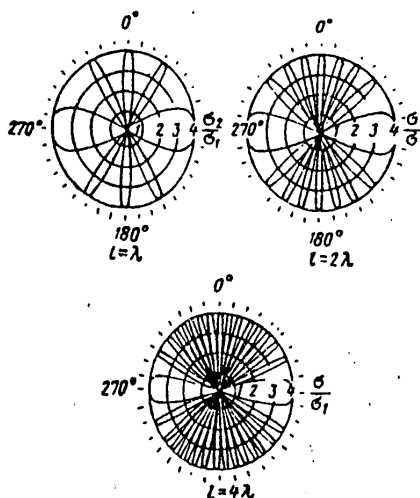


Figure 1.4. Polar plots of the function  $\sigma_2/\sigma_1$  for various values of  $L/\lambda$  and the angles  $\theta$ .

Real targets consist of a set of scattering elements with different reflecting properties, where each of these elements can additionally interact with the others. The mutual motion of the target and the radar, as well as the motion of individual elements of the target itself (for example, as a result of the natural vibrations of the aircraft or ship) exert a great influence on the nature of the fluctuations in the resulting return. It can be seen from Figure 1.5 that slight changes in the heading angle of an aircraft can change the instantaneous value of  $\sigma_t$  by a large amount.

The amplitudes of the returns and the effective back-scatter cross-sections of complex real targets are subject to random fluctuations. Consequently, the techniques of probability theory must be employed to characterize these quantities. They can be sufficiently completely described by the distributions and the spectrum of the fluctuations or by an autocorrelation function.

Let a complex target (aircraft, ship, ground structure), consisting of a set of arbitrarily arranged reflectors, contain an element as part of it which yields a stable reflected signal ("shining" point), the amplitude of which exceeds the total signal from the other elements. The amplitudes and phases of the returns of all of the other elementary reflectors will vary (in contrast to the "shining" point) as a function of the mutual motion of the target and the radar.

FOR OFFICIAL USE ONLY

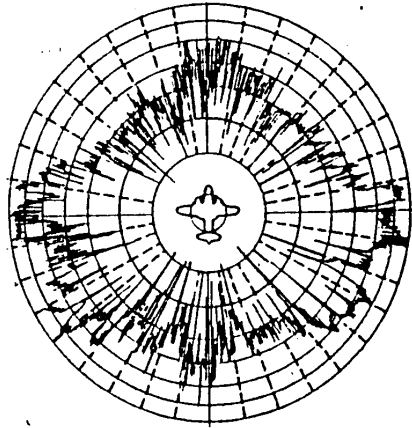


Figure 1.5. The effective back-scatter cross-section of a twin engine B-26 bomber as a function of azimuth. The measurements were made at a radar wavelength of  $\lambda = 10$  cm.

The resulting signal from such a target will be determined by the expression:

$$E = A \cos \omega t + \sum_{k=1}^n E_k \cos(\omega t - \varphi_k).$$

where  $A$  is the amplitude of the "shining" spot signal;  
 $E_k$  is the amplitude of the  $k$ -th element signal;  
 $\varphi_k$  is the phase shift of the  $k$ -th element.

With a change in the relative position of the radar station and the target, the ranges to the elementary reflectors and their effective cross-sections will also change. This leads to random changes in the amplitudes ( $E_1, E_2, \dots, E_k$ ) and the phases ( $\varphi_1, \varphi_2, \dots, \varphi_k$ ) of the reflected signals. As was demonstrated in paper [1], the two-dimensional probability distribution of the quantities  $E$  and  $\varphi$  for the composite signal can be described by the equation:

$$W(E, \varphi) = \frac{E}{2\pi v^2} \exp \left[ -\frac{E^2 + A^2 - 2AE \cos \varphi}{2v^2} \right], \quad (1.4)$$

where  $v$  is the amplitude dispersion.

In order to determine the probability density of the random resulting amplitude  $E$ , we integrate expression (1.4) over all possible values of the phase  $\varphi$  from 0 to  $2\pi$ :

$$\begin{aligned} W(E) &= \int_0^{2\pi} W(E, \varphi) d\varphi = \\ &= \frac{E}{v^2} \exp \left[ -\frac{E^2 + A^2}{2v^2} \right] \frac{1}{2\pi} \int_0^{2\pi} \exp \left[ \frac{AE}{v^2} \cos \varphi \right] d\varphi. \end{aligned} \quad (1.5)$$

It is well known that:

$$\frac{1}{2\pi} \int_0^{2\pi} \exp \left[ \frac{AE}{v^2} \cos \varphi \right] d\varphi = J_0 \left( \frac{AE}{v^2} \right). \quad (1.6)$$

FOR OFFICIAL USE ONLY

## FOR OFFICIAL USE ONLY

where  $J_0(AE/v^2)$  is a zero order Bessel function of an imaginary argument.

We derive the following from expressions (1.5) and (1.6):

$$W(E) = \frac{E}{v^2} \exp\left[-\frac{E^2 + A^2}{2v^2}\right] J_0\left(\frac{AE}{v^2}\right). \quad (1.7)$$

Equation (1.4) is called the generalized Rayleigh distribution. If  $A = 0$  (there is no stable component), then  
and the probability density  $W(E)$  is  
governed by a simple Rayleigh distribution:

$$W(E) = \frac{E}{v^2} \exp\left[-\frac{E^2}{2v^2}\right]. \quad (1.8)$$

Expressions (1.7) and (1.8) can be written in a more general form, if the following symbols are introduced:

$$a = \frac{A}{v}; \quad v = \frac{E}{v}; \quad dv = \frac{dE}{v}.$$

Then:

$$W(v) = v \exp\left[-\frac{v^2 + a^2}{2}\right] J_0(av),$$

$$W(v) = v \exp\left[-\frac{v^2}{2}\right].$$

Curves for the distribution  $W(v)$  are shown in the graph (Figure 1.6), which were plotted for various values of the constant component of [1]. It can be seen from the graph that for large values of the stable component  $a$ , the distribution of  $W(v)$  approaches a normal distribution. If there is stable component ( $a = 0$ ), the resulting signal is produced as the sum of solely the signals from the random reflectors. The mean relative value of this signal will be equal to:

$$\bar{v} = \int_0^\infty v \exp\left[-\frac{v^2}{2}\right] dv = \sqrt{\frac{\pi}{2}}.$$

The dispersion of the relative signal amplitude is:

$$(\overline{v - \bar{v}})^2 = 2 - \frac{\pi}{2}.$$

By converting from the value  $E$  in expression (1.7) to power  $P$ , we derive:



## FOR OFFICIAL USE ONLY

$$W(P) = \frac{1}{v^2} \exp \left[ -\frac{P + P_0}{v^2} \right] J_0 \left[ \frac{2\sqrt{PP_0}}{v^2} \right], \quad (1.9)$$

where  $P_0 = A^2/2$  is the power of the stable signal component;  $P = E^2/2$  is the power of the resulting signal, dissipated in a resistance of 1 ohm.

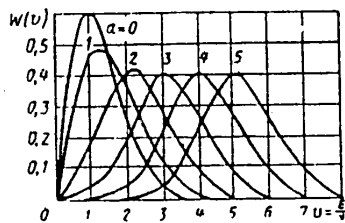


Figure 1.6. Curves for the distribution of the resulting signal amplitudes.

We shall introduce the symbol:

$$m = \frac{P_0}{v^2} = \frac{a^2}{2}. \quad (1.10)$$

Then the average power of the return will be equal to:

$$\bar{P} = v^2 + P_0$$

or, in other words:

$$v^2 = \frac{P}{1+m} = \frac{P}{1+\frac{a^2}{2}}. \quad (1.11)$$

Taking expressions (1.10) and (1.11) into account, we write expression (1.9) in the form:

$$W(P) = \frac{1+m}{P} \exp \left[ -m - (1+m) \frac{P}{P} \right] \times \\ \times J_0 \left[ 2 \sqrt{m(1+m) \frac{P}{P}} \right].$$

Since the effective back-scatter cross-section of the target,  $\sigma_t$  is proportional to the power of the return, then:

$$W(\sigma_t) = \frac{1+m}{\sigma_t} \exp \left[ -m - (1+m) \frac{\sigma_t}{\sigma_t} \right] \times \\ \times J_0 \left[ 2 \sqrt{m(1+m) \frac{\sigma_t}{\sigma_t}} \right]. \quad (1.12)$$

If there is no stable component ( $m = 0$ ), then the random quantity corresponding to the effective cross-section of the target, is distributed exponentially:

$$W(\sigma_t)_{m=0} = \frac{1}{\sigma_t} \exp \left[ -\frac{\sigma_t}{\sigma_t} \right], \quad (1.13)$$

## FOR OFFICIAL USE ONLY

where  $\sigma_t$  is the resulting effective radar cross-section of the target;  $\bar{\sigma}_t$  is the mean value of the resulting effective radar cross-section of the target.

In expression (1.12), the parameter  $m$  can be treated as the ratio of the effective radar cross-section of a stably reflecting element,  $\sigma_{t0}$ , to the average value of the effective cross-sections of all of the random reflectors,  $\sigma_t \Sigma$ . Then, for the relative effective radar cross-section,  $\sigma_t / \bar{\sigma}_t$ , the distribution densities (1.12) and (1.13) will assume the following forms:

$$W\left(\frac{\sigma_t}{\bar{\sigma}_t}\right) = (1+m) \exp\left[-m - (1+m)\frac{\sigma_t}{\bar{\sigma}_t}\right] \times \\ \times J_0\left[2\sqrt{m(1+m)\frac{\sigma_t}{\bar{\sigma}_t}}\right] \\ W\left(\frac{\sigma_t}{\bar{\sigma}_t}\right)_{m=0} = \exp\left[-\frac{\sigma_t}{\bar{\sigma}_t}\right].$$

The curves for  $W(\sigma_t / \bar{\sigma}_t)$  are depicted in Figure 1.7 as a function of  $\sigma_t / \bar{\sigma}_t$  for various values of  $m$  [1]. Using these graphs, one can estimate the probability of the appearance of various values of effective target radar cross-sections.

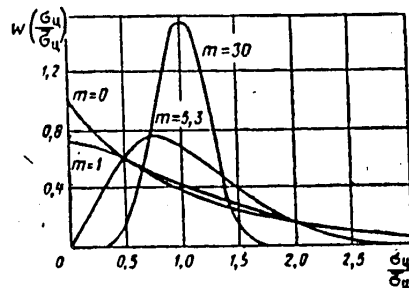


Figure 1.7. The effective radar cross-section distribution of a complex target.

Key: Ordinate =  $W(\sigma_t / \bar{\sigma}_t)$ .

As a rule, the spectral and correlational characteristics of returns, the autocorrelation function and spectrum of the signal, are used to describe the fluctuation variation in the amplitude of the reflected signal and the effective radar cross-section of the target as a function of time.

The statistical relationship between the values of the fluctuating voltage  $E$ , broken down into a time interval  $\tau$ , is described by means of the autocorrelation function  $R(\tau)$ :

$$R(\tau) = \lim_{T \rightarrow \infty} \frac{1}{T} \int_0^T E(t) E(t+\tau) dt,$$

where  $T$  is the observation time.

## FOR OFFICIAL USE ONLY

The maximum value of the autocorrelation function will occur when  $\tau = 0$ . The value of  $R(\tau)$  will fall off in step with the increase in  $\tau$ . The duration of an observation  $T$  should be chosen so that all of the characteristic fluctuations in the function  $E(t)$  are encompassed.

The autocorrelation function is closely linked to the signal fluctuation spectrum. If the changes in the amplitude of the fluctuating signal take the form of a steady-state random process,  $E(t)$ , in a specified time range of  $-T \leq t \leq T$ , then the fluctuation spectrum is determined by the relation:

$$A(f) = \int_{-T}^T E(t) e^{-i2\pi ft} dt.$$

while the spectral density is:

$$G(f) = \lim_{T \rightarrow \infty} \frac{1}{2T} |A(f)|^2.$$

If  $E(t)$  is the voltage across a resistance of 1 ohm, then  $G(f)df$  is the average power dissipated in a 1 ohm resistor in a frequency range of from  $f$  to  $f + df$ , while  $G(f)$  is the average power density, having the dimensions of power per unit bandwidth.

The following relationships exist between the spectral density and the autocorrelation function:

$$G(f) = 4 \int_0^{\infty} R(\tau) \cos 2\pi f \tau d\tau,$$

$$R(\tau) = \int_0^{\infty} G(f) \cos 2\pi f \tau df.$$

The probability distributions of the effective cross-sections of real targets and the nature of the change in the effective cross-sections as a function of time are usually determined experimentally.

### 3. Phase Front Fluctuations of a Return

For a complex target, there are also fluctuations in the phase front of the signal along with the fluctuations in the amplitude of the reflected signal.

To explain this phenomenon, we shall again turn to the target model consisting of two point isotropic radiators and compare the pictures of the phase fronts of this target and a single isotropic radiator (Figure 1.8).

The equal phase surfaces of a single point radiator will be concentric spheres with the center in the radiator. For a two point target, these surfaces will be other than spherical. The quantity which characterizes the bending of the phase

## FOR OFFICIAL USE ONLY

front can be found as a function of the angle  $\delta$  between normals to the equal phase surfaces of the single point and two-point radiators for various emission angles  $\phi$ .

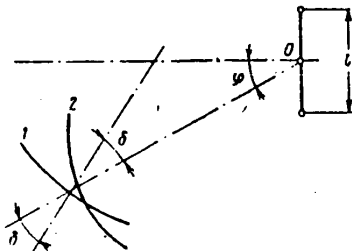


Figure 1.8. The phase fronts of a single point isotropic radiator and a target consisting of two isotropic radiators.

Key: 1. Equal phase surface of the two-point target;  
2. Equal phase surface of the single point radiator.

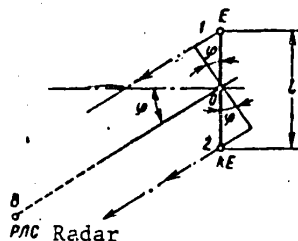


Figure 1.9. On the determination of the phase shift.

Let the radar be located at remote point B (Figure 1.9). Then the frequency incoming from point 1 will lag in phase the frequency from the single point source by an angle of:

$$\epsilon = \frac{2\pi}{\lambda} \frac{l}{2} \sin \varphi,$$

while the frequency incoming from point 2 will lead it by the same angle. If the amplitude of the transmitted signals are  $E$  and  $kE$ , where  $k < 1$ , then the vector diagram will have the form shown in Figure 1.10a. The resulting vector of the two point target field will be equal to the sum of the vectors  $\vec{E}$  and  $k\vec{E}$ . We find from Figure 1.10b:

$$\operatorname{tg} \delta = \frac{E \sin \epsilon + kE \sin (-\epsilon)}{E \cos \epsilon + kE \cos (-\epsilon)} =$$

$$= \operatorname{tg} \epsilon \frac{1-k}{1+k}.$$

$$\delta = \operatorname{arctg} \left( \epsilon \frac{1-k}{1+k} \right).$$

Calculating the value of  $\delta$  for various values of  $\phi$ ,  $k$  and  $l$ , one can construct the picture of the phase fronts of a two point target (Figure 1.11). The fluctuations of the phase front because of the continuous motion of the target relative to the radar are of a random nature. These fluctuations are manifest at the output of the receiver in the form of random changes in the error signal for the measurement of the angular position of the target, and for this reason, they are frequently called angular noise.

## FOR OFFICIAL USE ONLY

## FOR OFFICIAL USE ONLY

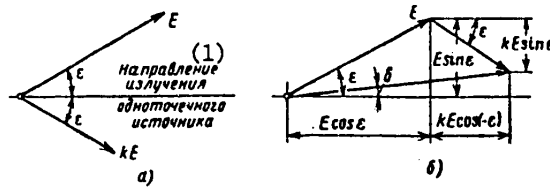


Figure 1.10. Vector diagrams of the field of a two-point target.

Key: 1. Direction of the emission of a single point source.

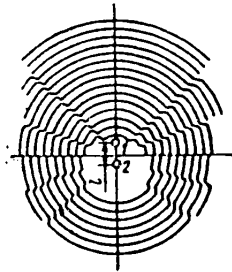


Figure 1.11. Equal phase surface cross-sections in the plane of the drawing. Target point 1 is the source of large amplitude oscillations [1].

#### 4. The Polarization Characteristics of a Return

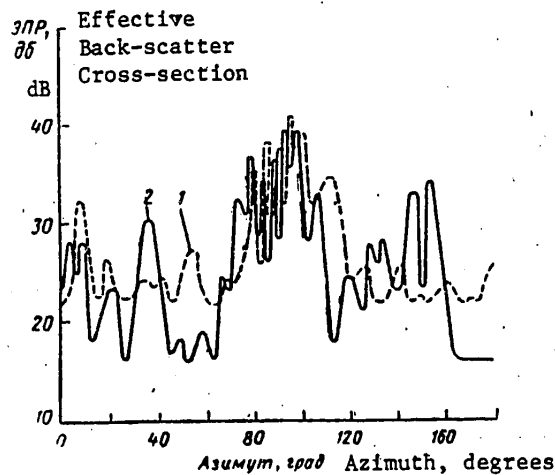


Figure 1.12. Experimental diagram of the effective radar cross-section of an aircraft as a function of azimuth, measured in the plane of the wings.

Key: 1. Vertical polarization of the incident wave;  
2. Horizontal polarization. Frequency of 75 MHz.

## FOR OFFICIAL USE ONLY

**TABLE 1.2** Results of Measurements of the Losses of a Radar Signal Reflected From an Aircraft ( $\lambda = 10$  cm)

<u>Incident Wave Polarization</u>	<u>Target</u>	<u>Changes in the Reflected Signal</u>	<u>Losses, dB</u>
Plane	Ideal	Reflects all of the energy; the polarization plane of the reflected signal is parallel to the polarization plane of the incident wave	0
Plane	Air-craft	A portion of the energy (-10 dB) is returned with transverse polarization and is attenuated by the receiver	0.5
Circular (reception with the same polarization as the transmission)	Air-craft	The reflected energy is split equally between orthogonal circular polarizations	3

Experimental studies confirm the dependence of the reflected signal intensity, and consequently also the value of the effective radar cross-section of the target on the kind of polarization of the transmitted signal (Figure 1.12). When electromagnetic oscillations are reflected from any object, the polarization of the reflected wave does not match the polarization of the incident wave in the general case, i.e., the reflected signal is depolarized. The degree of depolarization depends on the properties of the irradiated target and on the polarization of the incident field. Solids exist which reflect any polarization field without distortions: these are a sphere and a flat disc, irradiated in the direction of the axis. Another extreme case is a target which produces a reflected field with one polarization for any polarization of the incident wave. Such a target is a fine wire.

Objects of an arbitrary shape change the polarization of the incident field in various ways; in this case, attenuation of the signal is observed as a rule at the input to the receiver because of the depolarization (Table 1.2) [44].

##### 5. The Effective Back-Scatter Cross-Section of a Target for the Case of Diversity (Bistatic) Radar

In bistatic radar, the transmitter and receiver are located in different places. A separation angle  $\beta$  is formed between the transmitter-target direction and the receiver-target direction (Figure 1.13). If  $\beta = 0^\circ$ , bistatic radar reduces to the conventional monostatic case.

## FOR OFFICIAL USE ONLY

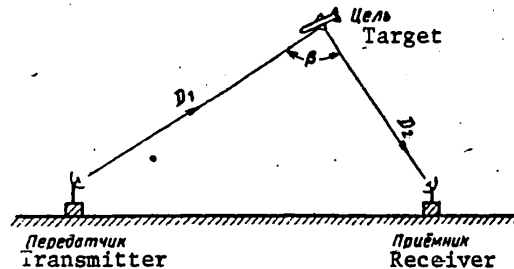


Figure 1.13. Radar using a spatially separated transmitter and receiver.

The range equation for bistatic radar has the following form:

$$P_{\text{rec.}} = P_{\text{np}} = \frac{P_{\text{изл}} G_{\text{изл}} G_{\text{пр}} \lambda^2 \sigma_{\text{цб}}}{(4\pi)^3 D_1^2 D_2^2 L_{\text{р пр}} L_{\text{р пр}}}$$

where  $P_{\text{пр}}$  is the received signal power;

$P_{\text{изл}}$  is the transmitted signal power;

$G_{\text{изл}}$  is the directional gain of the transmitting antenna;

$G_{\text{пр}}$  is the directional gain of the receiving antenna;

$\sigma_{\text{цб}}$  is the effective target back-scatter cross-section;

$D_1$  is the distance from the target to the transmitter;

$D_2$  is the distance from the target to the receiver;

$L_{\text{р пр}}$  are the radio wave propagation losses from the transmitter to the target;

$L_{\text{р пр}}$  are the radio wave propagation losses from the target to the receiver.

In this case,  $\sigma_{\text{цб}}$  is a measure of the energy scattered in the direction of the receiving antenna.

As has shown in the literature [28], for separation angles  $\beta \neq 180^\circ$ , the relationship between the values of the effective radar cross-sections for the case of monostatic and bistatic radar can be found if the following theorem is employed:

"At the limit, in the case of an infinitely small wavelength, the effective target cross-section, where the target is a sufficiently smooth solid, for the case of a diversity (bistatic) radar station with directions to the transmitter and the receiver determined by the vectors  $\vec{k}$  and  $\vec{n}$  respectively, equal to the effective

## FOR OFFICIAL USE ONLY

## FOR OFFICIAL USE ONLY

target cross-section in the case of a combined (monostatic) radar station, where the direction to the transceiver is determined by the vector  $\bar{k} + \bar{n}$ , where  $\bar{k} \neq \bar{n}$ ."

Here,  $\bar{k}$  is a unit vector directed from the transmitter to the target, while  $\bar{n}$  is a unit vector directed from the receiver to the target.

It is apparent that in those cases where the effective radar cross-section of a complex target is composed of the effective cross-sections of several elements, the transition from the bistatic to the monostatic case is accompanied by a change in the relative phases, and consequently, in the fine structure of the effective cross-section pattern of the target. It has been determined that when the effect of shading is taken into account and when the angle is limited to a certain range of values, the indicated theorem can be successfully employed. The influence of shading effects for a large aircraft is shown in Figure 1.14. It can be seen from the figure that in the case of bistatic measurements ( $\beta = 135^\circ$ ) the engines and fuel tanks on the wings of the aircraft prove to be "in the shade", while in the case of monostatic measurements, the reflections from them considerably increase the effective radar cross-section of the aircraft.

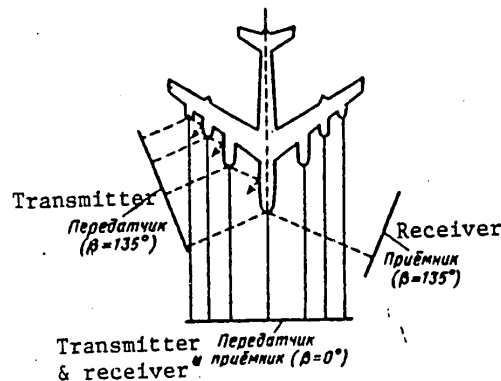


Figure 1.14. Electromagnetic energy scattering by the nose section of a large aircraft for two values of the separation angle.

It was found when comparing the results of monostatic and bistatic measurements using this theorem [28], that the maximum values of the effective cross-section, as well as the limits of variation in the effective cross-section obey the theorem with sufficient precision even for relatively large wavelengths. This can be seen from the graph of Figure 1.15a and 1.15b, in which the results of measuring the effective radar cross-section of the large aircraft depicted in Figure 1.14, are shown. During the measurements, the transmitter and axis of the aircraft were located in the same plane and the angle  $\theta$  was read out from the axis of the aircraft (from the nose) to the bisector of the angle formed by the transmitter, target and the receiver.



FOR OFFICIAL USE ONLY

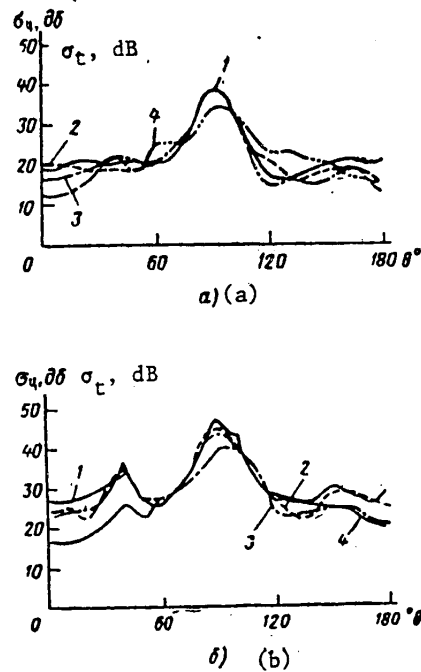


Figure 1.15. The effective back-scatter cross-sections of a large jet aircraft, measured at a frequency of 250 MHz for the case of horizontal polarization of the incident wave.

Key: a. Medians (every ten degrees);  
b. Maximum values (every ten degrees);

1.  $\beta = 0^\circ$ ;
2.  $\beta = 30^\circ$ ;
3.  $\beta = 60^\circ$ ;
4.  $\beta = 135^\circ$ .

The theorem considered here is not applicable to the case of  $\beta = 180^\circ$  (forward scattering). In this case, the effective radar cross-section of the target can be many times greater than for a monostatic radar (back-scattering). In the case of forward scattering, the effective radar cross-section of the target (if the wavelength  $\lambda$  is small as compared to the target dimensions) will be equal to:

$$\sigma_{tf} = 4\pi A^2 / \lambda^2,$$

where  $A$  is the target projection area.

FOR OFFICIAL USE ONLY

## FOR OFFICIAL USE ONLY

A sphere of radius  $a$  has an effective target cross-section for a monostatic radar station of  $\sigma_t = \pi a^2$ . Consequently, the ratio of the effective cross-sections for the case of forward and back-scattering for a sphere is equal to:

$$\frac{\sigma_{\text{f}}}{\sigma_{\text{b}}} = \left( \frac{2\pi a}{\lambda} \right)^2.$$

When  $a/\lambda = 10$ , the theoretical effective radar cross-section of such a target in the case of forward scattering is 36 dB greater than for back-scattering.

#### 6. Average Values of the Effective Back-Scatter Cross-Sections of Real Targets

The mean value of the effective cross-section  $\bar{\sigma}_t$ , is usually employed in the practical estimation of the range of a radar. This quantity can be derived by averaging the values of  $\sigma_t$  for various directions of the incident wave.

TABLE 1.3.

Average Values of Effective Back-Scatter Cross-Sections

Radar Target	Effective Cross-Sections, $\text{m}^2$
Nose cone of a ballistic missile	0.2
Fighter	3 - 5
Medium bomber	7 - 10
Long range bomber	15 - 20
Transport aircraft	up to 50
Cruiser	14,000
Low tonnage transport	150
Medium tonnage transport	7,500
Large tonnage transport	15,000
Trawler	750
Small submarine on the surface	140
Launch	100
Submarine conning tower	1
Man	0.8

Average values of the effective radar cross-sections of various real targets are given in Table 1.3, which were obtained as a result of the statistical generalization of a large number of measurements at centimeter band wavelengths.

As a rule, the maximum detection range of such targets was measured,  $R_{\text{max}}$ , and then  $\sigma_t$  was determined from the basic radar equation.

## FOR OFFICIAL USE ONLY

## CHAPTER TWO. THE EXPERIMENTAL STUDY OF THE EFFECTIVE BACK-SCATTER CROSS-SECTIONS OF TARGETS

## 1. Methods of Experimentally Studying Effective Back-Scatter Cross-Sections

If the atmospheric absorption of electromagnetic energy, ground or sea returns and other limiting factors are not taken into account, then radar range in free space is determined by the formula:

$$R_{\max} = A \left( \frac{1}{\sqrt{\sigma_t}} \right) \quad (2.1)$$

where  $A$  is a factor which combines the radar parameters.

It is apparent that the basic method of reducing the radar detection range for an object to be protected using antiradar camouflage is the reduction of the value of the effective radar cross-section of such an object. The successful resolution of this problem not only reduces the detection range of the object being defended, but additionally does the following:

--Reduces the target detection probability and the probability of autoguidance systems of missile armaments which use radar locking onto it;

--Allows for a significant reduction in the power of jamming transmitters installed in the object being protected (if  $\sigma_t$  is reduced by a factor of  $n$ , then the power of the jamming transmitter installed in this object to protect it can be reduced by a factor of  $n$ );

--Makes it possible to the size and weight of false radar targets which simulate the actual object with a reduced  $\sigma_t$ ;

--Boosts the camouflage effect of hydrometeors and sea and ground returns.

To achieve the requisite camouflage effect when protecting one military or industrial facility or another, it is essential to know not only its overall effective radar cross-section, but also to determine which elements of the structure specifically contribute the major share of the reflected signal. In other words, it is necessary to ascertain which portions of the object's surface must be camouflaged first of all. To obtain such data by means of theoretical research is an extremely complex problem, and at times, even impossible. For this reason, the major method of studying the effective radar cross-sections of real objects is experimentation at the present time. An advantage of the experimental method of study is the fact that it makes it possible to obtain a detailed reflection pattern in the elevation and azimuth planes and to ascertain the fluctuation and polarization characteristics of the return. The precision of the experimental method is sufficient for the design of a false target which simulates the real target with a high degree of reliability. The data obtained in this fashion can

FOR OFFICIAL USE ONLY

## FOR OFFICIAL USE ONLY

be utilized for the solution of the inverse problem: identification of the signal from a real object against a background of signals and false targets.

One of the most obvious methods of measuring  $\sigma_t$  is the study of the reflecting properties of an object under full scale conditions. It can be seen from the radar range equation:

$$P_{\text{rec}}/P_{\text{trans}} = \frac{P_{\text{rp}}}{P_{\text{max}}} = \frac{G^2 \lambda^4 \sigma_t}{(4\pi)^3 R^4} \quad (2.2)$$

That if the radar is calibrated, then the value of  $\sigma_t$  can be calculated by measuring the transmitted and reflected powers,  $P_{\text{trans}}$  and  $P_{\text{rec}}$ .

However, the performance of such measurements in a real situation entails considerable organizational and technical difficulties and requires considerable material outlays. For this reason, the reflective properties of objects are studied at the present time primarily under laboratory conditions or on special test sites. Both the objects themselves or mock-ups of them made to full scale, as well as models of the targets being studied can be used in this case. The use of mock-ups and models makes it possible to not only study the secondary emission pattern of the object in detail, but also to determine the influence of its individual structural components on the total value of the effective radar cross-section and the structure of the reflected signal. The studies consist in sequentially removing the elements being studied from the model, their reflective properties and comparing the results obtained with the reflected signal level received from the model of the entire object.

## 2. Specific Features of Electromagnetic Simulation

A model which differs from the original by a scale of  $n = 1/z$  is placed in the field of the electromagnetic radiation, the wavelength of which should be  $n$  times shorter than when irradiating the actual target. In accordance with the requirements of the experiment, the model is rotated in one plane or another. Its secondary emission field acts on the receiver at the appropriate frequency, is converted to an electrical signal of a definite level, which is then registered on an auto-recorder tape, photographic film or on magnetic tape. The polar plots obtained in this way make it possible to ascertain the level of the reflected signal as a function of the angular position of the model.

The possibility of a simple change in the scales of the electromagnetic systems is a direct consequence of Maxwell's linear equations. It is sufficient to meet the similarity conditions when modeling that the dimensions of the target and the wavelength for the measurements be changed by the same number of times, while the quantity  $E/H$  be the same for the model and the real object (Table 2.1).

Small models of aircraft, missiles and ships are turned out of an entire piece of metal, usually, aluminum or magnesium. Models of large dimensions are fabricated from wood or fiberglass and then coated with several layers of conductive paint.

## FOR OFFICIAL USE ONLY

To perform measurements on models, one must correctly choose the transceiving equipment, and additionally, meet the three following main requirements:

1. A plane wave should impinge on the model.
2. Clutter due to reflections from foreign objects (walls, stands, supports, etc.) should be minimal.
3. The elements for fastening the models should not have an influence on the structure of the electromagnetic field reflected from it.

TABLE 2.1.

Relationships Between the Parameters of a Model and a Real System (Target)

Quantity	Real System	Model
Length	$l$	$l' = l/n$
Time	$t$	$t' = t/n$
Frequency	$f$	$f = fn$
Wavelength	$\lambda$	$\lambda' = \lambda/n$
Specific conductivity	$\gamma$	$\gamma' = \gamma n$
Dielectric permittivity	$\epsilon$	$\epsilon' = \epsilon$
Antenna gain	$G$	$G' = G$
Effective back-scatter cross-section	$\sigma_t$	$\sigma'_t = \sigma_t/n^2$

In order for the effective radar cross-section concept to have any meaning, the value of the effective cross-section should be determined and measured for a certain reference standard incident field. Usually, a plane wave field is chosen as the reference standard field. An antenna radiates a spherical wave, and only with increasing distance from the radiator does the wave front approximate a plane front. However, in step with increasing distance of the model from the antenna, the received energy falls off rapidly, and for this reason, this distance is chosen as small as possible ( $R_{\min}$ ), but nonetheless such that the wave front differs little from a plane one. If the distance  $R_{\min}$  exceeds the dimensions of the test site or laboratory, then a special lens is placed between the radiator and the target to equalize the incident wave front.

As a rule, the electromagnetic field irradiates not only the model, but also the support on which it is mounted as well as the surrounding objects, so that the resulting back-scatter field at the receiver takes the form of a combination of the useful field from the model and spurious fields. Especially great interference is obtained because of returns from walls when operating in closed rooms. In order to reduce this kind of clutter to a minimum, measurements in closed

FOR OFFICIAL USE ONLY

## FOR OFFICIAL USE ONLY

rooms are made in so-called anechoic chambers. An anechoic chamber is created by means of covering the walls of the room in which the measurements are made with radio absorbing coatings. Free space conditions are simulated in this way.

Anechoic chambers, the fabrication and application of which have become possible because of the existence of high quality radio absorbing materials, make it possible to study the effective radar cross-sections of various targets and test radar equipment in short periods of time with a high precision, regardless of the weather.

Radio absorbing materials for anechoic chambers are materials which absorb radio waves in a wide range of frequencies. For this, they are made with a "matched" input, i.e., the impedance of the material at the surface is equal to the impedance of free space and gradually increases with increasing material thickness. The majority of samples of such materials are made from flexible or solid plastic foam with interspersed particles of absorbing material. To improve the matching to free space, the exterior surface of the material (coating) is made with a spine covered appearance. Hair mats impregnated with an absorbing composition can also be used in anechoic chambers. For the meter wavelength band, individual pyramids made of absorbing plastic foam are produced with a height of about 2 m. The radio absorbing materials employed in anechoic chambers operate effectively in a wide range of wavelengths shorter than a certain ultimate wavelength which is governed by the thickness of the material as well as the average value of the dielectric permittivity. The reflection from their surface depends little on the incidence angles.

Radio absorbing materials are produced by the American company of "Emerson and Camin" in the form of sheets of flexible or solid plastic foam. They are fastened to the surfaces being camouflaged with glue or special plastic clamps. The materials are sometimes made in the form of bricks from which walls are built up. The solid materials for floor decking are covered on the top with sheets of fabric glass laminate. This same company also produces, besides the sheets of absorbing material, finished panels faced with a coating. The dimensions of the panels are 1,800 x 1,800 mm<sup>2</sup> and 2,700 x 1,200 mm<sup>2</sup>.

Returns from the support stands on which the model is secured can also be reduced by means of radio absorbent materials. These stands or supports frequently fabricated from plastic foam. To reduce the returns from the supports, they are given the shape of a cone or inclined cylinder, while the surface is made with a toothed shape.

The background radiation can likewise be reduced by shaping the transmitter antenna directional pattern so that its minimum is directed towards the most dangerous re-reflectors. Because of the fact that the power appearing at the receiver input changes in accordance with a  $1/R^4$  law, it is advantageous to choose the spacing between the antenna and the model less than the distance to the interfering objects.

## FOR OFFICIAL USE ONLY

It makes sense to select the dimensions of anechoic rooms great enough so that the target can be set up as far as possible from the back wall, which must additionally be covered with the best of the absorbing materials available to the experimenter. For example, anechoic chambers having a length of 40 to 50 m have been built in the U.S.

If the dimensions of the model are so great that the distance to it should exceed 30 to 40 m, special open test sites are employed. The effective radar cross-sections of targets can be studied at such test sites just as if the targets were located in free space and at a separation boundary. In the latter case, the transmitting antenna and the target are placed at the surface of the earth at such a height that with the interaction of the forward and return beams from the earth, a maximum is obtained in the interference picture. Such a test facility will be described below in more detail.

### 3. Instrumentation Systems for the Study of Effective Back-Scatter Cross-Sections Using Models

The major difficulties which are encountered in the study of effective radar cross-sections are related to the segregation of the return signal from the transmitter signal and the suppression of undesirable returns from surrounding objects. At the present time, the following main types of measurement systems are employed:

- CW systems;
- Pulsed;
- Systems utilizing the doppler effect.

*A CW System.* This is the least expensive system. It is usually employed for working with small models, where the measurements are made in anechoic chambers at distances of up to 15 m from the model.

A block diagram of a CW instrumentation system is shown in Figure 2.1. The system consists of a transmitter and receiver (1, 7), connected to the corresponding arms of a twin T-waveguide bridge, hybrid tee 5. Tuning units 4 and matched load 3 are connected to one of the arms of the bridge, while foreign antenna 9 is connected to the other which serves simultaneously for transmission and reception. When using such a bridge, one must consider the fact that half of the received "and transmitted" power is fed to the receiver, while half is lost in the load. The waveguide tee should be made with strictly symmetrical arms. Only in this case will there be complete decoupling between the transmitter and receiver, while the received return is split equally between the matched load and the receiver. In practice, the load is intentionally slightly mismatched so that part of the signal is reflected from it into the arm of the tee to which the receiver is connected. This signal, the amplitude and phase of which is adjusted by means of the tuning units, is used to compensate for parasitic background returns. The ratio of the energy remaining following compensation in the arm of the tee, to which the receiver is connected, to the energy in the transmitter arm is called the degree of system decoupling. The requisite degree of decoupling increases with a decrease

FOR OFFICIAL USE ONLY

## FOR OFFICIAL USE ONLY

in the effective radar cross-section of the object being studied, with an increase in the requisite precision of the measurements and range to the target. To reduce

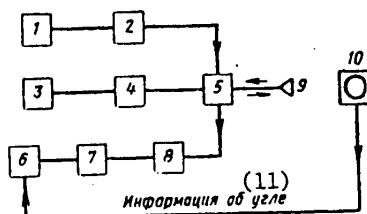


Figure 2.1. Block diagram of a CW system for the measurement of effective back-scatter cross-sections.

- Key:
1. Regulated oscillator;
  2. Decoupler;
  3. Matched load;
  4. RF tuning units;
  5. Hybrid T-joint;
  6. Autorecorder;
  7. Receiver;
  8. Mixer;
  9. Transceiving horn antenna;
  10. Support for the model;
  11. Information on the angle.

temperature influences on the level of decoupling, the waveguide T-joint and the antenna are fabricated from Invar, while the tuning rods in the arm of the matched load are made of quartz.

Extremely stringent requirements are placed on the stability of the oscillator, since a frequency deviation in it leads to the unbalancing of the bridge, a degradation of the decoupling and consequently, to a reduction in the receiver sensitivity. It is figured that in a system operating in the 10 cm band, the requisite degree of stability should amount to  $10^{-5}$  for a isolation level of 85 dB and  $5.8 \cdot 10^{-6}$  for an isolation of 100 dB. Modern industrial samples of microwave oscillators provide the stability needed to maintain the requisite compensation level during the entire measurement time and can be used as transmitters and beat frequency oscillators in superheterodyne receiving systems.

The following procedure is used for measurements made with such systems.

At the start of the measurements, the model is taken off of the support. The controls of the tuning unit are set in a position such that no signal is detected in the receiver arm. This means that the fields produced by returns from the supports and background clutter have been cancelled out. After the model is mounted in place, an uncompensated signal appears in the receiving arm of the waveguide T-joint from the target, which is registered by the recorder. The model can be rotated in this case  $360^\circ$  in azimuth or its position varied in the vertical plane. Then a



## FOR OFFICIAL USE ONLY

reference standard for which the effective radar cross-section is known is substituted for the model (sphere, cylinder, corner reflector) and the uncompensated signal from the selected reference standard is recorded.

By comparing the returns from the model being studied with the return from the reference standard, the effective radar cross-section of the model is determined directly. To obtain satisfactory precision with such measurements, it is necessary that the effective radar cross-section of the reference standard be of the same order of magnitude as the effective radar cross-section of the model being measured.

The calibration of the equipment will be correct only in the case where the reference standard and the model are irradiated by a plane wave. If the irradiating wave is other than plane, i.e. its phase front is distorted, then the reflected field will depend on the nature and magnitude of these distortions. In order to check the correctness of the obtained return patterns from complex models, it is necessary to make measurements of the field reflected from a flat plate, the pattern of which is well known [10].

If the transmitted wave is plane, then the angular width of the main lobe of the secondary emission pattern of a plate of width  $a$  will be defined by the equation  $\theta = \lambda/a$ . The sidelobes will be twice as narrow as the main lobe. The level of the first sidelobe should be 4.7 times less than the main one; the level of the next one should be 7.8 times less, etc.

A check of the ratio of the levels is simultaneously a check of the linearity of the entire receiving equipment channel. The measurement of the patterns of plates with different widths  $a$  and their comparison with the calculated ones makes it possible to determine at which dimensions the pattern begins to be distorted so much that the irradiating field cannot be considered plane any longer [10].

One of the variants of CW measurement systems is a *frequency modulated* CW system. The operational principle of such a system consists in the following.

A signal at a frequency of  $f_0$ , which is transmitted at a point in time  $t_0$  and reflected by the scattering target (the model) at a range of  $R$ , is returned to the receiver after  $\tau = 2R/c$  sec. Let the frequency of the transmitted signal change at a rate of  $df/dt$  Hz/sec, and then the frequency of the received signal will be:

$$f = f_0 + \frac{2R}{c} \frac{df}{dt}.$$

If a small portion of the energy at a frequency of  $f_0$  is used as the heterodyne frequency and it is mixed with the received signal, then we obtain the difference frequency:

$$f_p = f - f_0 = \frac{2R}{c} \frac{df}{dt}.$$

The signals reflected from objects located at ranges other than  $R$  yield other values of  $f_p$ . Interference from these signals can be avoided by means of tuned amplifiers and filters with a high degree of selectivity. The value of the effective radar target cross-section will be proportional to the amplitude of the received signal.

## FOR OFFICIAL USE ONLY

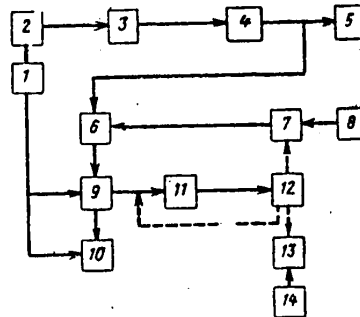


Figure 2.2. Block diagram of a pulsed system for effective radar cross-section measurements.

- Key:
1. Pulse generator and time sweep;
  2. Trigger pulse amplifier;
  3. Modulator;
  4. Magnetron;
  5. Transmitting antenna;
  6. Receiver and AFC system;
  7. Waveguide attenuator;
  8. Receiving antenna;
  9. Gated amplifier;
  10. Oscilloscope;
  11. Servo-amplifier;
  12. Servomotor for the autorecorder pen and waveguide attenuator drive;
  13. Autorecorder;
  14. Information source for the angle of rotation of the model support.

A pulsed system takes the form of a simplified radar adapted for operation with models set up at comparatively short ranges (Figure 2.2).

The pulse technique makes it possible to obtain a high transmission power and provides the capability of tuning out interfering signals by means of using special gating circuits. Pulses of from 0.1 to 1.0 microseconds are used in the equipment at repetition rates of from 500 Hz to 25 KHz. The intermediate frequencies of the superheterodyne receiver run from 30 to 60 MHz with a bandwidth of up to 10 MHz. For the indicated pulse widths, no antenna switchers are used, but separate antennas are used for transmission and reception. This is due to the fact that the comparatively long switching and reset time of antenna switches (gas dischargers) impedes normal operation with one antenna in the case of small ranges (up to 50 m) from the model being studied. The limitations related to the selection of the minimum range are practically eliminated, if nanosecond and sub-nanosecond pulse widths are used in the equipment. Pulse systems with pulse widths of one nanosecond and shorter exist, something which makes it possible to obtain a resolution of 15 cm and less. It is natural that such narrow pulses require a very wide intermediate frequency bandwidth.

FOR OFFICIAL USE ONLY

## FOR OFFICIAL USE ONLY

*Doppler Measurement Systems.* The measurement principle in such systems consists in the following.

The reflecting object is moved relative to the observer at a definite velocity  $v_r$  by means of a mechanical system. The moving object is irradiated with an electromagnetic field (with a wavelength  $\lambda$ ). The signal reflected from it will have a frequency which now differs from the frequency  $f$  by the amount  $\Delta f$  (the doppler frequency):

$$\Delta f = 2v_r/\lambda$$

The  $\Delta f$  frequency is segregated in the receiving equipment by means of comparing the reflected signal frequency with the transmitter signal frequency. The amplitude of the  $\Delta f$  frequency signal will be proportional to the effective radar cross-section of the moving object. A block-diagram of one of the variants of such a measurement system is shown in Figure 2.3.

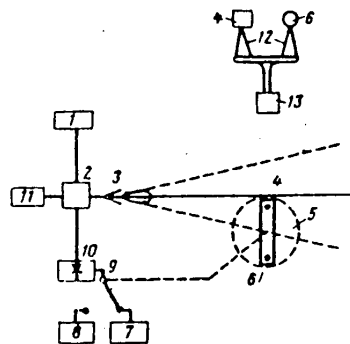


Figure 2.3. A measurement installation using rotation of the model and reference standard, based on the utilization of the doppler effect.

Key: 1. CW oscillator; 2. Waveguide tee-joint; 3. Antenna; 4. Model; 5. Rotating angle mounting bracket; 6. Reference standard; 7, 8. The equipment which receives and records the signal reflected from the model and the reference standard; 9. Switch; 10. Mixer; 11. Load; 12. Stands for fastening the model and the reference standard; 13. Rotational drive with the switch.

The object being studied is mounted on a rotating angle bracket and irradiated by a horn antenna. A reference standard reflector mounted in the place of the model at the same radial distance from the center of rotation is used to calibrate the return level. The position of the transmitting antenna is chosen so that only one object is irradiated. Thus, during the rotation of the mounting bracket, the model and the reference standard alternately fall in the irradiating field. The return from the rotating body is fed to the receiving arm of a waveguide tee-joint and is mixed there with the reference signal from the oscillator. As a result of such mixing, a difference frequency  $\Delta f$  is segregated, which is then amplified and fed to the recorder. If the objects are located at a distance  $r$  from the center of

## FOR OFFICIAL USE ONLY

—

## FOR OFFICIAL USE ONLY

antenna and the object as well as the range to the object remain within limits acceptable for practice. In order to be able to simultaneously measure the effective cross-sections of several objects, three rotating stands are positioned at distances of 150, 360 and 750 m from the radar building (Figure 2.4). Three devices for raising the antennas (to a height of up to 12 m) are set up around the periphery of the building, each of which supports transmitting and receiving antennas.

Simultaneously with monostatic measurements, bistatic measurements (two position) can be made at transmitter--target--receiver separation angles  $\beta$  of up to  $120^\circ$ . For this, there are three tracks on the test sites along with the device for raising the antenna moves as well as a bus with the equipment.

The main equipment complex consists of transceiver systems, each of which operates in one of seven frequency subbands, something which makes it possible to continuously cover a range of from 0.1 to 12 GHz; seven additional receiver systems are housed in the bus with the equipment and are used for the two-position measurements. There are also six sets of circular antennas with diameters of from 0.6 to 9 m and a set of polarizing units for each frequency band.

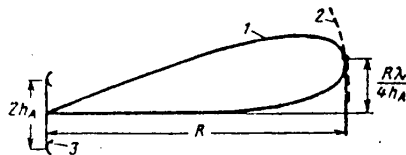


Figure 2.5. Idealized antenna directional pattern of the RAT SCAT facility.

Key: 1. Equal field intensity curve;  
2. Equal phase curve;  
3. Mirror image of the antenna.

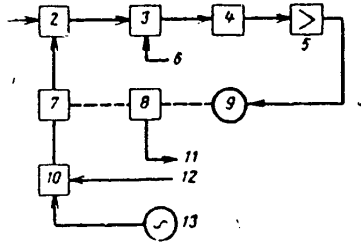


Figure 2.6. Block diagram of the receiver of the RAT SCAT facility.

Key: 1. Signal from the RF mixer;  
2. Intermediate frequency amplifier (60 MHz);  
3. Gating circuit;  
4. Error detector;  
5. Amplifier;  
6. Timing circuit;  
7. Reference attenuator;  
8. Digital and analog devices; 9. Drive; 10. Gating circuit; 11. Signal to the recording equipment; 12. Timing circuit; 13. Reference signal generator.

\* \* \*

The minimal peak power of each of the seven transmitters is 1 KW. The oscillators for the transmitters in the five upper subbands are designed around TWT's; triode oscillators are used in the two lower subbands. The pulse width can be carried in all seven subbands from 0.1 to 1 microsecond, while the repetition rate can vary from 500 to 5,000 Hz.

FOR OFFICIAL USE ONLY

Superheterodyne receivers with automatic gain control at an intermediate frequency, which amounts to 60 MHz, are used in the system. The bandwidth is 2 to 10 MHz. The primary amplifier channel is coupled to the reference signal oscillator, to obtain a linear output signal proportional to the value of the effective radar target cross-section in decibels (Figure 2.6). A range gating circuit passes the signal reflected from the object; the circuit passes the reference signal after approximately half of the interval between pulses. These two signals are compared with respect to amplitude, and the difference signal is used as an error voltage in a tracking circuit which controls the angle of rotation of the shaft of a precision reference attenuator. The tracking system generates the error signal; the level of the signal proportional to the effective radar cross-section in decibels is determined from the position of the reference attenuator shaft. This is accomplished by means of analog and digital coding devices. Such a method provides for automatic compensation for the nonlinearity of the intermediate frequency amplifiers.

The control consoles and recording equipment make it possible for the operator to monitor and control all of the timing circuits of the radar, the position and angular velocity of the rotating devices, the position of the reference standard reflector as well as the choice of antenna polarization and reference pulse amplitude.

The radar return is recorded in polar and cartesian coordinates on two autorecorders. A digital recording is also made at the same time on punched tape, which makes possible to record data incoming via the azimuth channel in intervals of 0.1, 0.2, 0.4, 1, 2 and 4 degrees.

FOR OFFICIAL USE ONLY

FOR OFFICIAL USE ONLY

CHAPTER THREE. REDUCING THE EFFECTIVE RADAR CROSS-SECTIONS OF OBJECTS BY USING POORLY REFLECTING SHAPES AND RADIO ABSORBANT MATERIALS

1. The Use of Poorly Reflecting Shapes

Having obtained exhaustive data on the effective radar cross-section of the object being protected, one can set about solving one of the major problems of antiradar camouflage: reducing the radar visibility of the object by means of reducing its effective back-scatter cross-section.

Reductions in the effective radar cross-sections of various targets can be achieved in two ways:

--By imparting a poorly reflecting shape to the object being protected;

--By using radio absorbent materials.

It is obvious that the maximum masking effect can be achieved with an efficient combination of both methods.

The general principle for the use of poorly reflecting shapes is the imparting of such a shape to the object that the maximum of the reflected electromagnetic energy is deflected to the side away from the direction to the radar receiver. This phenomenon can also be supplemented with chaotic scattering in various directions. The most characteristic poorly reflecting shape which deflects the maximum of the reflected energy in the direction of the receiver is an inclined plane or pyramid. A characteristic feature of a cone is the deflection of the maximum of the secondary emission pattern from the direction to the radar and the scattering of the reflected energy in various directions.

Comparative values of the effective radar cross-sections of simple reflectors are shown in Figure 3.1, for which the geometric areas  $S$  of the surfaces being irradiated are equal ( $1 \text{ m}^2$ ). Objects, in the structural design of which flat or cylindrical surfaces normal to the direction of irradiation, as well as corner reflectors, predominate have the greatest value of  $\sigma_t$ , where the geometric dimensions are the same. These objects are easily observed by radars at long ranges. Consequently, a basic condition for the use of poorly reflecting shapes is the priority replacement of structures having such surfaces with conical, pyramidal or flat surfaces with a particular angle of inclination with respect to the horizontal.

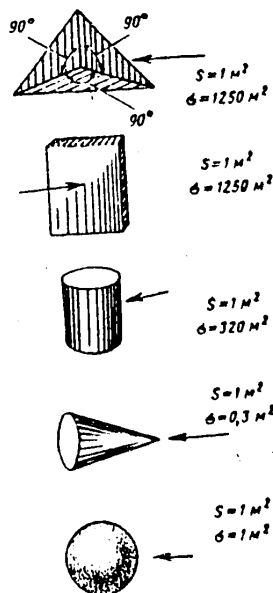
First of all, it is necessary to eliminate from the structure of the object being protected those corner reflectors which have large values of  $\sigma_t$  with small boundary dimensions, where the signals from such reflectors are stable on the display of a radar set. Dihedral and trihedral corner reflectors can be formed by the combination of the side of a ship and a smooth sea surface as well as by the combination of deck and superstructure surfaces. The surfaces of buildings, in conjunction with smooth pavements and bridges, form powerful corner reflectors with large surface dimensions.

## FOR OFFICIAL USE ONLY

If it is impossible to employ poorly reflecting shapes on an object because of structural design requirements, antiradar shields are used. A shield takes the form of a current conducting sheet, which is installed with an inclination to the vertical wall of the object being camouflaged (buildings, docks, the walls of mooring berths, etc.). A drawing depicting the protection of a submarine in its berth with an antiradar shield is shown in Figure 3.2. As has been reported in the foreign press, although such shields do not completely camouflage the protected objects, they nonetheless considerably reduce the power of the reflected signals, something which in turn has an impact on the clarity of the image on the display screen.

Some foreign specialists believe that such effects (although to a lesser extent) can be achieved if the vertical surfaces of the object being protected are not made smooth, but with a relief (corrugated). Such a ceramic plate is shown in Figure 3.3, which is proposed in the FRG for use as camouflage for residential buildings and industrial enterprises. Components which absorb radio waves can be introduced into the lower portion of the plate.

Moreover, West German specialists have proposed that grooves, channels and cup-shaped projections or depressions be made in the exterior surfaces of buildings to reduce the reflected radar signal power for the purposes of camouflaging industrial and residential buildings. To mask vertical planes and straight lines which form the outline of a building, it is recommended that the flat surfaces be broken up with grooves, which run in arbitrary directions; the rectangular outlines of foundations, doors, windows and entrances are to be provided with projections and cup-shaped add-ons, which distort the shape of these objects. Panels can be installed at an angle of  $45^\circ$  to the wall of a building above windows and doors and grooves, channels and projections can be made on the outside of the panels [7].



+ Figure 3.1. Comparative values of the effective radar cross-sections of reflectors of various geometrical shapes.

\*

Considerable work is underway in the U.S. to reduce the reflectivity of the warheads of ballistic missiles by means of imparting a poorly reflecting geometric shape to them. It is reported in published materials that the effective radar cross-section of a warhead, usually assumed to be  $0.2 \text{ m}^2$ , can be reduced by a factor of almost 1,000. As is well known, the theoretically ideal poorly reflecting shape is an infinite cone, viewed from the vertex. The nose-cones of missiles being developed in

FOR OFFICIAL USE ONLY



## FOR OFFICIAL USE ONLY

the U.S. at the present time have a minimal effective radar cross-section because the electrical characteristics of an infinite cone are reproduced in them with the greatest possible precision. This is done by means of imparting a cone shape to the missile nose cone with an ablation shield, in order to reduce back-scattering to a minimum, as well as by making appropriate changes in the outlines of the base of the nose cone to reduce diffraction. Sharpening the nose cone of a warhead not only reduces its effective radar cross-section, but also attenuates the shock wave and leads to less surface heating, something which considerably reduces ionization. In this case, a higher penetration velocity through the atmospheric layers is achieved and sharp aerodynamic braking of the nose cone begins at considerably lower altitudes. The problems of the enemy in tracking the missile warhead and intercepting it are thereby complicated a great deal.

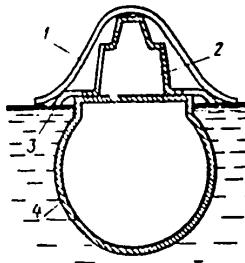


Figure 3.2. Antiradar shield on a submarine.

Key: 1,3. Shield;  
2. Conning tower;  
4. Hull.

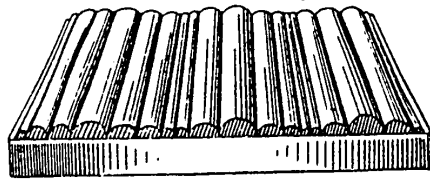


Figure 3.3. Ceramic plate which scatters the radio wave energy impinging on it.

Despite the fact that a pointed shape for missile nosecones is theoretically the most advantageous, it proves necessary in practice to round off the sharp points of the cone somewhat for the purpose of reducing its burn-up.

A shape close to a hemisphere, but having a specially designed double curvature to reduce the energy flux reflected in the direction of irradiation can be the optimal one for the base of the conical surface of a missile nose cone. To reduce diffraction and back-scattering, it is proposed that radio absorbant coatings be used on the back side of a missile warhead in areas having sharp edges and projections.

The back-scattering from a missile nose cone is a function of frequency. The energy radiated back in the direction of the irradiating source due to diffraction reaches a maximum when the wavelength approaches the dimensions of the warhead. The energy of the radio waves scattered from the sharp point of the cone and from the sharp edges of the missile warhead increase in direct proportion to wavelength:

## FOR OFFICIAL USE ONLY

## FOR OFFICIAL USE ONLY

the greater the wavelength, the greater the back-scattered energy is and the smaller the vertex angle of the cone, the smaller the back-scattering is.

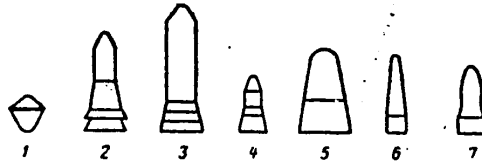


Figure 3.4. Nosecones of U.S. ballistic missiles.

- Key: 1. Mark 2 (Atlas, Thor missiles);  
 2. Mark 3 (Atlas missile);  
 3. Mark 5 (Titan 1 missile);  
 4. Mark 6 (Minuteman missile);  
 5. Mark 6 (Titan 2 missile);  
 6. Mark 7 (Skybull missile);  
 7. Mark 11, 11A (Minuteman missile).

The nosecones of ballistic missiles in U.S. armaments are shown in Figure 3.4.

## 2. General Information on Radio Absorbent Materials

In the middle of the Second World War, the English employed aircraft radar to search for submarines, something which sharply increased losses in the German fleet. To retain the major tactical advantage of the submarine - the fact that it is hidden, the Germans set about the design of radio absorbing materials. The conning towers and extendible equipment of submarines were covered with such materials. The coatings were supposed to absorb the electromagnetic energy incoming from the radar transmitter and reduce the submarine detection range by an aircraft radar.

In the opinion of foreign specialists, radio absorbing materials are a promising means of antiradar camouflage at the present time too for military and industrial objects. They are being developed primarily to shield aircraft for the purpose of facilitating the penetration of aircraft and missiles to an air defense line.

The operational principle of such materials consists in the fact that the absorbed radar energy is converted to other kinds of energy in the material itself. In this case, the phenomena of electromagnetic wave absorption, scattering and interference occur. In the case of electromagnetic energy absorption, the incident wave field is attenuated because of the conversion of the field energy to heat.

FOR OFFICIAL USE ONLY

FOR OFFICIAL USE ONLY

Such a process is primarily explained by the presence of dielectric and magnetic losses in the absorbing camouflage material. The scattering process is the conversion of the electromagnetic energy flux which propagates in a certain direction in the material to fluxes in various directions. The radio wave interference phenomenon (on analogy with optical interference) is responsible for the reflectivity of an absorbing material in the direction of greatest secondary emission from its surface.

In terms of structural design, absorbing materials can be broken down into two main types:

1. Radio absorbant coatings - materials which are applied to the surface (as a rule, metal surface) of the object being protected.
2. Radio absorbant construction materials: such materials, which are used for the construction of military or industrial facilities, combine, along with good strength characteristics, the property of absorbing radio waves transmitted by enemy search radars.

The following requirements are placed both on these and other material:

- Minimal radio wave reflection from the surface being protected;
- Maximum electromagnetic wave absorption;
- A wide frequency range of absorbed energy;
- High strength characteristics;
- Minimum size and weight;
- Capable of operating in a wide range of positive and negative temperatures.

Radio absorbant materials can be broken down into two main types, according to the operational principle: narrow band types, which are interference materials and broadband types, absorbing materials. In narrow band interference coatings, the secondary radio emission is suppressed because of the interference of the radio waves reflected from the exterior surface of the coating and the surface of the object being camouflaged. In broadband absorbing materials, because of their definite structure, there are no reflections from the external surface of the material and almost all of the electromagnetic wave energy entering the camouflage coating is gradually attenuated and converted to heat by virtue of the induction of scattered currents and magnetic hysteresis or high frequency dielectric losses.

Depending on the electrical and magnetic properties, radio absorbing materials can be broken down into dielectric and magnetic-dielectric types.

## FOR OFFICIAL USE ONLY

## 3. Some Questions of Theory

An absorbing material will correspond to its designation in the case where there is no electromagnetic wave reflection from the external surface while the energy penetrating into such a material is completely absorbed in it. Meeting these conditions is achieved through the appropriate choice of the electrical properties of the material, primarily the complex dielectric permittivity and the complex magnetic permeability:

$$\begin{aligned}\epsilon &= \epsilon' - j\epsilon'', \\ \mu &= \mu' - j\mu''.\end{aligned}$$

The imaginary components of the permeability and permittivity are due to losses in the material. We shall consider the conditions for the absence of electromagnetic energy reflection from the absorbing material. Let this material with electrical parameters of  $\epsilon$  and  $\mu$  have the form of an infinite plane, where a radio wave arrives from the external space ( $\epsilon_1\mu_1$ ) normal to the plane (Figure 3.5).

The field of such a wave at the surface of the absorbing material and the field inside the material will be described by Maxwell's equations [5, 9]:

$$\left. \begin{aligned} E_x &= E_m(e^{jkz} + se^{-jkz}) \\ H_y &= \frac{E_m}{12\pi}(e^{jkz} - se^{-jkz}) \end{aligned} \right\} z > 0, \quad (3.1)$$

$$\left. \begin{aligned} E'_x &= E'_m e^{jk'z}, \\ H'_y &= E_m \sqrt{\frac{\epsilon}{\mu}} e^{jk'z} \end{aligned} \right\} z < 0. \quad (3.2)$$

Here  $k = 2\pi/\lambda$  and  $k' = kn$  are the wave factors for the ambient medium (the air) and the absorbing material respectively,  $n = \sqrt{\epsilon\mu}$  is the complex index of refraction in the absorbing medium;  $s$  is the coefficient of radio wave reflection from the surface of the coating.

If boundary conditions are used which the field must satisfy at the surface of the material (the separation boundary of the media), i.e., when the tangential components of the electric and magnetic fields are equal, we obtain the following expression for the reflection factor:

$$s = \frac{\sqrt{\frac{\epsilon}{\mu}} - 1}{\sqrt{\frac{\epsilon}{\mu}} + 1}.$$

It is apparent that the factor  $s$  will be equal to zero (there is no reflection from the coating) when the dielectric permittivity and magnetic permeability of the material are equal,  $\epsilon = \mu$ .

FOR OFFICIAL USE ONLY

FOR OFFICIAL USE ONLY

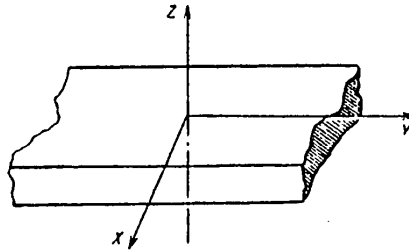


Figure 3.5. Schematic explaining the derivation of equations (3.1) and (3.2).

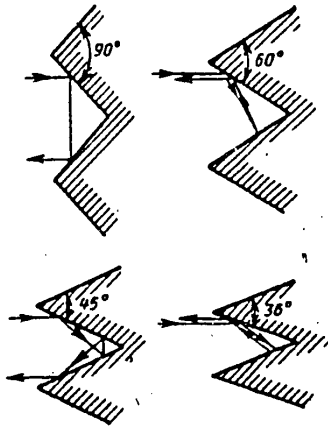


Figure 3.6. The influence of the angle at the vertex of the spines of the exterior surface of a coating on the number of reflections within the cells.

The expressions for  $s$  can be rewritten in a different form:

$$s = \frac{m-1}{m+1},$$

where  $m = z_1/z_2$ , and  $z_1$  and  $z_2$  are the complex impedances of the first and second media in which the wave propagates.

If the first medium is the ambient air, then  $z = 377$  ohms. In the case where the second medium is an absorbing material, it is necessary for the lack of a reflection that the equality  $z_2 \approx z_1$  be observed, from which it follows that  $\sqrt{\mu_2/\epsilon_2} = 377$  ohms, or

$$\sqrt{\frac{\mu_2}{\epsilon_2}} = 377 \text{ ohms}$$

$$\sqrt{\frac{\mu_{207n}}{\epsilon_{207n}}} = 1.$$

Thus, if the radio absorbing material has  $\mu_{2 \text{ rel}} \approx 1$  (nonmagnetic dielectric), then it is necessary that  $\epsilon_{\text{rel}}$  also be close to unity. A material having such properties should be porous (for example, rubber or polystyrene foam). However, it is also difficult in this case to meet the condition  $\epsilon = \mu$  for the input layer.

To reduce residual reflections, the exterior surface is not made smooth, but rather with relief, by arranging pyramidal projections over the entire surface (spines). In order to increase the number of reflections between the spines (and consequently, reduce the reflections from the coating surface), it is advantageous to make the angle small at the vertex of a spine (Figure 3.6).

FOR OFFICIAL USE ONLY

## FOR OFFICIAL USE ONLY

A material which such properties can operate in a rather frequency range, given the condition that the imaginary components  $j\epsilon$  and  $j\mu$ , which are due to energy losses when it passes through a layer of the selected material, are sufficiently large.

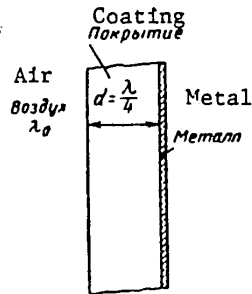


Figure 3.7. A radio absorbent interference coating with a thickness of a quarter wavelength, glued onto a metal sheet.

The effectiveness of a coating is improved if its absorption factor gradually increases from the outside surface of the coating to the protected surface. Multilayer dielectric radio absorbent materials ( $\mu_{rel} = 1$ ) are used for this purpose, where these materials have a permittivity  $\epsilon$  which increases from the exterior surface deep within the coating.

While the bulk of the energy impinging on absorbing protective coatings is converted to heat before the electromagnetic waves reach the reflecting surface of the protected object, in interference (narrow band) coatings, the lack of a reflection from the object being camouflaged is achieved through the interference of two radio waves: the one reflected from the exterior surface of the coating and the one from the surface to which the coating is applied (Figure 3.7). Naturally, in this case, the spacing between the reflecting surfaces (the coating thickness) should be

such as to provide for the out-of-phase addition of the reflected waves. In other words, the suppression of the incident wave occurs when its phase shift in the layer is  $\phi = \pi$ , i.e., when the layer thickness  $d$ , is equal to an odd number of quarter wavelengths:

$$\phi = (2b - 1)\pi,$$

where  $b = 0, 1, 2, \dots$

$$d = (2b - 1)\lambda/4n.$$

The masking effect of radio absorbing materials (coatings) is effective only in the case where the linear dimensions of the flat surfaces of the protected objects (targets) or the radii of curvature of their surfaces with a complex shape considerably exceed the wavelength in the coating material, i.e., when the following condition is met:

$$\frac{2\pi}{\lambda} \sqrt{S} > 10,$$

where  $S$  is the cross-section area of the body.

## FOR OFFICIAL USE ONLY

When the wavelength exceeds the maximum diameter of an object, so-called Rayleigh scattering is observed. In this case, scattering by an object with a finite conductivity proves to be almost the same as for an object with infinite conductivity, something which can be seen directly from the expression for the propagation constant:

$$\gamma = \omega \sqrt{\mu \epsilon \left(1 + j \frac{\eta}{\omega}\right)},$$

where  $\eta$  is the conductivity.

In fact, at sufficiently long wavelengths, the second term in the expression for  $\gamma$  begins to predominate, because of which, a coating with a finite conductivity will behave as an ideal conductor and the incident electromagnetic energy will not be able to penetrate into such a coating and will be absorbed in it. Experimental studies performed with metal spheres and cones with vertex angles of 60°, 90° and 120° have demonstrated that in the region of Rayleigh scattering, applying a coating to the surface of a sphere even leads to a slight increase in the back-scattering, and consequently, the effective radar cross-section of the sphere. However, in the region of resonance scattering ( $[2\pi/\lambda]a \geq 0.4$ , where  $a$  is the radius of the sphere), just as is to be expected, back-scattering decreases when a coating is applied.

Back-scattering by cones in the Rayleigh region when a coating is applied increases considerably (by 20 dB), and the back-scattering level begins to fall off in step with an increase in the diameter of the base of the cone, i.e., as the region of resonance scattering is approached.

#### 4. Narrow Band Interference Coatings

The simplest interference coating takes the form of a resonant absorber, consisting of a homogeneous dielectric layer applied to the metal surface being protected. The thickness of the dielectric layer  $d$ , its dielectric constant  $\epsilon$  and the tangent of the dielectric loss angle,  $\tan \delta$ , are chosen so that the reflection factor for the incidence electromagnetic waves is equal to zero.

Camouflage interference coatings are manufactured abroad from various plastics or rubber, filled with graphite powder or carbonyl iron. Merits of such coatings are their considerable mechanical strength, flexibility, comparatively small thickness and low weight. A major drawback consists in the fact that absorption takes place in a narrow band of frequencies. This is related to the basic condition for obtaining a nonreflective interference coating: its thickness is a function of the transmitter wavelength as well as the dielectric permittivity  $\epsilon$  and the magnetic permeability  $\mu$  of the material itself, i.e.:

$$d = \frac{\lambda}{4\sqrt{\epsilon\mu}}.$$

FOR OFFICIAL USE ONLY

## FOR OFFICIAL USE ONLY

In order to meet this condition, it is necessary to precisely choose the quantities,  $\epsilon$ ,  $\mu$  and the thickness of the coating. The coatings can be rather thin for short wavelengths with large dielectric and magnetic losses in the material. Interference materials work well only in the case of normal incidence of the radio waves on their surface. At other incidence angles, the reflection factor of the coating increases sharply.

TABLE 3.1

## Characteristics of Narrow Band Camouflage Coatings

Brand of Material	Thickness, mm	Wavelength Range, cm	Bandwidth, %	Weight, kg/m <sup>2</sup>	Reflector
MX1	2	3-3.4	10	7	Copper
MX3	2	-	10	9	Fabric
MS1	4	-	24	17	Copper
MS3	4	9.1-10.5	24	17	Fabric



Figure 3.8. The power reflected from the MX1 coating as a function of wavelength for the case of normal incidence.

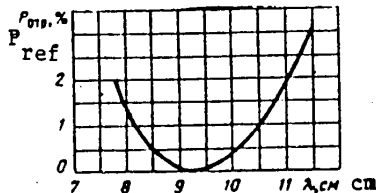


Figure 3.9. The power reflected from the MS1 coating as a function of the wavelength for the case of normal incidence.

The type MX and MS radio absorbent coatings developed by the English firm "Plessey Company", can serve as the most characteristic example of narrow band interference materials (Table 3.1). The basis of the coatings is rubber which is mixed with carbonyl iron. The back side of the materials is coated with copper sheet or flexible brass fabric. In the latter case, the coating can bend to fit the shape of the camouflaged object.

The bandwidth of MS material is considerably wider than that of MX because of the large content of magnetic material, and consequently, the large values of  $\mu$  and



the characteristic impedance. These materials take up little space, and if their back side is firmly fastened to the solid surface of the camouflaged object, they are good conductors of heat, and can absorb and dissipate approximately one watt/cm<sup>2</sup>. During a short-term exposure of such materials to a field with a power of approximately 200 KW on a surface of a few tens of centimeters, no changes were observed in their properties.

Curves showing the power of the reflected signals as a function of the wavelength and the angle of incidence for the MS1 and MX1 materials are plotted in Figures 3.8 - 3.10. They all have a narrow absorption band, and moreover, the power of the returns rises rapidly with an increase in the angle of incidence.

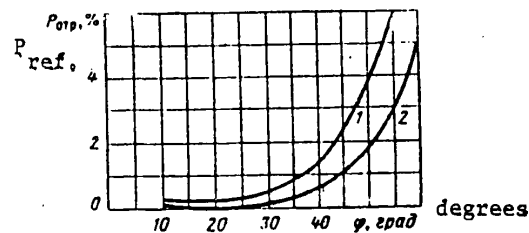


Figure 3.10. The power reflected from the MS1 coating as a function of the angle of incidence  $\phi$  at a wavelength of 3.2 cm.

Key: 1. Horizontal polarization;  
2. Vertical polarization.

Type MX and MS coatings with a small thickness and low weight have a comparatively high mechanical strength, something which makes it possible to use them for the antiradar camouflage of small mobile objects: motor vehicles, tanks, small ships, buoys, the helmets and weapons of night patrols, etc. [21, 30, 39].

The RS radio absorbing interference coating, designed for operation in the three centimeter band, was developed in the U.S. The coating is manufactured in the form of flexible plastic sheets 1.75 mm thick, with which metal objects of any shape can easily be covered. This covering provides for a reduction in the reflected power by a factor of 100 (as compared to reflection from a metal surface) at a wavelength of 3.2 cm. The material is distinguished by good strength characteristics, it can operate both at high (up to 205 °C) and below freezing temperatures, as well as in conditions of solar radiation, wind and rain. A square meter of such a covering weighs about 5 kg.

It should be noted that the production process for the fabrication of thin sheet and film interference coatings, which have good radio engineering and mechanical properties, is extremely complex.

Here, for example, is how a radio absorbent material is fabricated for a resonant frequency of  $7.5 \cdot 10^9$  Hz. The technology was developed by the American firm of "Dupont de Nemours Company". It is first of all necessary to fabricate the so-called neoprene absorbing cement, the composition of which includes the following components: 150 parts neoprene, 3 parts phenyl- $\beta$ -naphthylamine, 7.5 parts zinc oxide, 6 parts calcined magnesium oxide, 0.75 parts stearic acid, 84 parts furnace black and 494 parts xylol. At first, the phenyl- $\beta$ -naphthylamine, magnesium oxide,

## FOR OFFICIAL USE ONLY

zinc oxide, and furnace black are mixed in a special mixer for three minutes at a temperature of 43 °C. Then the temperature is lowered to 35 °C, neoprene is added to the mixer and the temperature is again increased up to 88 °C for seven minutes. The mixing is carried out at this temperature for five minutes. The resulting composition is placed in a rubber mill, where the zinc oxide is added to it at room temperature. Such a mixture, which is prepared in a cold rubber mill, is placed in a paddle mixer and half of the xylol contents are added, after which the intermixing continues for another 5.5 hours. The cement solution prepared in this manner contains 33.7 percent solid material by weight and is filtered through a fabric filter to remove the insoluble clumps. Then a homogeneous composition is prepared from the filtered mass, which is suitable for application to a flat surface with a conventional putty knife. For this, 171 parts by weight of neoprene cement is mixed with 12.6 parts by weight of graphite and 42 parts toluene. Such a solution is applied to the surface of glass plates (coated beforehand with a polyvinylchloride film 0.025 mm thick) and dried for 30 minutes at room temperature. Yet another coating layers are applied in the same way. The finished coating is removed from the glass plate, kept at a temperature of 70 °C for 24 hours to remove the solvent and is vulcanized at a temperature of 140 °C for an hour.

The vulcanized film 0.5 mm thick contains 11.9 percent (by volume) graphite and 22.7 percent (by volume) furnace black. Three such films are placed one on top of the other and pressed. The finished film is firmly joined to the metal foil.

It is recommended that graphite and acetylene black be used to absorb lower frequencies, and in this case, their content in the film is increased up to 25-50 percent (by volume).

Also of interest is the work underway abroad on the design of radio absorbent materials which take the form of a system of dipoles oriented in a dielectric and arranged at a distance of a quarter wavelength from the metal surface of the object being camouflaged. It is believed that such a system will make it possible to extend the bandwidth in which narrow band materials operate. It has been determined that for each length of the dipole used in the absorbing system there exists a lattice constant for the grid formed by the dipoles such that the reflection factor is minimal.

Under actual modern combat conditions, a large number of radars will be used simultaneously which have various working wavelengths. In this case, narrow band interference coatings will have little effectiveness. Broadband radio absorbent materials are considered more promising. As a rule, they have considerable thickness and weight, but nonetheless can camouflage the objects they protect against radar stations operating at different frequencies.

##### 5. Broadband Radio Absorbent Coatings and Materials

The development of broadband radio absorbent coatings, which were intended for camouflaging submarines, started during the Second World War in Germany. The coverings consisted of a number of layers, the conductivity of which increased with depth. The layers were separated by a foam-like plastic with a dielectric

FOR OFFICIAL USE ONLY

## FOR OFFICIAL USE ONLY

permittivity close to unity. Absorption was good in a range of wavelengths from 4 to 13 cm. However, because of the great thickness and considerable weight, the covering samples which were developed did not find practical application.

Many industrial companies and scientific research organizations abroad are working on such materials at the present time. It is believed that the use of absorbing coatings on aircraft and missiles will make it possible to significantly facilitate their penetration of air defense zones of an enemy, saturated with radars operating in a broad range of frequencies. The opinion has been put forward that if even the speed of a camouflaged object is reduced through of such materials, the then slow nuclear weapons vehicle which is poorly visible on a radar screen can prove to be more dangerous than a fast vehicle which produces a strong return and is detected by the radar at a great range. A merit of such materials is also the fact that they do not have to cover the entire camouflaged object, but only the "shining" areas of its surface which are determined during the process of studying the effective radar cross-sections of various targets.

TABLE 3.2

Characteristics of Broadband Camouflage Coatings

Brand	Lower Limit of the Wave-length Range, cm	Maximum reflected power, %	Thickness, mm	Weight per Square Meter, kg	Cost per Square Meter, Dollars
AN-W-72	1.5	1.5	3.2	0.4	48.5
AN-W-73	4.0	1	9.5	0.8	54
AN-W-74	8.6	1	15.9	1.2	63
AN-W-75	12.5	1	25.4	2.0	72
AN-W-77	32.0	1	53.5	3.5	117
AN-W-79	66.0	1	114.3	8.0	140

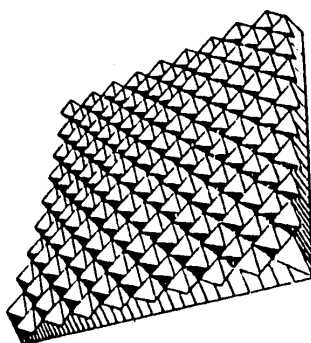


Figure 3.11. AF-11 radio absorbent material, the outer surface of which is corrugated.

The American company "Emerson and Camin" produces the AN-W series of radio absorbent materials, which are recommended for use on aircraft and objects exposed to the open air (Table 3.2). The company advertises this material as light, flexible and a sheet covering which can assume the form of the object being protected. The dimensions of a sheet are 600 x 600 mm. The covering parameters do not depend on the weather and do not change at temperatures of from -55 to +150 °C. A neoprene fabric covered with nylon is applied to the material, which is glued to any surface.

## FOR OFFICIAL USE ONLY

## FOR OFFICIAL USE ONLY

The type RM "Echosorb" broadband radio absorbent material was also developed by the same company to camouflage aircraft and space vehicles. It takes the form of a flexible silicone foam capable of operating for a long time at high temperatures (up to +260 °C). The power reflection factor in a range of wavelengths of from 4 cm and shorter does not exceed 2 percent. Changes in the polarization plane of the incident energy or the angle of incidence have little effect on a change in the reflection factor. The material is produced in the form of sheets 300 x 300 mm. At a thickness of 9.5 mm, the weight of one square meter of the material is 2.98 kg. A variant of the RM "Echosorb" has been developed for a range of wavelengths of 8 cm and shorter. It weighs 6.85 kg/m<sup>2</sup>, while the thickness is 28.6 mm [43].

The English firm of "Plessey Company" produces the AF series of broadband radio absorbent materials, which are intended for camouflaging stationary objects or objects which move at a slow velocity (Figure 3.11). These coverings are specifically recommended for use in camouflaging the superstructures of ships, buildings, port facilities, canals, etc. [7, 30].

The AF-10 material is fabricated from two layers of porous rubber, mixed with carbon dust. The absorption increases gradually from the first layer to the second. The covering layers have the following characteristics:

	<u>First Layer</u>	<u>Second Layer</u>
Characteristic impedance, ohms	225	190
Attenuation, dB/m:		
At a frequency of 3,000 MHz	125	210
At a frequency of 10,000 MHz	540	970

In the case of normal incidence of a beam on the first layer, the power reflection factor in a range of wavelengths of 3 to 10 cm is 6 percent. The corrugation of the surface reduces it down to 1 percent in the 10 cm band and down to 0.2 percent in the 3 cm band. Because of the relief surface, the reflection factor depends little on the angle of incidence.

The AF-11 coating which is intended for wavelengths of 5.7 cm and shorter has finer absorber grains and less weight than the AF-10.

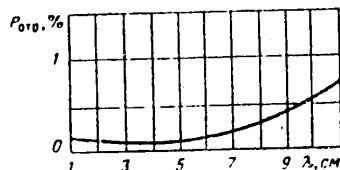


Figure 3.12. The electromagnetic power reflected from AF20 material as a function of wavelength for the case of normal incidence.

## FOR OFFICIAL USE ONLY

## FOR OFFICIAL USE ONLY

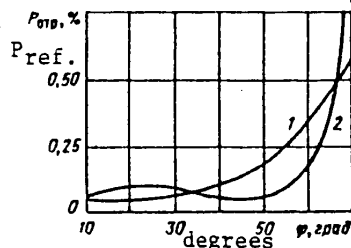


Figure 3.13. The electromagnetic power reflected from AF-20 material as a function of the angle of incidence at a wavelength of 3 cm.

Key: 1. Horizontal polarization;  
2. Vertical polarization.

The lightest and hardest covering is the AF-20 type. It consists of pressed grains of polystyrene foam, surrounded by a tough carbon film. The front side is likewise corrugated, just as the AF-11 material. The AF-20 materials can be used in open air if their surface is protected by a layer of hydrophobic siliceous paint. In this case, atmospheric moisture can form individual drops, which do not increase reflections, on the corrugated surface of the covering. The reflection factor from such a coating does not exceed one percent with respect to power in a wide range of wavelengths (Figures 3.12, 3.13).

Ferrites have found widespread applications in recent years for the manufacture of broadband radio absorbant materials. Coverings made of such materials are distinguished by light weight and small thickness. The American company of "Conductron" manufactures material based on ferrites, intended for camouflaging the nose cones of ballistic missiles. It provides for the absorption of electromagnetic energy at meter and decimeter wavelengths. Other broadband materials by the same firm make it possible to absorb radio emissions in a range from meter to centimeter wavelengths. Coatings of materials of this type have a thickness of 6.3 to 12.7 mm and attenuate the reflected radiation by a factor of 20 to 1,000. One of these coatings 5 mm thick (a square meter of this coating weighs 4.9 kg) provides for a reflection attenuation in a range of frequencies from 40 to 3,000 MHz down to 1 percent in the center of the band and down to 7 percent at the edges. The "Conductron" company is working on the design of a radio absorbent material to camouflage aircraft and missiles, which simultaneously has thermal shielding and radio absorbent properties. It is thought that ablation heat shield coverings can be obtained with the introduction of plastics into the composition of the radio absorbent coverings developed by this company.

The radio absorbent fabric developed in the FRG is also of interest. It is proposed that ground objects be camouflaged with panels of such fabric: aircraft on airfields, tanks, ordinance, missile installations, etc. The fabric has a layered grid structure, the cells of which are filled with graphite powder along with a binder. In some layers of the fabric, the graphite powder particles are arranged so that they do not fill the cells completely or uniformly, leaving air gaps. The camouflage panels consist of three or five layers, where the dimensions of the cells in the layers are not the same [7].

Radio absorbent coverings for so-called anechoic chambers are produced abroad in a wide assortment. Their structural design and use were treated in the previous chapter. The most widespread type of absorbing material for anechoic chambers is

## FOR OFFICIAL USE ONLY

## FOR OFFICIAL USE ONLY

FR "Echosorb", which is used in the form of light foam blocks. It has a reflection factor of one percent in a wavelength range of 0.6 to 12 cm with a thickness of 5 cm (type FR-330) and in a range of wavelengths of up to 66 cm with a material thickness of 20.3 cm (type FR-350).

The "Echosorb" CHW material is especially recommended for operation at low frequencies. It is produced in the form of solid or hollow pyramids, built into blocks, as well as in the form of individual pyramids with a height of up to 1.8 m (CHW-560) for frequencies below 50 MHz.

Absorbent antiradar structural materials occupy a special place among the means of antiradar camouflage. West German specialists are intensively involved in their development. For example, they have proposed using porous concrete in the form of individual construction blocks for shielding against radar detection of buildings. Because of the presence of air bubbles in porous concrete, the radio wave absorption in it considerably exceeds the absorption in conventional concrete. For more intense absorption, it is recommended that graphite be mixed in the porous concrete. A multilayer absorbing construction material design with different grain and pore sizes in the layers has also been developed in the FRG (Figure 3.14). The outer layer, which is irradiated by the electromagnetic energy first, amounts to half of the material thickness (having the form of plates or blocks) and contains the largest grains. Underneath it is a layer in which the grains are considerably smaller, and even lower is a layer of silica with graphite added. For practical purposes, a three-layer absorbing plate is recommended, the outer layer of which (11 cm) consists of grains with a diameter of 10 to 20 mm; the second layer (3 cm) contains grains 1 to 3 mm in diameter. Underneath it is a layer of fine pebbles with graphite added, where the diameter of the pebbles is equal to approximately 0.7 mm. Radio waves which penetrate into the second layer are partially refracted and scattered back to the outer layer and partially absorbed in the pores of the second layer.

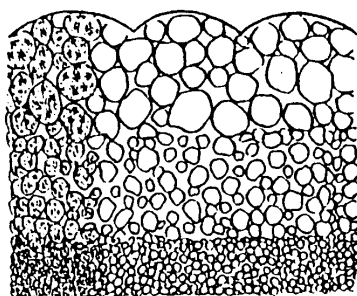


Figure 3.14. The structure of a three-layer radio absorbent construction material.

Sometimes, two of these layers is sufficient to achieve the requisite effect. The third fine-grained layer absorbs part of the electromagnetic energy and reflects part of it, and it is attenuated when passing back through the layers with pores and hollow places of greater size.

Work is intensively underway abroad on the study of the radio absorbing properties of plasma for its utilization as a means of antiradar camouflage for missiles and space vehicles. It was reported in the press that a radar emission absorption effect and a considerable decrease in the effective backscatter cross-section can be achieved with the radar probing of a metal sphere

## FOR OFFICIAL USE ONLY

partially covered with a plasma layer. The plasma layer can be extremely thin as compared to the radar wavelength.

#### 6. Measuring the Characteristics of Radio Absorbent Materials

The basic parameter to be measured, which must be known both during the process of fabricating the material and in the final stage when testing the finished sample, is the reflection factor of the coating  $s$ . The study of the properties of radio-absorbent materials can be carried out using various techniques. The radio frequency method has become the most widespread. In this case, the field intensities  $E_A$  and  $E_R$  of electromagnetic waves reflected from the absorbing material and from a flat metal reflector respectively, where the latter has the dimensions of the coating and is mounted in the same place, are compared:

$$s = E_A/E_R$$

A sample measurement set-up is shown in Figure 3.15. The transmitting and receiving horns are positioned on supports, which can be moved in a vertical plane along a semicircular arc. The sheet of absorbing material being tested is placed in the center of the arc. The polarization is changed by rotating the horns about the axis.

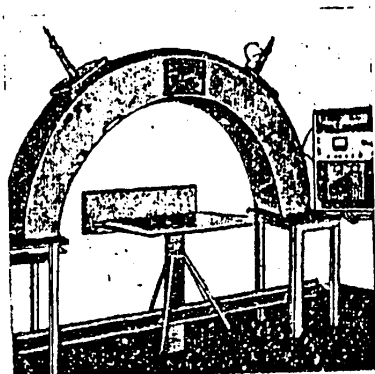


Figure 3.15.

Set-up for measuring the reflection factor of radio absorbent materials.

The transmitting horn transmits the microwaves which are modulated with square wave pulses, which pass through the graduated attenuator. The receiving horn is loaded into a semiconductor detector, which is coupled with a cable to an amplifier tuned to the modulation frequency.

Having arranged the horns so as to obtain the requisite angles of incidence and polarization, the metal sheet is placed in the center of the arc. Then the attenuator is set so a sufficiently high reading is obtained at the output of the amplifier.

FOR OFFICIAL USE ONLY

FOR OFFICIAL USE ONLY

Then the metal sheet is replaced by the absorbing material being tested, and the attenuation inserted with the attenuator is reduced until the previous reading is obtained at the amplifier output. The difference in the two attenuator readings yields the value of the power reflection factor:

$$s = 10 \log(P_1/P_2) \text{ dB,}$$

where  $P_1$  is the power level reflected by the material;  $P_2$  is the power level reflected by the metal sheet.

The measurement frequency range is governed by the property of the horns and the parameters of the RF generator. At lower frequencies, considerable errors appear because of the increase in the dimensions of the horn and the surface areas of the tested materials as compared to the spacing between them. In this case, the reflection factor can be determined from the standing wave ratio (SWR). The installation includes a horn, which is matched to free space. The dimensions of the horn are chosen so that the aperture angle of the exiting beam does not exceed 12 degrees. The covering sheet is placed in front of the horn so as to obtain the requisite irradiation angle.

The techniques have been developed and the equipment designed at the present time for the rapid determination of the dielectric constants and tangent of the dielectric loss angle of radio absorbent materials. However, it is thought that despite the importance of these quantities, they are rather difficult to determine at a directly specified point on a real object. It has been reported in the press that it is obviously expedient to evaluate promising radio absorbent materials in the future based on such variables as the capacitance and losses at audio frequencies, which are measured directly on the object protected with the covering.



## FOR OFFICIAL USE ONLY

## CHAPTER FOUR. THE MASKING PROPERTIES OF TERRAIN AND HYDROMETEORS

## 1. The Effective Back-Scatter Cross-Section of Surface Distributed Targets

The camouflage effect of surrounding terrain objects consists in producing clutter interference as a result of electromagnetic wave reflections from the surface of the ground or sea, as well as from inhomogeneities in the atmosphere. The intensity of these returns depends on the condition of the atmosphere, the nature of the terrain around the radar station, the wavelength as well as the resolving power of the radar. With a sufficiently high intensity, such clutter can significantly reduce the operational effectiveness of the radar or even completely preclude the possibility of radar operation.

The specific effective back-scatter cross-section is taken as the measure of the intensity of returns to characterize the masking reflections from distributed objects (grass cover, plowed land, forest, shubbery, a sea surface, etc.). The back-scatter level is usually taken equal to the effective back-scatter cross-section of one square meter of distributed surface targets and is designated  $\sigma_y$ . We shall assume that a radar, located in an aircraft flying at an altitude  $H$ , has a pulse width  $\tau$  and an antenna directional pattern width at the half power level of  $\theta$ . At each given point in time, the signal acting on the receiver input is the result of the adding of the signals reflected from elementary reflectors arranged in a random manner within the bounds of the reflecting area of the surface. The geometric area of a distributed target section ("the resolving area"), as can be seen in Figure 4.1, will be equal to:

$$S_{ra} = \frac{c\tau}{2} R\theta \sec \varphi, \quad (4.1)$$

where  $\phi$  is the angle of antenna beam inclination to the horizontal.

The value of the effective radar cross-section of a surface distributed target,  $\sigma_{ra}$ , is defined as the product:

$$\sigma_{ra} = \sigma_y S_{ra} = \frac{c\tau}{2} \sigma_y R\theta \sec \varphi. \quad (4.2)$$

It can be seen from the derived expression that the effective back-scatter surface area of such targets depends not only on the scattering properties of the surface, governed by the quantity  $\sigma_y$ , but on the oblique range, angle of wave incidence and radar parameters. The signal from the surface target produces a rather intense luminescent blip on the radar screen, as well as a "background", which interferes with the observation of point targets located within the bounds of this surface area" ships, tanks, industrial objects, etc. A target on the ground or water surface can be detected by the operator only in the case where its signal is

## FOR OFFICIAL USE ONLY

segregated from the pips produced by the masking returns from the background surrounding the target. Experimental data show that on a PPI display, one can segregate a return from a reflecting surface on which a point target is located from the reflecting areas adjacent to it which do not have point targets only when the contrast factor is equal to:

$$K = \frac{\sigma_{pt} + \sigma_s}{\sigma_{pt}} \leq 1.3 + 1.4, \quad (4.3)$$

where  $\sigma_{pt}$  is the effective radar cross-section of a point target and  $\sigma_s$  is the effective radar cross-section of a surface target.

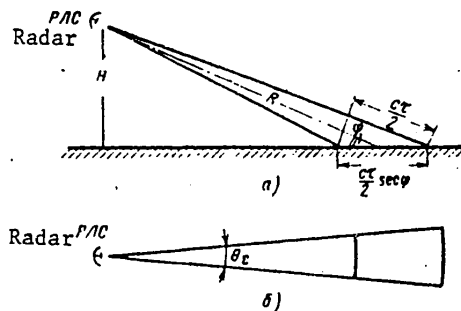


Figure 4.1. The reflecting surface area in the vertical (a) and horizontal (b) when scanning a ground or sea surface with a pulsed aircraft radar.

To improve the observability of point targets, it is necessary to reduce  $\sigma_s$ , something which as can be seen from formula (4.2) can be accomplished by narrowing the directional pattern in the horizontal plane  $\theta$  and reducing the pulse width  $\tau$ .

However, it must be noted that an improvement in the observability of a camouflaged object through a reduction in  $\tau$  will not occur as rapidly as follows from expression (4.2), since when  $\tau$  is shortened, the bandwidth of the receiver must be extended, because of which its internal noise increases.

The effective radar cross-section of a surface target is also governed by the quantity  $\sigma_y$ , which in turn depends on the unevenness of the surface, the incident angle of the electromagnetic energy, the wavelength, the polarization and the dielectric permittivity of the irradiated surface.

As is well known, irradiated surfaces in radar are broken down into smooth and rough. A smooth surface is depicted on a display screen in the form of a dark spot, since in this case, the incident beam is reflected away from it in accordance with the laws of geometric optics and does not return to the receiver. In the case of a rough surface, a portion of the scattered energy returns back to the antenna and produces a bright region on the screen. The transition from a mirror to diffuse reflection is related to the unevennesses of the irradiated surface.

## FOR OFFICIAL USE ONLY

## FOR OFFICIAL USE ONLY

A surface can be considered smooth if the height of the uneven places on it,  $h$ , with an angle of inclination of the antenna beam to the horizontal,  $\phi$ , and a wavelength  $\lambda$  satisfies the expression:

$$h \leq \frac{\lambda}{16 \sin \phi}. \quad (4.4)$$

The majority of surface targets have an unevenness value which does not satisfy expression (4.4). For such rough surfaces which produce a diffuse reflection, the specific effective radar cross-section is justified as a sinusoidal function of the angle  $\phi$ :

$$\sigma_y = \sigma_0 \sin \phi, \quad (4.5)$$

where  $\sigma_0$  is the specific effective radar cross-section when  $\phi = \pi/2$ .

## 2. The Reflecting Properties of a Ground Surface

For centimeter band radars, the majority of dry land is a rough surface, primarily because of vegetation. The reflecting surface of such objects consists of reflectors which move little (hills, tree trunks, etc.) and reflectors which are in chaotic motion with the action of the wind (grass, leaves and tree branches). The stronger the wind, the more intensive their motion. For this reason, reflections from trees, shrubbery and natural terrain features covered with vegetation consist of a brightly expressed constant signal and a signal which fluctuates in amplitude and phase. Radar returns from a surface covered with vegetation undergo seasonal changes. Moreover, the nature of electromagnetic wave reflections from all surfaces depends strongly on their humidity and the presence or absence of snow cover.

The specific effective radar cross-sections of a ground surface covered with forest is shown in Figure 4.2 as a function of the angle of antenna beam inclination to the horizontal,  $\phi$ , and summary graphs of the function  $\sigma_y = f(\phi)$  are plotted in Figure 4.3 based on the results of averaging the data for various types of terrain. As can be seen from this figure, the values of  $\sigma_y$  for various terrains occupy a region with comparatively clear-cut boundaries, so that one can judge the overall character of the terrain from which an echo is received based on the value of  $\sigma_y$ . Thus, for example, the range of values of  $\sigma_y$  for forested terrain at various angles to the horizontal has an extent of no more than 5 dB. The specific radar cross-section for desert terrain depends greatly on the nature of the soil and the surface inhomogeneities, and averages 13 dB less than for forested regions. Measurements made over three various regions of broken rocky desert yield very loose results, where the course of the  $\sigma_y = f(\phi)$  curve for a desert has almost the same form as for forested terrain. The back-scattering by sandy desert (even, dry sand) proves to be the least of dry land. Back-scattering by the sea, as a rule, is less than the scattering by dry land, and the values of  $\sigma_y$  occupy a region 10 to 15 dB wide.

FOR OFFICIAL USE ONLY

## FOR OFFICIAL USE ONLY

Electromagnetic energy scattering by built-up regions always exceeds the scattering by forested terrain. The range of possible values of  $\sigma_y$  for built-up regions of the earth's surface is extremely wide (20 to 30 dB).

In antiradar camouflage, the nature of the background against which a particular camouflaged object is located is of very great importance, since the background frequently provides no small return, and sometimes a greater return than the object being scanned, which in this case, will not be detected.

When taking step directed towards the reduction of the effective radar cross-section of any ground object, its size, shape and the material from which it is made must be taken into account, as well as the reflectivity of individual background areas surrounding the object being camouflaged.

A priority task in camouflaging ground objects of extensive area should be the equalization of the radar return coefficients of the object being camouflaged and the ambient background. This is achieved through the use of radio absorbent construction materials and coverings in conjunction with poorly reflecting shapes and shields. By reducing the effective radar cross-section of a camouflaged object and somewhat boosting the returns from individual background areas close to the object, the contrast boundaries between the target being camouflaged and the background are erased. Individual structures (bridges, roads, dams, etc.) or group objects (concentrated troupes or equipment, plants, warehouses, electric power stations, airfields) are camouflaged in this way.

Thus, for example, it is recommended in one of the foreign references [38] that concrete asphalt highways and landing strips at airfields be camouflaged taking into account the surrounding background.

In the case of vertical scanning of a concrete strip, up to 60 percent of the incident energy is reflected in the direction of incidence. In the case of irradiation at an angle of  $45^\circ$ , the amount of energy reflected in the direction of arrival is zero. In intermediate cases, the return factor falls in a range between zero and 60 percent.

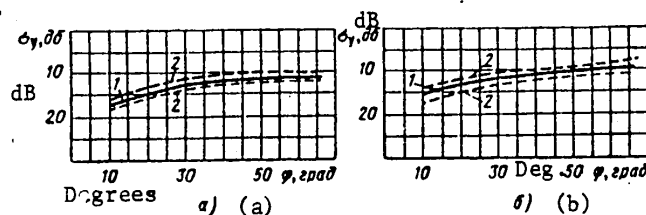


Figure 4.2. The specific effective radar cross-section,  $\sigma_y$ , of forested terrain as a function of the angle of beam inclination to the horizontal,  $\phi$ .

Key: a. Temperate zone forest; b. Tropical forest; 1. Average value; 2. Range encompassing 70 percent of all measurements.

FOR OFFICIAL USE ONLY

## FOR OFFICIAL USE ONLY

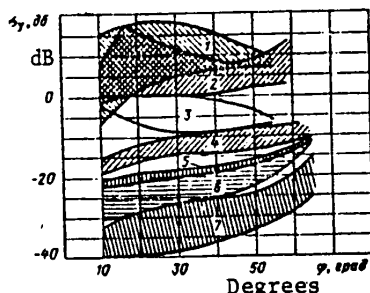


Figure 4.3. The specific effective radar cross-section,  $\sigma_y$ , as a function of the angle of beam inclination to the horizontal,  $\phi$ .

- Key: 1. Industrial regions of a city;  
 2. Commercial regions of a city;  
 3. Residential regions of a city;  
 4. Forested terrain;  
 5. Broken rocky desert;  
 6. Sandy desert;  
 7. Sea for a wind speed of from 5 m/sec to 7 m/sec (the larger values of  $\sigma_y$ ).

To shield against radar detection, the return factor must be chosen in a manner applicable to the surrounding terrain. If a road (airstrip) runs through a pine forest, then the factor must be reduced from 60 to 29 percent, and if in open fields, down to 10 percent while among rocks, down to 49 percent etc. For this purpose, roughness can be imparted to a concrete surface of a road by means of channels, the spacing between which depends on the surrounding terrain. The concrete surface is broken down into fields, in which the grooves run in different directions. The edges of the strip are camouflaged with shrubbery having a large scattering cross-section so as to disrupt the symmetry and distort the outlines of the strip.

When implementing antiradar camouflage measures for various ground objects, one must take into account the fact that the enemy has surveillance radars for ground targets and radars for detecting the fire positions of mortars and artillery.

The practically straight-line propagation of the ultrashort waves used in radar limits the effectiveness of the ground station to the visible horizon. In other words, by having reconnaissance data on the arrangement of enemy radar stations in a terrain, one can compute the boundaries of their detection areas from the well-known formula:

$$R = 3.57(\sqrt{h} + \sqrt{H}).$$

where  $R$  is the line of sight range, km;

$h$  is the radar station antenna height in m;

$H$  is the height of the object in m.

The positioning of objects to be probed outside the bounds of this zone cannot be detected by ground radars, no matter what kind of tactical and technical data they have.

## FOR OFFICIAL USE ONLY

## FOR OFFICIAL USE ONLY

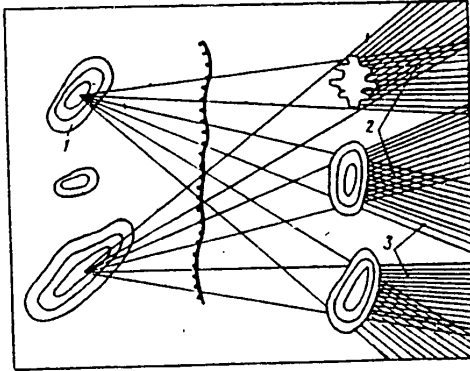


Figure 4.4. The plotting of invisibility fields.

Key: 1. Enemy radar positions;  
 2. Invisibility fields of two radars;  
 3. Invisibility fields of one radar.

In many cases, the terrain relief also does not allow the detection of targets by means of ground radars. Objects which are concealed behind natural shields: hills, mountains, forests - are not detected by ground stations. This circumstance, in the opinion of foreign specialists, makes it possible to use the terrain relief on a widescale to conceal troop groupings, combat materiel, and individual ground objects in the so-called invisibility fields of the enemy radars.

Such fields can be plotted on a map of the terrain in the following manner (Figure 4.4) [11]. Straight sighting lines are run from the locations of the enemy radars through possible high crests, the edges of local objects and natural shields. Then, profiles of the terrain are plotted using the sighting lines. The enemy will not see in the sight profiles located behind terrain objects, since a region of radio shadow is formed behind them which is due to the line of sight propagation of VHF band radio waves.

### 3. The Masking Properties of Returns from a Sea Surface

Signals reflected from a sea surface can make it significantly more difficult for aircraft, ship or shore radars to detect targets on the water and in the air flying at low altitude.

The nature of the average signal levels reflected from various sea targets and sea waves as a function of their observation range by a ship radar is shown in Figure 4.5. It can be seen from the figure that small sea targets (launches, small boats, buoys or the extendable surface gear of submarines, the effective radar cross-sections of which are commensurate with the cross-section of a buoy) will be reliably camouflaged at certain ranges by returns from sea waves.

Sea returns have a very complex nature. The specific effective radar cross-section,  $\sigma_y$ , of a sea surface depends on the angle of antenna beam inclination, the wavelength and the radiation polarization, as well as the state of the sea and the wind strength.

## FOR OFFICIAL USE ONLY

## FOR OFFICIAL USE ONLY

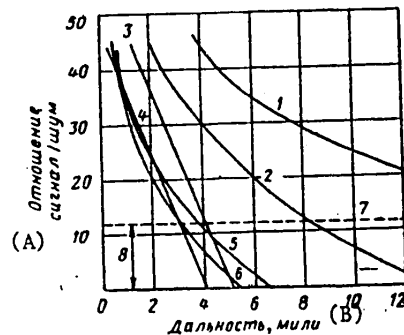


Figure 4.5. The average levels of the returns from various sea targets [as a function of range].

- Key: 1. Ship with a displacement of 10,000 tons;  
 2. Ship with a displacement of 1,000 tons;  
 3. Sea wave clutter incoming from a range of up to 9 km;  
 4. Clutter from a range of up to 7 km;  
 5. Launch;  
 6. Buoy;  
 7. Limiter level;  
 8. Range of signal variation which can be displayed on the screen.  
 A. Signal to noise ratio;  
 B. Range, miles.

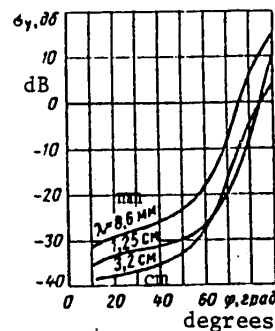


Figure 4.6. The quantity  $\sigma_y$  for a sea surface as a function of the angle of inclination of the directional pattern and the wavelength of the radar.

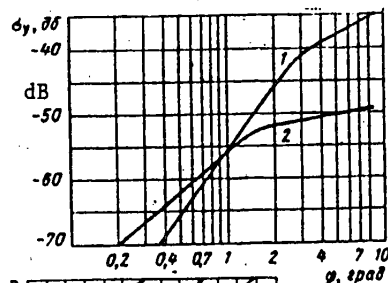


Figure 4.7. The quantity  $\sigma_y$  for a sea surface as a function of the beam inclination angle.

- Key: 1. Quiet sea;  
 2. Moderate wave agitation on the sea.

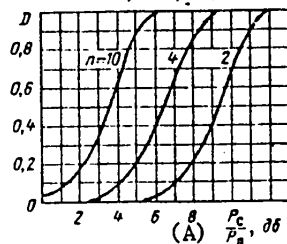


Figure 4.8. The probability of radar detection of a constant amplitude pulse packet with a random phase for  $F = 10^{-6}$ .

- Key: A.  $P_{sig}/P_{clutter}$ , dB.

As a rule, the value of  $\sigma_y$  increases with an increase in the inclination angle, something which is confirmed by the graph of Figure 4.6. The curves were plotted from averaged experimental data for various sea states and wind speeds which varied in a range of from 3.7 to 45 km/hr.

## FOR OFFICIAL USE ONLY

## FOR OFFICIAL USE ONLY

At small angles of inclination of the antenna beam to the horizontal ( $\phi < 10^\circ$ ), the dependence of  $\sigma_y$  on the state of the sea is expressed especially sharply (Figure 4.7). A critical inclination angle exists,  $\phi_{cr}$ , at which the slope of the curve which characterizes the rise in  $\sigma_y$  with an increase in  $\phi$  changes sharply. A formula has been derived empirically which expresses the quantity  $\sigma_y$  for a sea surface as a function of the angle  $\phi$ , which yields good agreement with experimental data:

$$\sigma_y = 10e^{-0.5(90^\circ - \phi)^{0.7}}$$

The specific effective cross-section  $\sigma_y$  increases with an increase in frequency: in the millimeter wavelength band, it is approximately 8 to 12 dB greater than in the centimeter band (Figure 4.6). It was ascertained as a result of numerous experiments that the specific effective radar cross-section of a sea surface is approximately a  $\lambda^{-4}$  function of the wavelength in the case of a quiet sea and approximately a  $\lambda^{-1}$  function in the case of wave agitation.

The quantity  $\sigma_y$  is expressed as a function of the polarization in the following manner: in the case of a quiet sea, horizontally polarized signals yield a significantly smaller reflection in the direction to the radar than vertically polarized transmissions. The difference in the returns with the different kinds of polarization decreases substantially in the presence of wave agitation.

A strong dependence of return intensity on the sea surface and sea wave agitation is observed. With an increase in wave agitation,  $\sigma_y$  increases up to a certain limit, and then decreases. Thus, at a wavelength of 3.0 cm, this limit begins at a change in the sea wave height of from 0.6 to 1 m. The quantity  $\sigma_y$  also depends on the direction of the wind. A reflected signal will be more intense when the antenna beam is directed counter to the wind. When the beam is oriented in the direction of the wind, the return intensity will be 5 to 10 dB less.

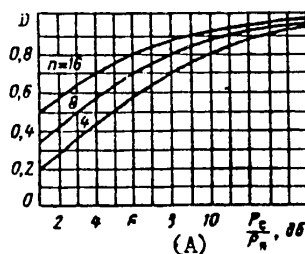


Figure 4.9. The probability of radar detection of a mildly fluctuating pulse packet in the case of a Rayleigh distribution for the amplitudes (when  $F = 10^{-5}$ ).

Key: A.  $P_{sig}/P_{clutter}$ , dB.

The procedure proposed in paper [40] can be used for practical calculations of the masking effect of sea waves when detecting surface water targets with a ship-board radar.

The problem of detecting the useful signal (the signal from a target on the water surface) in the presence of interference (sea wave clutter) is a probabilistic



## FOR OFFICIAL USE ONLY

problem. When solving such a problem, it is expedient to specify the false alarm probability,  $F$ , at which a minimum signal passage probability,  $M$ , or a maximum detection probability,  $D$ , is assured (the Neumann-Pearson criterion).

In terms of the processing technique for the received signals, a shipboard PPI radar is close to the optimal processing system for an incoherent pulse train. The detection characteristics of an optimum receiver with square-law summing at the output of an incoherent packet of radar signals,  $n$ , are shown in the graphs of Figure 4.8 and 4.9 for various  $F$ .

To segregate the useful signals in the final unit of a radar with a reliability no less than the specified value, it is necessary that the signal/interference ratio at the output of the detection system be no less than a threshold value  $(P_c/P_\pi)_{\text{нпд}}$ .

The calculation of the  $P_{\text{sig}}/P_{\text{int}}$  ratio at the output of the system can be accomplished using the basic radar equation:

$$\frac{P_c}{P_\pi} = \frac{\bar{\sigma}_n}{\bar{\sigma}_\pi} \left( \frac{\gamma_r/R}{\gamma_\pi/R} \right)^4, \quad (4.6)$$

where  $\bar{\sigma}_n$  and  $\bar{\sigma}_\pi$  are the probability values of the effective radar cross-sections of the target and the sea wave agitation;  $\gamma_c$  and  $\gamma_\pi$  are attenuation functions [for the signal and interference respectively];  $R$  is the range to the target being detected;  $P_c$  and  $P_\pi$  is the back-scattered signal and interference power [respectively].

In the special case where the observation is made at grazing angles,  $\phi$ , close to the critical angle  $\phi_{\text{cr}}$ , expression (4.6) can be simplified, by reducing it to the form:

$$\frac{P_r}{P_\pi} = \frac{\sigma_n}{\sigma_\pi \frac{c\tau}{2} \theta R \sec \varphi}, \quad (4.7)$$

where  $\theta$  is the width of the antenna directional pattern in the horizontal plane;

$$\sec \phi = h/R \quad (4.8)$$

( $h$  is the installation height of the radar antenna).

The quantity  $\phi_{\text{cr}}$  can be computed from the formula:

$$\sin \varphi_{\text{cr}} = \frac{\sqrt{\lambda}(h_1 + h_2)}{2\theta R},$$

where  $h_1$  and  $h_2$  are the referenced heights of the radar antenna and the target.

## FOR OFFICIAL USE ONLY

Values of the critical grazing angle are given in Table 4.1 as a function of the state of the sea surface.

Based on expressions (4.7) and (4.8), one can write the condition for reliable detection of a target and a water surface against a background of sea wave clutter:

$$\sigma_{\text{ц}} \geq \left( \frac{P_{\text{с}}}{P_{\text{ш}}} \right)_{\text{пор}} \sigma_{\text{ц}} h \frac{c^2}{2} \theta. \quad (4.9)$$

TABLE 4.1

Состояние поверхности моря Sea Surface State		Критический угол $\phi_{\text{кр}}$ , град. при длине волны $\lambda$ , см (C)	
баллы (A)	средняя высота волн, м (B)	10	3
1	0.15	4.7	1.4
2	0.45	1.6	0.47
3	0.9	0.8	0.24
4	1.8	0.4	0.12
5	3.2	0.22	0.07
6	5	0.14	0.04
7	7.6	0.095	0.03

Key: A. Intensity rating;  
B. Average wave height, m;  
C. Critical angle,  $\phi_{\text{кр}}$ , degrees, for a wavelength  $\lambda$ , cm.

*Example.* We shall determine the masking effect of sea waves when detecting surface targets with a "Don" chipboard radar having the following parameters:  $\tau = 1$  microsecond,  $\theta = 1$  degree, the pulse repetition rate is  $F_{\pi} = 800$  Hz, the antenna rotational speed is  $\Omega = 15$  r.p.m.,  $h = 20$  m and we specify the following values:  $D = 0.9$ ,  $F = 10^{-5}$  and  $\sigma_{\text{т}} = -15$  dB (the wave height is more than 2 m).

We find the number of pulses to be integrated:

$$n = 0.5 (\theta F_{\pi} / \Omega) \approx 4. \quad n = 0.5 (\theta F_{\pi} / \Omega) \approx 4.$$

From the graph of Figure 4.9 we determine the ratio  $(P_{\text{sig}}/P_{\text{clutter}})_{\text{thresh.}} = 13$  dB substituting all of the data in expression (4.9), we obtain:

$$\sigma_{\text{т}} \geq 12 \text{ dB} \approx 16 \text{ m}^2.$$

Thus, the calculations show that in the case of sea wave agitation rated at 4 points and above, surface targets having an effective radar cross-section of less than

FOR OFFICIAL USE ONLY

## FOR OFFICIAL USE ONLY

16 m<sup>2</sup> can be detected only with great difficulty against the background of sea wave clutter using the "Don" shipboard radar with the antenna mounted at a height of 20 m: launches, small boats, submarines running submerged with periscope up, etc. And in this case, if measures to reduce the radar contrast are taken into account, the masking effect of sea waves will also be extended to ships of greater displacement.

## 4. The Masking Effect of Hydrometeors

Water vapor condensation products in the atmosphere are called hydrometeors. They can be observed in the form of rain, fog, snow or hail. When falling in the target detection field of a radar, hydrometeors reduce its detection range or mask the target. The masking effect of hydrometeors is amplified with a shortening of the radar wavelength.

Hydrometeors (atmospheric precipitation) take the form of an aggregate of a large number of individual elementary reflectors, which fill a certain volume and which are perceived as a single volume distributed target.

The elementary reflectors which form the overall signal are distributed within the bounds of a reflecting volume  $V$ . In the case of pulsed radar, the reflecting volume will be equal to (see Figure 1.2):

$$V = \frac{\pi}{4} R^2 \theta_{na} \theta_{yn} \frac{c\tau}{2}.$$

Then the effective radar cross-section of a distributed volumetric target can be found from the formula:

$$\sigma_v = \sigma_y V = \frac{\pi}{4} \sigma_y R^2 \theta_{na} \theta_{yn} \frac{c\tau}{2}.$$

The specific radar cross-section,  $\sigma_y$ , is governed by the nature of the bulk target. If the bulk target takes the form of an aggregate of homogeneous reflectors - rain drops, hail stones, snow flakes - then the value of  $\sigma_y$  depends on the distribution density of such reflectors in space, on the effective cross-section of each of the particles,  $\sigma_i$ , and on the polarization of the incident wave [45]. The specific effective cross-section per unit volume of hydrometeors will be equal to:

$$\sigma_y = \sum_i \sigma_i N_i, \quad (4.10)$$

where  $N_i$  is the number of particles per cubic meter.

In the case where fogs, clouds and precipitation consist of spherical water or ice particles and their diameter is much less than the wavelength, the effective radar cross-section of a particle can be computed from Rayleigh's well-known formula:

FOR OFFICIAL USE ONLY

## FOR OFFICIAL USE ONLY

$$\sigma_t = \frac{\pi^2 d^6}{\lambda^4} \left( \frac{n^2 - 1}{n^2 + 2} \right)^2, \quad (4.11)$$

where  $n$  is the complex index of refraction.

For water, the factor  $\left( \frac{n^2 - 1}{n^2 + 2} \right)^2$  varies from 0.90 to 0.92 and depends slightly on the temperature when  $\lambda$  changes from 0.8 to 10 cm. It is almost constant for ice and is equal to 0.19.

By substituting expression (4.11) in formula (4.10), we obtain:

$$\sigma_y = \frac{\pi^2 \sum_i N_i d_i^6}{\lambda^4} \left( \frac{n^2 - 1}{n^2 + 2} \right)^2.$$

It is more convenient in practice to express the quantity  $\sigma_y$  in terms of the water content of clouds or fogs,  $W$  in  $\text{g/m}^3$ , and the rain intensity as  $I$ , in  $\text{mm/hr}$ . Then the specific cross-sections for clouds and fogs will be:

$$\sigma_y = 13.2 \cdot 10^{-18} \frac{W^2}{\lambda^4}; \quad (4.12)$$

and for rain:

$$\sigma_y = 6.2 \cdot 10^{-11} \frac{I^{1.4}}{\lambda^4}. \quad (4.13)$$

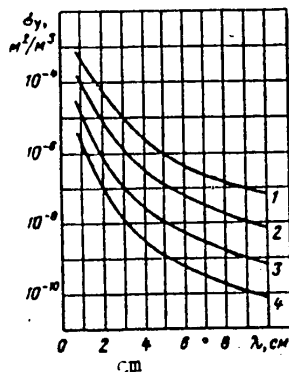


Figure 4.10. The value of the specific effective radar cross-section for rain of various intensities.

Key: 1. Heavy rain (16 mm/hr);  
2. Moderate rain (4 mm/hr);  
3. Light rain (1 mm/hr);  
4. Drizzle (0.25 mm/hr).

It follows from equations (4.12) and (4.13) that for the same radar, with values of  $W$  and  $I$  which are encountered in nature, the return from clouds and fog is approximately four orders of magnitude less than the signal reflected from atmospheric precipitation. For this reason, in practice it is necessary to consider only the masking effect of precipitation (rain, snow, hail).

## FOR OFFICIAL USE ONLY

The specific effective radar cross-section  $\sigma_y$ , is shown in Figure 4.10 as a function of the rain intensity for various wavelengths. It can be seen from the figure that with an increase in the wavelength, the return from the rain falls off.

The power of the echo signal received from a target, taking into account radio wave attenuation, can be determined from the main radar equation, written in the following form:

$$P_{rr} = \frac{P_{trans} G^2 \lambda^2 \sigma_n}{(4\pi)^2 R^4} \gamma_1, \quad (4.14)$$

where  $\gamma_1$  is a coefficient which takes into account the signal attenuation over the radar-target path which is due to the influence of atmospheric gases, fog, clouds and precipitation.

The power of returns from atmospheric formations is determined from the relationship:

$$P_r = \frac{P_{trans} G \lambda^2 \sigma_p}{(4\pi)^2 R^4} \gamma_1. \quad (4.15)$$

It is proposed in the literature [41] that the masking effect of precipitation be characterized by a comparative relationship between the range of a radar in the absence of precipitation on the path and when precipitation is present.

In the first case, the signal to noise ratio at the radar receiver input is equal to  $P_{rec}/P_n$ , and in the second case it is  $P_{rec}/(P_n + P_r)$ , where  $P_n$  is the power of the receiver noise.

Assuming that the target can be detected at the same signal to noise ratio, and equating the two latter relationships, taking into account formulas (4.14) and (4.15), we obtain:

$$\frac{P_{trans} G^2 \lambda^2 \sigma_n}{(4\pi)^2 R_0^4 P_n} = \frac{P_{trans} G^2 \lambda^2 \sigma_n \gamma_1}{(4\pi)^2 R^4 (P_n + P_r)},$$

from which:

$$R_0^4 = \frac{R^4}{\gamma_1} + \frac{R^4 P_r}{P_n \gamma_1}.$$

Taking into account only the masking effect of atmospheric precipitation, we find:

$$R_0^4 = R^4 \gamma_1^{-1} + 5.2 \cdot 10^{-1} \gamma_1^{-1} R^4. \quad (4.16)$$

The first term in equation (4.16) takes attenuation into account, while the second considers the masking return from the precipitation. Using the known radar range

FOR OFFICIAL USE ONLY

## FOR OFFICIAL USE ONLY

for good weather without precipitation,  $R_0$ , one can determine its range under specified meteorological conditions,  $R$ , from the graphs plotted using the above equation. Curves characterizing the change in the range of a radar with the following parameters in a drizzle as well as in light, moderate and heavy rain are shown in Figure 4.11. The wavelength is  $\lambda = 3.2$  cm; the power per pulse is  $P_{\text{trans}} = 50$  KW, the pulse width is  $\tau = 0.6$  microseconds and the antenna gain is  $G = 28.6$  dB.

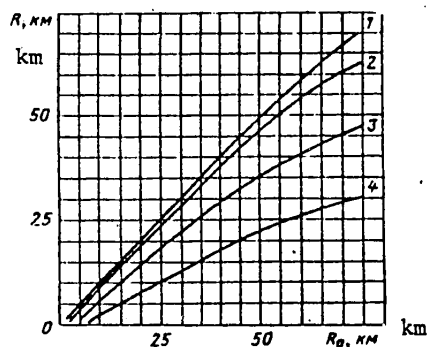


Figure 4.11. The reduction in the detection range,  $R$ , of a 3 cm band radar for rain of various intensities.

Key: 1. Drizzle;  
2. Light rain;  
3. Moderate rain;  
4. Heavy rain.

An analysis of the curves shows that for moderate (4 mm/hr) and heavy (16 mm/hr) rains, radar operation is degraded quite significantly. For example, while the range is 75 km in good weather without precipitation, moderate rain reduces it to 48 km while heavy rain reduces it to 30 km.

## FOR OFFICIAL USE ONLY

## FOR OFFICIAL USE ONLY

## CHAPTER FIVE. ARTIFICIAL RADAR REFLECTORS AND THEIR USE

## 1. General Information

An artificial radar reflector is understood to be a special device which is characterized by the fact that the radar signal reflected from it has parameters which are specified beforehand (power, directionality, polarization, etc.).

Such reflectors find the widest application to the anti-radar camouflage for various objects: distorting the shore outline or the contours of water surfaces; imparting reflective properties similar to the properties of surrounding terrain to water surfaces, air strips and highways, etc. In this case, such a distorted picture of the portion of the terrain on which the camouflaged target is located can be created on the screens of the enemy radars that its surveillance under poor visibility conditions will be made a great deal more difficult or altogether impossible.

Artificial reflectors play a no less important part when they are used as decoy radar targets. The function of such targets is to mislead the enemy, overload his target acquisition and fire control radar, and in the final analysis sharply reduce the effectiveness of his fire power.

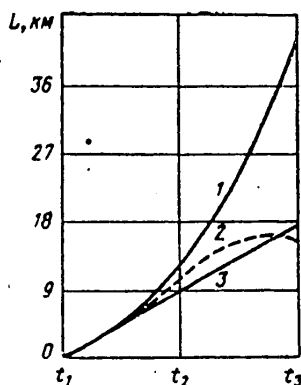


Figure 5.1. Extent of the propagation zones of a "cloud" of chaff, ejected from a ballistic missile in various portions of its trajectory and in various directions.

- Key: 1. In the plane of the trajectory in the direction of its major axis;  
 2. Perpendicular to the plane of the trajectories;  
 3. In the plane of the trajectory in the direction of its minor axis;

$t_1$  is the end of powered phase;  
 $t_2$  is apogee;  
 $t_3$  is the final section.

Radar decoys, which are spaced a certain distance from the true target, will attract a missile with a radar homing device to it; in this case, the probability of destroying the protected target is considerably reduced.

FOR OFFICIAL USE ONLY

One of the requisite conditions for the effective use of decoy targets is that they have a sufficient effective radar cross-section which is comparable to the cross-section of actual targets. In this case, changes in the effective radar cross-sections of the decoy and the effective cross-section of the protected object as a function of the direction of their irradiation by the radar should be identical.

To be added to this are such requirements as simplicity of the device, economy, small size and weight, as well as the capability of the mass utilization of decoy targets.

Decoys are widely used in the protection of the most diverse military and industrial facilities: air, space, sea and ground installation.

An especially great effect can be achieved with decoy targets in the case of air and space objects, primarily ballistic missiles. More than 50 various false targets having an overall volume complexity of 100 times greater than the missile warhead can be ejected from one missile. The extent of the propagation region of a "cloud" of decoy targets jettisoned from a ballistic missile at various points in its flight and in various directions relative to the trajectory is shown in Figure 5.1 [7]. The identification of a missile warhead against a background of false targets is possible in principle, but requires extremely complex and expensive equipment. The use of artificial radar reflectors as camouflage tools and decoy targets, in conjunction with a reduction in the radar contrast of the camouflaged objects, makes it possible to confuse the operation of enemy radars to a considerable extent.

One of the promising trends in the refinement of various kinds of radar systems is the increasing of their selectivity up to a level which makes it possible to reliably discriminate an artificial reflector from the true target based on a set of secondary criteria which are frequently related to the fine structure of the return.

The parameters which characterize radar signals reflected from actual objects are the following:

- The carrier frequency (taking into account the doppler shift in it due to the motion of the object);
- The average power and the changes in it as a function of range, azimuth and elevation angle;
- The level of fluctuations in the power (or effective radar cross-section) and the spectral composition and probability distribution of the fluctuations;
- The pulse width and waveform;
- The polarization of the electromagnetic wave.

It is desirable that the signal reflected from an artificial reflector (especially if this reflector is used as a distracting decoy) be identical to the return from the camouflaged target with respect to the majority of the parameters enumerated above.



FOR OFFICIAL USE ONLY

The following kinds of artificial radar reflectors will be treated in this chapter: dipole and corner reflectors; Luneberg lenses and variants of them; antenna arrays (Van-Atta arrays); guided decoys (both passive and with an active response).

## 2. Dipole Reflectors

Dipole reflectors (dipoles) are one of the most widespread means of producing camouflage jamming. They can also be used to produce individual decoy targets (in the form of compact clouds) for the purpose of disrupting the operation of automatic target tracking systems of radars or homing warheads.

Dipole reflectors take the form of half-wave passive antennas tuned to the working wavelength of the radar being suppressed. If such a dipole falls in the transmission region of a radar, the frequency of which matches the resonant frequency of the dipole, intense oscillations are excited in it and it becomes an electromagnetic energy radiator.

To obtain the resonance conditions, the length of a dipole  $l$  is chosen somewhat less than half of the radar wavelengths.

The shortening factor for the dipole is equal to:

$$y = 2l/\lambda.$$

Strips of metallized paper or foil (for meter wavelengths) or a metallized neutral fiber or glass fiber (for centimeter wavelengths) are used as such reflectors.

The dipoles scattered in the air produce a secondary emission field, a portion of the energy of which gets to the input of the radar receiver, and an intense return will be observed on its displays, which is reminiscent of noise interference in terms of its structure.

Besides producing camouflage jamming, dipole reflectors are also used to create decoy radar targets which make it difficult to observe the situation on radar screens and which interfere with the operation of automatic fire control systems which receive information from target acquisition and indication radars.

The following conditions must be met to produce solid intense jamming with dipole reflectors, i.e., such interference that the camouflage target cannot be seen on the radar screen against such a background:

- 1) The intensity of the return from a dipole cloud should exceed the signal level from the camouflaged target;
- 2) The signal power from a dipole cloud should not be significantly less with a change in the carrier frequency of the suppressed radar;

## FOR OFFICIAL USE ONLY

- 3) Displays of the signals reflected from dipole clouds and from the camouflaged targets on radar screens should not be seen separately, but in the automatic output tracking devices, it should be impossible to segregate them.

The first condition will be met if the effective radar cross-section of a cloud of  $N$  dipoles,  $\sigma_N$ , enclosed in one reflecting volume, is equal to or greater than effective cross-section of the target being camouflaged,  $\sigma_t$ .

In order to determine the number of dipoles  $N$  necessary for camouflaging any target with an effective back-scatter cross-section  $\sigma_t$ , it is necessary to know the effective cross-section of one dipole,  $\sigma_d$ , and the cloud of dipole reflectors,  $\sigma_N$ .

The following factors have an impact on the value of the effective radar cross-section of a dipole:

- The orientation of the dipole relative to the direction of the incoming wave;
- The polarization of the incident electromagnetic wave;
- The radar carrier frequency;
- The dipole dimensions.

It is well known that the effective radar cross-section of a single half-wave dipole varies in accordance with the law:

$$\sigma_d = 0.86\lambda^2 \cos^4 \theta,$$

where  $\theta$  is the angle between a normal to the dipole and the direction to the radar.

If the dipole is arranged parallel to the electrical field intensity vector,  $\vec{E}_1$ , then the intensity of the reflected electromagnetic energy is maximal and the effective radar cross-section of the dipole is equal to:

$$\sigma_{d \max} = 0.86\lambda^2. \quad \sigma_d \max = 0.86\lambda^2.$$

When the dipole is oriented perpendicular to the vector  $\vec{E}_1$ , the value of  $\sigma_d$  tends to zero.

We shall determine the mean value of the effective radar cross-section of a dipole, when the probability is the same for any orientation of it in space. By employing the theorem of the mean from probability theory, we obtain the following expression for finding the average value of the effective radar cross-section of a dipole reflector:

$$\bar{\sigma}_d = \frac{1}{4\pi} \int_0^{2\pi} \int_0^\pi \sigma(\theta, \varphi) \sin \theta d\theta d\varphi. \quad (5.1)$$

FOR OFFICIAL USE ONLY

## FOR OFFICIAL USE ONLY

The angles  $\theta$  and  $\theta$  are shown in Figure 5.2.

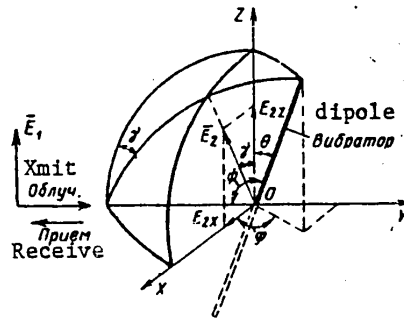


Figure 5.2. On the calculation of the reflection from an elementary dipole in the case of an arbitrary orientation of the dipole.

By substituting the value of  $\sigma(\theta, \phi)$  in expression (5.1), we obtain:

$$\bar{\sigma}_R = \frac{0.86\lambda^2}{4\pi} \int_{\varphi=0}^{2\pi} \int_{\theta=0}^{\pi} \cos^4 \theta \sin \theta d\theta d\varphi$$

or

$$\bar{\sigma}_R = 0.17\lambda^2.$$

If the electrical field intensity vector of the incident wave is oriented parallel to the Z axis, then the size of the electric field vector radiated by the dipole in the direction opposite to the incoming wave will be determined by the expression:

$$E_z = E_0 \cos \theta \sin \psi,$$

where  $E_0$  is the maximum value of the electrical field intensity  $E_2$  (in the equatorial plane when the vector  $\bar{E}_1$  is oriented parallel to the axis of the dipole);  $\psi$  is the angle between the dipole and the direction in which the reflected field is observed.

The components of the vector  $\bar{E}_2$  in line with the OZ and OX axes will be equal to the following respectively:

$$E_{2z} = E_0 \cos \gamma,$$

$$E_{2x} = E_0 \sin \gamma,$$

But

$$\cos \gamma = \frac{\cos \theta}{\sin \psi}.$$

Then

$$E_{2z} = E_0 \cos \theta \sin \psi \cos \gamma = E_0 \cos^2 \theta;$$

$$E_{2x} = E_0 \cos \theta \sin \psi \sin \gamma = -\frac{1}{2} E_0 \sin 2\theta \cos \varphi.$$

## FOR OFFICIAL USE ONLY

## FOR OFFICIAL USE ONLY

Thus, the effective back-scatter cross-section of a half-wave dipole will depend on the plane of polarization of the radar receiving antenna. If the antenna receives the vector component of the reflected electrical field  $E_{2Z}$ , the polarization of which is the same as in the incident wave, then the effective cross-section of the reflector is:

$$\sigma_{dZ} = \sigma_{d \max} \cos^4 \theta.$$

In the case where the component  $E_{2X}$  is received, which is perpendicular to  $E_{2Z}$ , the effective radar cross-section of the reflector will be equal to:

$$\sigma_{dX} = \sigma_{d \max} \sin^2 2\theta \cos^2 \phi.$$

We shall determine the average effective back-scatter cross-section of a cloud of dipole reflectors. We shall assume that there are  $N$  randomly arranged reflectors in the radar return volume. The phase relationships between the intensities of the reflected fields of the individual dipoles, because of their random arrangement in space relative to each other and the direction to the radar, will also be random.

By employing the techniques of probability theory, it can be demonstrated with a random distribution of the phases of the electromagnetic waves reflected from the dipole reflectors, the most probable value of the resulting electrical field intensity  $E_{2N}$ , is equal to the mean geometric value of the field intensities produced by the pairs of reflectors, i.e.:

$$E_{2N} = \sqrt{\sum_{i=1}^N \sum_{k=1}^N E_i E_k}.$$

where  $E_i$  and  $E_k$  are the field intensities produced by individual reflectors.

Assuming that  $E_i = E_k = E_{2d}$ , where  $E_{2d}$  is the intensity of the reflected electric field of a single dipole, we obtain:

$$E_{2N} = E_{2d} \sqrt{N};$$

and the average effective radar cross-section of the "cloud" of dipoles we be equal to:

$$\bar{\sigma}_N = \bar{\sigma}_d N = 0.17 \lambda^2 N. \quad (5.2)$$

It can be seen from formula (5.2) that with a decrease in the wavelength, the effective radar cross-section of a single dipole falls off sharply, and for this reason, a larger number of dipoles is needed to obtain a specified effective radar cross-section of a "cloud".

FOR OFFICIAL USE ONLY

## FOR OFFICIAL USE ONLY

The number of dipole reflectors,  $N$ , needed to simulate a target, can be determined by knowing the average values of the effective cross-section of the target,  $\sigma_t$ , and a single reflector  $\sigma_d$ :

$$N = \frac{\sigma_t}{\alpha \sigma_d},$$

where  $\alpha$  is a factor which takes into account the number of effective dipoles.

Since when dipoles are dumped from an aircraft, some of them are broken, deformed or tangled in clumps with the action of the opposing wind flow, the value of the coefficient  $\alpha$  is chosen in a range of from 0.1 to 0.3. When designing the dipoles, an effort is made to obtain as large number of effective reflectors as possible and the highest rate of their dispersal with minimum weight, volume and material consumption per unit of back-scattering surface. The effective radar cross-section of a dipole cloud,  $\sigma_N$ , is shown in Figure 5.3 as a function of the time which has passed since the moment they were jettisoned. A rise in the effective radar cross-section was observed in the first three to four minutes. Over this time, the dipoles fly apart and form the cloud. The cloud was produced at an altitude of 3,000 m by ejecting a packet of dipoles from the aircraft. The observation was made using a radar at a wavelength of  $\lambda = 9.2$  cm [8].

Figure 5.3. The influence of the number of dipoles in a cloud on the value of its effective radar cross-section.



- Key: 1. Number of dipoles (strips) in the packet is  $N = 3.75 \cdot 10^6$ , horizontal polarization of the receiving antenna;  
 2. Number of dipoles in the packet is  $N = 0.625 \cdot 10^6$ , vertical polarization.  
 A. Effective back-scatter cross-section,  $m^2$ ;  
 B. Time from the moment the packets of chaff are jettisoned, minutes.

As was stated above, the resulting signal reflected from the dipole cloud takes the form of the sum of signals which are random in phase and amplitude from a large number of reflectors. Therefore, the amplitude of the resulting signal from one repetition period of the radar probe pulse to the next does not remain constant, but changes with time in a random manner.

FOR OFFICIAL USE ONLY

## FOR OFFICIAL USE ONLY

An experimental study of returns from a cloud of dipole reflectors showed that the spectral width of the amplitude fluctuations in the reflected signal is governed by the rate of motion of the dipole relative to each other and relative to the radar station, as well as by the wavelength of the transmitting radar.

It can be assumed with sufficient precision that the distribution of the dipole velocity and the spectrum of the returns from them obey a Gaussian law. For this reason, the spectral width of the returns from the dipoles is

$$\delta f_{0.5} = 5(v_d/\lambda),$$

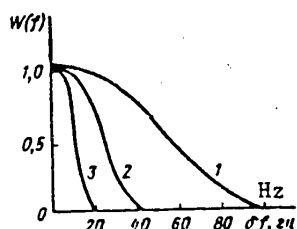
where  $\delta f_{0.5}$  is the half-power spectral width, in Hz;

$v_d$  is the average rate of dipole travel, cm/sec;

$\lambda$  is the radar wavelength in cm.

The width of the fluctuation spectra can range from tens to several hundreds of hertz. For example, it is 10 to 40 Hz at a frequency of 3,260 MHz (Figure 5.4).

Figure 5.4. Spectra of the return from dipole chaff in the centimeter band ( $f = 3,260$  MHz).



- Key; 1. When the dipoles are dumped from an aircraft and when the wind speed is up to 40 km/hr;  
 2. When the dipoles are dumped from an aircraft and the wind speed is about 16 km/hr;  
 3. When the dipoles are dumped from a slowly moving dirigible.

Usually, glass fiber or metallized strip dipoles are packaged in a packet in such a number that each packet simulates the actual target in terms of its reflective properties. To produce jamming interference for radars operating at meter wavelengths, it is sufficient to have a few tens of metallized strips in a packet. For counter measures against centimeter band radar, the number of dipoles in a packet runs up to tens of thousands.

When camouflaging a certain space, such a number of reflectors should be ejected into each reflecting volume that their total average effective radar cross-section is equal to or greater than the total effective cross-section of the targets being camouflaged which are located within this volume.

In this case, with any position of the radar antenna within the bounds of the selected zone, the returns from the dipoles in one reflecting volume will be

## FOR OFFICIAL USE ONLY

observed on the display screen to merge with the returns from dipoles in adjacent reflecting volumes.

The number of dipole packets,  $n$ , which must be dumped into each reflecting volume to effectively camouflage the targets being protected, can be determined from the formula:

$$n = (\bar{\sigma}_t m / \bar{\sigma}_N) \eta$$

where  $\bar{\sigma}_N$  is the average effective back-scatter cross-section of a dipole packet cloud;

$\bar{\sigma}_t$  is the effective radar cross-section of the target being camouflaged;

$m$  is the number of targets falling within the reflecting volume which are being camouflaged;

$\eta$  is a safety factor which takes into account the fact that not all of packets dumped from the jamming vehicle will open up.

The timewise interval for dumping  $n$  packets of  $N$  reflectors to produce a solid jamming field on the screen of a radar display depends on the resolving volume of the radar,  $V_p$ , which is governed by the range resolution of the radar,  $\Delta R$ , and the angular coordinates ( $\Delta\phi$ ,  $\Delta\epsilon$ ). The greater the resolving volume, i.e., the worse the radar resolution, the smaller the number of dipole packets which are needed to suppress the radar.

Packets of reflectors which form discrete compact clouds of dipoles are thrown from the jamming delivery vehicle (or from the object being camouflaged) to produce the false radar returns.

One of the major drawbacks to dipole reflectors as a means of antiradar camouflage consists in the comparatively small time they act on the radars being suppressed. This time depends on the ejection altitude of the dipoles, their rate of descent (approximately 40 to 50 m/min), as well as on the wind speed and can reach several tens of minutes, being considerably reduced in rain or snow.

The cloud formed by dipole reflectors of the same length produces a masking effect in a narrow range of frequencies: the bandwidth does not exceed 5 to 10 percent of the center frequency. The bandwidth can be extended by increasing the length and width of the dipoles or by putting together packets of strips of different lengths. Naturally, the material consumption increases in this case and the reflector production technology becomes more complicated.

Dipole reflectors were used for the first time as a means of antiradar camouflage by English air forces during an attack on Hamburg in July of 1943, and were widely used thereafter by the belligerents during the course of the Second World War. Dipole reflectors were manufactured from foil or metallized paper.

## FOR OFFICIAL USE ONLY

FOR OFFICIAL USE ONLY

The English and American air forces dropped more than 20,000 tons of aluminum foil over German territory during the war. The Germans themselves acknowledged that as a result of the comprehensive use of active jamming and dipole reflectors by the allies, the effectiveness of German air defense was reduced by 75 percent. According to data on the foreign press, the use of such techniques made it possible to save about 450 aircraft and spare the lives of 4,500 flight crew members from just the American Airforces operating in England.

In addition to half-wave dipoles, long metallized strips (up to 120 meters long) were also used, which were dropped from aircraft on special parachutes. During the Second World War, packets of dipoles or long metallized strips were thrown out manually by crew members. However, a special automatic device was designed as early as the end of the war. Then shells, mortars and rockets filled with dipole reflectors were used for the first time. Such 82.5 mm caliber rockets were used, in particular, from launch positions on allied ships during the invasion landing in Normandy in 1944. Some 76,800 metallized strips from 12.7 to 406 mm long were placed in the warhead of a rocket, the jettisoning of which jammed radars operating in a wide range of frequencies.

Dipole reflectors remain an extremely effective means of antiradar camouflage at the present time for air and sea military objects. Work is underway abroad on increasing the effective cross-section of dipoles, extending the frequency range and improving their mechanical characteristics. Foreign specialists are devoting considerable attention to the development of equipment for automatically dumping packets of dipoles from an aircraft. Such devices are usually installed in an external container or inside the aircraft in the tail compartment. The automatic devices are remote control. The rate at which the packets are dumped is set beforehand, but it can be changed during the flight by the pilot.

Modern jet aircraft are much faster than the aircraft of the Second World War period, and for this reason, they cover a distance greater than the size of the resolution volume during the time of dipole packet dispersal. In other words, the camouflaging aircraft, which dumps the dipoles, travels at a high velocity and does not conceal itself. In order to eliminate this deficiency, special aircraft rockets have been developed at the present time which make it possible to eject reflectors in front, behind, up, down and to the side.

A small aviation rocket has been developed in the U.S. which is equipped with a device for producing false radar targets by means of scattering dipole reflectors over a specified distance. The device is placed in the nose cone of the rocket. It consists of a tank with compressed gas, a firing pin with a trigger mechanism intended for destroying the tank and a device which automatically separates the nose cone of the rocket with the charge of dipoles from the rocket motor. The replacement of the explosive charge usually employed to scatter dipoles by a tank of compressed gas makes it possible to produce a false radar target with a more uniform distribution of the dipoles, and moreover, provides for safety when shipping, storing and using such rockets in practice.



## FOR OFFICIAL USE ONLY

American specialists have proposed a device for scattering dipole reflectors from ballistic missiles. A container with the dipoles and a special mechanism are mounted in the nose cone of the missile. The device is actuated by a clock mechanism after a certain time interval following launch. The explosion of the detonator following the actuation of the device releases a spring and opens the walls of the container with the dipoles. The clock mechanism begins to operate at the moment the missile is launched. Special camouflage rockets, mortar projectiles and shells are being developed which can be launched from shipboard and ground installations. Thus, a special artillery shell for placing false targets of dipoles has been constructed in France. It is proposed that the shell be used to confuse radars which determine the coordinates of artillery and mortar batteries based on the trajectory of shells or mortar projectiles.

An original technique of launching dipole reflectors from a moving ship has been patented in the U.S. It is proposed that an additional mast and air blast blower with a pipe fastened to this mast be installed on the ship. The dipoles which are blown out form a cloud over the sea surface. It has been experimentally established that dipoles scattered in the air provide greater returns than when floating on the water. Calculations show that it is necessary to immediately throw out a large number of dipoles, approximately  $6 \cdot 10^7$  with an overall weight of about 1 kg to provide effective camouflage in the 3 and 10 cm bands for 1 mile of travel (1.85 km).

### 3. Corner Reflectors

A corner reflector takes the form of a structure of two or three mutually perpendicular conducting planes (sides). A valuable property of corner reflectors is their capability of reflecting a considerable portion of the energy falling within the bounds of the interior angle in a direction opposite to the irradiation. It is as if the corner is a mirror, the plane of which is always perpendicular to the direction of irradiation. Because of this property, corner reflectors have large effective radar cross-sections, even in the case where they are small, something which makes it possible to use them to simulate various targets.

Corner reflectors are used to create individual or group decoy targets, to increase the effective radar cross-sections of various objects (beacons, buoys, spar buoys, small ships, targets, etc.), reduce the contrast of the radar image of industrial and military installations down to the level of their surrounding background as well as to distort the shore outlines of bodies of water.

The problem of electromagnetic energy scattering by corner reflectors was solved by A.N. Shchukin. Despite the assumptions made in this case which simplify the solution of the problem, the design formulas which were derived are in good agreement with experimental data [6].

We shall analyze the physical phenomena which are the basis for the engineering design of reflectors with the example of the simplest (dihedral) corner reflector.

FOR OFFICIAL USE ONLY

## FOR OFFICIAL USE ONLY

We shall assume that the direction of propagation,  $M$ , of the incident electromagnetic wave is perpendicular to the edge of the reflector and forms an angle  $\phi$  with a normal to the horizontal plane of the reflector (Figure 5.5).

At the internal faces of the corner, which are sufficiently distant from the edges, the incident wave excites a surface current density of:

$$\vec{j} \approx \frac{c}{2\pi} [\vec{n} \vec{H}_i],$$

where  $c$  is the speed of light;

$[\vec{n} \vec{H}_i]$  is the vector product of the unit vector  $\vec{n}$ , normal to the plane of the side and the magnetic field intensity of the incident wave,  $H_i$ .

The elementary current moment of the incident wave is:

$$d(Ih)_i = j_i dS,$$

where  $dS$  is a surface element of a side.

The elementary current moment, in terms of its effect, is similar to an elementary dipole. The direction of the current moment  $D(Ih)_i$  is perpendicular to the plane containing  $\vec{n}$  and  $\vec{H}_i$  (Figure 5.5). The phase shift between the elementary moments  $d(Ih)$  is governed by their mutual positions on the sides of the corner and the direction of the incident wave. The surface currents excited in the side of a corner by an incident wave produced a secondary electromagnetic field which excites secondary surface currents in the adjacent side. The back-scattering caused by the secondary surface currents corresponds to the wave reflection from the corner which obeys the laws of optics; it has a considerable level for incident wave directions which fall in a range of  $\pm 45^\circ$  around the bisector of the interior angle of the reflector.

It is well known that the effect of a metal surface with a dipole arranged on it can be replaced by the action of a virtual mirror image. Then, for an actual elementary dipole  $d(Ih)_i$ , which is located on side  $S_1$  of the corner, one can construct its mirror image  $d(Ih)_r$  on face  $S_1$ . The phases of the elementary current moments  $d(Ih)_i$  and  $d(Ih)_r$  are identical or differ from each other by  $\pi$ , depending on whether the direction of the current moment  $d(Ih)_i$  is perpendicular to or parallel with edge  $AB$ . If the phase of the current moments flowing along the surface of edge  $AB$  is taken as the initial phase, then the phase of the current moment  $d(I, h)_r$  will be equal to:

$$\theta = \frac{2\pi}{\lambda} (ac_i) = \frac{2\pi}{\lambda} (ac),$$

where  $ac$  and  $a_1c_1$  are the distances from points  $a$  and  $a_1$  to the plane of the incident wave front of  $S_n$ , which passes through the corner reflector edge  $AB$ .

FOR OFFICIAL USE ONLY

## FOR OFFICIAL USE ONLY

The electromagnetic oscillations produced by currents  $d(Ih)_r$  in the case of omnidirectional propagation reach the planes parallel to the incident wave front, having equal phases. In particular, their phase in the  $S_n$  plane which runs through the corner reflector edge AB, is equal to zero. In reality, the oscillations reaching point a at face  $S_1$  lead the oscillations reaching point 0 by the following phase angle, where point 0 falls on edge AB:

$$\theta_1 = 2\pi/\lambda$$

The current moment  $d(Ih)$  at point a also has the same phase shift (lead). The oscillations excited by the current moment  $d(Ih)_r$ , reaching the  $S_n$  plane, phase lag the oscillations excited by the current moment at point 0 by an angle of:

$$\theta = \frac{2\pi}{\lambda} (a_1 c_1).$$

Thus, the phase of the oscillations excited by the current moment  $d(Ih)_r$ , when these oscillations reach the  $S_n$  plane, will be equal to zero, since:

$$\theta_r = \theta_1 - \theta = \frac{2\pi}{\lambda} (ac - a_1 c_1).$$

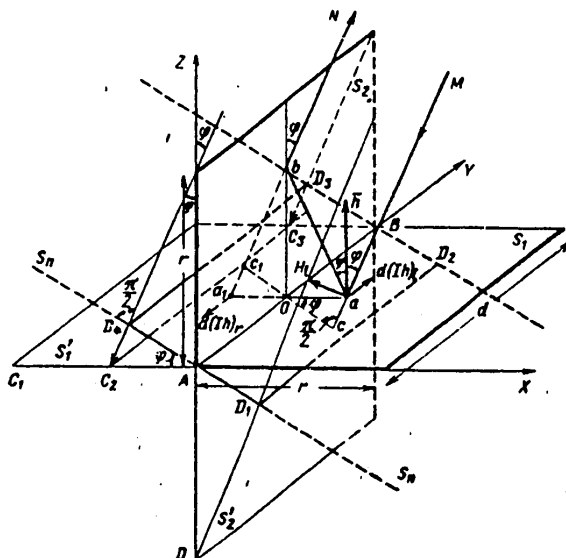
Consequently, the incident wave front is simultaneously the plane of the wave front scattered by the dihedral reflector and propagating in a direction opposite to the incident wave.

We shall determine the density of the energy flux reflected by the corner reflector in the direction of the transmitter. The wave incident to the corner reflector and perpendicular to its edge, and polarized so that the magnetic field intensity vector  $H_1$  falls in the propagation plane (Figure 5.5), excites a surface current density  $j_1$  having an amplitude equal to:

$$\begin{aligned} j_{11} = -j_{12} &= \frac{c}{2\pi} H_1 \cos \varphi \text{ в } \text{плоскости } S_1, \\ &\text{in face} \\ j_{13} = -j_{14} &= \frac{c}{2\pi} H_1 \sin \varphi \text{ в } \text{плоскости } S_2. \end{aligned}$$

The direction of these current planes is parallel to the edge AB of the corner reflector. For this reason, the back-scattering produced by the secondary currents  $j_r$  in the direction opposite to the irradiation can be treated as the radiation of two dipoles located in the  $S_1$  and  $S_2$  plane having current moments of  $Ih_{r1}$  and  $Ih_{r2}$ , which correspond to the scattering of all of the elementary dipoles  $d(Ih)_{r1} = j_{r1} dS_1^1$  and  $d(Ih)_{r2} = j_{r2} dS_2^1$ .

## FOR OFFICIAL USE ONLY



These current moments are equal to:

$$h_{r1} = -\frac{c}{2\pi} H_1 \int dS' \cos \varphi.$$

$$I h_{,2} = -\frac{c}{2\pi} H_2 \int dS'_2 \sin \varphi.$$

The secondary currents, the effect of which was replaced by the effect of a fictive mirror image, flow in faces  $S_1$  and  $S_2$ , and therefore the reflected waves are emitted from these sides. Because of this, only the action of those surface currents on face  $S_1'$  is taken into account, the radiation of which in a direction opposite to the incident wave passes "through" face  $S_2$ , i.e., the integration on face  $S_1'$  is carried out only within the limits of the area  $AC_2C_3B$ .

Thus,

$$I_{h,1} = -\frac{c}{2\pi} H_1 S_1 \lg \eta \cos \varphi =$$

$$= -\frac{c}{2\pi} H_1 S_1 \sin \varphi,$$

$$lh_{r2} = -\frac{c}{2\pi} H_2 S_2 \sin \varphi$$

or

$$lh_{r,z} = lh_{r,1} + lh_{r,2} = -\frac{c}{2\pi} H_d (S'_1 + S_2) \sin \varphi.$$

## FOR OFFICIAL USE ONLY

The latter expression shows that the back-scattering by a rectangular corner reflector in a direction opposite to the transmission can be replaced by back-scattering by a flat conducting plate,  $D_1$ ,  $D_2$ ,  $D_3$  and  $D_4$  (Figure 5.5), the area of which is equal to the projection of the faces of the corner reflector onto the plane of the incident wave. The substitution of an equivalent smooth plate lying in the incident wave plane for the dihedral corner reflector makes it possible to extremely simply calculate the effective radar cross-section of a dihedral corner reflector,  $\sigma$ , in any direction lying in a plane normal to an edge of the corner reflector:

$$\sigma = 4\pi \frac{S_{\Sigma}^2}{\lambda^4}.$$

The quantity  $S_{\Sigma}$  is the area of the equivalent plate and depends on the direction of the rays impinging on the face of the corner reflector. If the areas of the faces are the same,  $S_{\text{face}}$ , then:

$$S'_{\Sigma} = 2S_{\text{face}} \sin \psi \quad S'_{\Sigma} = 2S_{\text{face}} \sin \psi$$

and the effective radar cross-section of the corner reflector is:

$$\sigma = 16\pi \frac{S_{\text{face}}^2}{\lambda^4} \sin^4 \psi.$$

The resulting expression is correct for angles of  $\psi < 45^\circ$ ; when  $\psi > 45^\circ$ , the factor  $\sin \psi$  must be replaced by  $\cos \psi$ .

Strictly speaking, the methods of geometric optics can be used only in the case where the angle between the direction of the incident ray and the bisector of the angle between the faces does not exceed  $45^\circ$ . In the case of incidence angles close to a normal to one of the faces, it is necessary to take into account the diffraction pattern which coincides with the pattern of the plate forming the face.

A dihedral corner reflector yields the greatest return in the case where its faces make an angle of  $45^\circ$  with the direction to the transmitter. In this case,

$$S_e = S_{e \text{ max}} = \sqrt{2} S_{\text{face}}$$

and

$$\sigma_{\text{max}} = 8\pi (S_{\text{face}}^2 / \lambda^2).$$

The nature of the change in the effective radar cross-section of a dihedral reflector as a function of the angle between the direction of the incident beam and

## FOR OFFICIAL USE ONLY

## FOR OFFICIAL USE ONLY

the bisector of the angle between the sides is shown in Figure 5.6. The dashed line in the same figure also shows the change in the reflectivity of a smooth conducting plate with an area equal to  $S_e$ . The effective back-scattering surfaces of a dihedral reflector and a smooth conducting surface will be equal only when the incident angles are  $0^\circ$  and  $45^\circ$ .

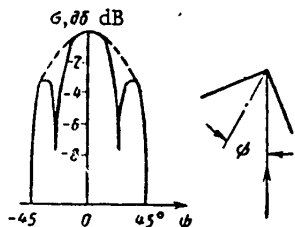


Figure 5.6. The effective radar cross-section of a dihedral corner reflector as a function of the angle between the incident beam and the bisector of the corner.

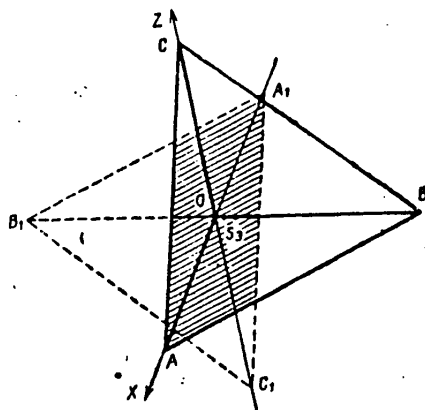


Figure 5.7. The equivalent smooth surface,  $S_e$ , of a trihedral corner reflector in a direction which forms the following angles with its faces:  $\alpha = 38^\circ 30'$ ,  $\beta = 72^\circ 30'$  and  $\gamma = 57^\circ 10'$  ( $S_e/S_{e \text{ max}} = 0.86$ ).

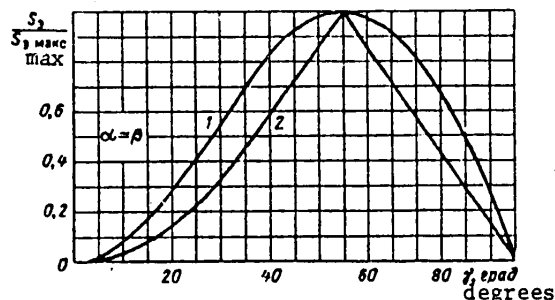


Figure 5.8. The curve for  $S_e/S_{e \text{ max}}$  of trihedral corner reflectors as a function of the direction of wave incidence.

Key: 1. Triangular sides;  
2. Square sides.

## FOR OFFICIAL USE ONLY

## FOR OFFICIAL USE ONLY

Dihedral corner reflectors find extremely little application in practice, since they scatter a considerable portion of the energy in the direction opposite to the transmission, where this transmitted radiation is in plane perpendicular to an edge. This deficiency of a dihedral corner has been eliminated by adding a third side, perpendicular to the two others.

The calculation of the effective radar cross-section of a trihedral corner reflector is carried out in a manner similar to the case considered above, i.e., by means of finding the area of the equivalent smooth surface  $S_a$ . The equivalent smooth surface is plotted in Figure 5.7 for a trihedral right-angled corner reflector.

For such reflectors, the maximum of the reflected energy falls in a direction which forms the following angles with its sides:  $\alpha = \beta = \gamma = 54^\circ 45'$ , i.e., when

$$\cos \alpha = \cos \beta = \cos \gamma = 1/\sqrt{3}.$$

For this direction, the equivalent smooth plate areas,  $S_{e \max}$ , are equal to:

$a^2/\sqrt{3}$  for a reflector with triangular sides, and

$a^2\sqrt{3}$  for a reflector with square sides, where  $a$  is the edge length of the trihedral reflector.

The relative value of  $S_e/S_{e \max}$  is plotted in the graph of Figure 5.8 as a function of the directions of the incident wave, which fall in a plane normal to one of the sides, when  $\alpha = \beta$ .

The maximum values of the effective radar cross-sections of trihedral corner reflectors are determined by the following formulas:

- 1) For reflectors with triangular sides:

$$\sigma = \frac{4}{3} \frac{\pi a^2}{\lambda^2};$$

- 2) For reflectors with sides in the form of right-angled sectors of a circle:

$$\sigma = \frac{16}{3} \frac{\pi a^2}{\lambda^2};$$

- 3) For reflectors with square sides:

$$\sigma = 12 \frac{\pi a^2}{\lambda^2}.$$

FOR OFFICIAL USE ONLY

## FOR OFFICIAL USE ONLY

Thus, the effective radar cross-sections of corner reflectors with triangular, circular and square sides, given the same edge length, are in a ratio of 1:4:9. These ratios, which are derived from the laws of geometric optics, will be correct only with the sufficiently large dimensions of the sides as compared to the wavelength.

Since the effective radar cross-section of a corner reflector is proportional to  $a^4$ , the detection range of such reflectors by radars will be proportional to the linear dimensions of the corner edge for the case of free space. In other words, a corner reflector with an edge length of  $a = 2$  m will be detected by an aircraft radar at twice the detection range of a corner reflector with an edge length of 1 m. It can be seen from the formulas cited above that corner reflectors can be used effectively on in the centimeter and millimeter bands.

The effective radar cross-section of a corner reflector with square sides is nine times greater than that of a reflector with triangular sides, given the same size of a side  $a$ , although the only half as much metal is needed for the fabrication of a reflector with triangular sides. However, the reflector with triangular sides has a wider directional pattern for the secondary emission, and moreover, its construction is sturdier.

The major characteristic of a corner reflector is the dependence of the effective radar cross-section on the direction of the incoming incident wave. Experimental data show that when the irradiation angle changes by  $\pm(20$  to  $30)$  degrees with respect to the optimal, the effective radar cross-section of a corner reflector falls off by 8 to 10 dB. Compensated corner reflectors are used to produce a more uniform directional pattern (Figure 5.9a). When the angles  $\phi$  and  $\theta$  between the incident ray and the bisector of the corner angle exceeds 30 degrees, electromagnetic waves start to be reflected from the additional compensating reflectors also. It can be seen from the graphs shown in Figure 5.9b that the use of additional reflectors substantially increases the level of the reflected power. The ratio of the dimensions  $b/a$  governs the degree of compensation. The optimum ratio is  $b/a = 1$ . If the quantity  $b$  is high, then so-called overcompensation begins and there is a trough in the center of the reflector back-scatter pattern.

Corner reflectors are frequently set up on the surface of the ground or water. In this case, it is necessary to take into account the influence of the separation surface on the back-scatter pattern of a corner reflector in the vertical plane, which takes on a multiple lobe character. For better observability of such a reflector, it is necessary to incline it in the vertical plane. The inclination angle is chosen depending on the direction in which it is necessary to have the maximum reflected energy. Thus, for example, this angle is 35 degrees for ship radars. The inclination angle must be chosen in a similar manner to produce the maximum return for aircraft radars located at a great distance from the corner reflector.

Special structures of several corners are used to provide an intense return in all directions from a false target made of corner reflectors.



## FOR OFFICIAL USE ONLY

A widespread design is the so-called octahedral group. It can be put together from three flat metal sheets, arranged so that they form eight trihedral corner reflectors. Depending on the position of such a group relative to the transmitter, various reflection patterns are obtained (Figures 5.10 and 5.11).

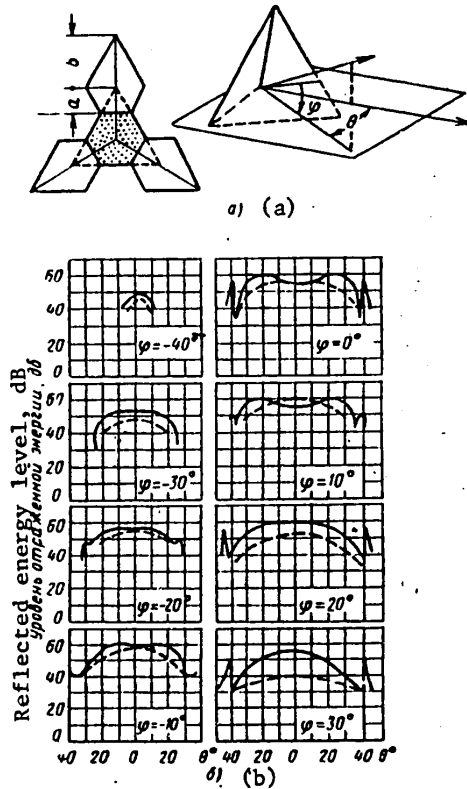


Figure 5.9. A trihedral corner reflector with supplemental corners (a) and the return patterns (b). The solid lines in the graph apply to a reflector with supplemental compensating corners; the dashed lines apply to a reflector without the compensating corners.

A more uniform reflection pattern can be obtained in the horizontal plane by means of a group of five trihedral corner reflectors, arranged in a circle (Figure 5.12). In the group of five reflectors, all of the axes of symmetry are arranged in one horizontal plane, and for this reason, the effective radar cross-section of such a

## FOR OFFICIAL USE ONLY

## FOR OFFICIAL USE ONLY

group is approximately twice that of an octahedral group and the main lobes of the reflection pattern are of greater width.

It is impossible in practice to obtain an omnidirectional return pattern from a stationary structure of corner reflectors which would not have numerous maxima and minima because of interference. For this reason, structures made of a group of corner reflectors are employed, which rotate in the azimuthal plane. The cut-up nature of the return pattern is smoothed out considerably in this case (Figure 5.13). The number of revolutions of such a structure depends on the type of oscillations generated by the radar transmitter. In the case of CW radar, a few revolutions per minute are sufficient. In the case of pulsed operation, the number of r.p.m. of the reflector should be 25 to 50 percent of the pulse repetition rate [37].

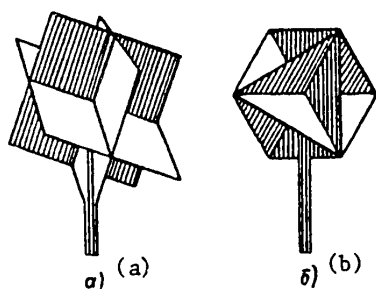


Figure 5.10. Group reflectors.

Key: a. Made of cells with square sides;  
b. Made of cells with triangular sides.

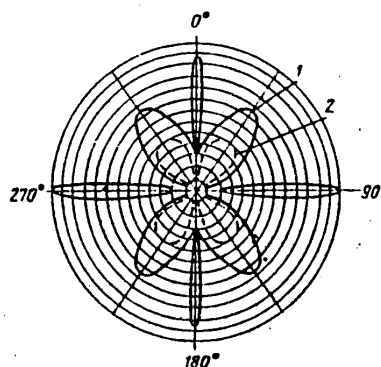


Figure 5.11. Patterns of the returns from the group reflectors depicted in Figure 5.10.

Key: 1. With square sides;  
2. With triangular sides.

One of the major requirements in the fabrication of corner reflectors is the precise observance of the perpendicularity of the sides. Even a slight deviation of the angle between them from 90 degrees can produce interference phenomenon which significantly reduce the size of the effective back-scatter cross-section. The reduction in the effective cross-section with a deviation in the interior angles of the corner reflector from right angles is explained by the disruption of the in-phase nature of the field in the aperture of the reflector because of the difference in the travel of the rays. The relative effective radar cross-section of a corner reflector with triangular sides is shown in Figure 5.14 as a function of the precision of its fabrication. The greater the linear dimensions of the sides, the more precisely the angle of 90 degrees between them should be maintained (Figure 5.14). This is one of the drawbacks to corner reflectors. The effective

## FOR OFFICIAL USE ONLY

FOR OFFICIAL USE ONLY

radar cross-section of a corner reflector increases with increasing size of its sides,  $a$ , given a definite error in the manufacture,  $\Delta$ , and a constant wavelength,  $\lambda$ .

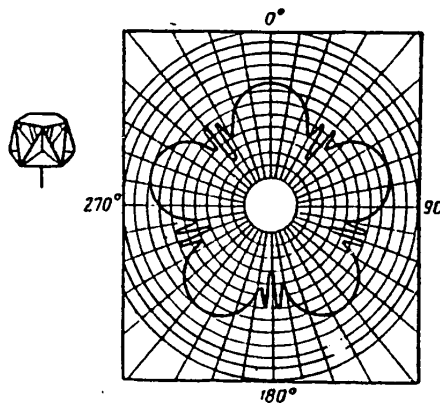


Figure 5.12. Pattern of the return in a horizontal plane from a five cell corner reflector.

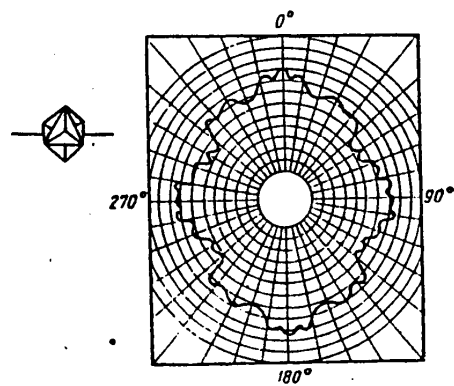


Figure 5.13. The pattern of the return from a five cell corner reflector when it continuously rotates in the azimuthal plane.

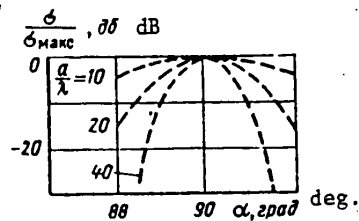


Figure 5.14. The effective radar cross-section of a trihedral corner reflector as a function of the angle between the sides for various ratios of the edge length to the wavelength.

It can be seen from the curve shown in Figure 5.15 that there is a limit beyond which it is not expedient to increase the dimensions of a corner reflector for a given fabrication precision  $\Delta$ . For example, with an error of  $\Delta = 0.5$  degrees ( $\alpha = 89.5$  degrees), the ultimate length of a rib amounts to  $a_{\max} = 60\lambda$ .

For corner reflectors with large dimensions of the sides, the deviation of the angle between them from 90 degrees should not exceed  $\Delta = 0.5$  degrees - 1 degree.

FOR OFFICIAL USE ONLY

FOR OFFICIAL USE ONLY

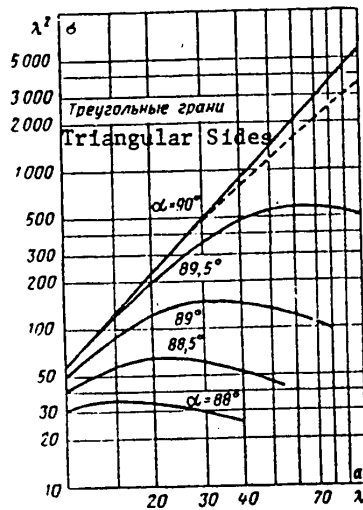


Figure 5.15. The relationship between the precision in the fabrication of a corner reflector and the dimensions of the sides.

In a trihedral corner reflector, the incident wave is reflected from the three planes, each of which changes the direction of rotation of wave polarization to the opposite direction. If the radar antenna is circularly polarized with a right-rotation, then because of the odd number of reflections from the faces of the corner reflector, the reflected field will have a left circular plane of polarization, and consequently, the radar will not detect such a target. Various steps are taken to eliminate this phenomenon, which reduced to the fact that the property of a so-called asymmetrical target is imparted to the corner reflector.

The simplest way of designing a corner reflector for circularly or elliptically polarized radars consists in placing a dielectric plate in front of one of the sides of the reflector a slight distance from it, as shown in Figure 5.16. Because of this plate, the phase difference between the horizontally and vertically polarized components, the wave energy reflected from the inside plate is not 90 degrees, but falls between 0 and 180 degrees. As a result of the addition of this wave to the component of the field reflected at the same point in time from the outer

surface of the plate, elliptical polarization of the wave occurs, which can be broken down into two waves with circular polarization in different directions and different amplitudes. The thickness of the plate and the spacing from the metal side is determined experimentally.

A widespread type of reflectors for radars with circular polarization is a corner reflector, in the aperture of which an array of parallel wires is placed. This reflector will be a wideband one for circularly polarized waves. It has the same return pattern as the conventional trihedral reflector, however, its effective radar cross-section is 6 dB less. Moreover, such a reflector back-scatters a field with linear polarization just a corner reflector does only in the case where the polarization plane of the incident wave is at an angle to the elements of the array. However, if the electrical field vector lines up with the direction of the wires, then the reflector will behave as a flat plate having an area equal to the aperture of the corner reflector. This drawback can be eliminated if the wire arrays are not placed in the aperture of the reflector, but rather in front of its sides at a spacing of  $\lambda/8$  from them. When both linear components of a circularly polarized wave, which are shifted relative to each other in time and space by 90 degrees are reflected from one of the sides with such an array, they receive an additional 90 degree shift, because of which a linearly polarized wave appears.

FOR OFFICIAL USE ONLY

## FOR OFFICIAL USE ONLY

It can be broken down into two waves with circular polarization in opposite directions, of which only one will produce a pip on a radar screen. In contrast to a reflector with an array in the aperture, this structural design is a narrow-band one, i.e., it operates only in a definite range of frequencies.

A variant of the corner reflector is the biconical reflector (Figure 5.17). It has a uniform circular secondary emission pattern in the horizontal plane. The effective radar cross-section of such a reflector when the polarization plane of the field is parallel to the axis is the same as for a cylinder of radius:

$$r_{\text{avg}} = (1/2)(r_{\text{max}} + r_{\text{min}})$$

and having a height  $h$ , i.e.:

$$\sigma = 2\pi r_{\text{avg}}^2 h^2 / \lambda^2.$$

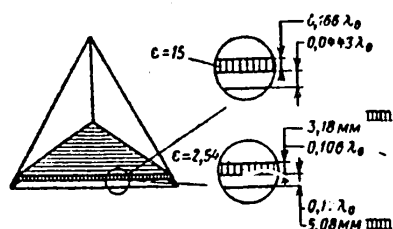


Figure 5.16. A corner reflector for radars using circular polarization.

The fabrication of such reflectors with the requisite precision is quite difficult, and for this reason they have not yet found mass application.

We shall now touch upon some questions of the use of corner reflectors for the purposes of antiradar camouflage.

As is well known, when scanning the ground or sea surface, the intensity of radar returns is governed by the distributed targets which have significantly different reflective properties. Modern aircraft radars make it possible to discriminate the outlines of cities, large industrial enterprises, railroad centers, contrasting objects (with respect to the intensity of the radar return) (rivers outlining cities, bridges, dams, etc.), as well as individual and group targets. Using corner reflectors, one can distort the image of such objects by means of changing the reflective properties of individual sections of the ground or water surface.

The major goal which is pursued in this case is a reduction of the radar contrast of the camouflaged objects down to the level of the background surrounding them by virtue of increasing the effective radar cross-sections of individual portions of the surface, where such objects are located. Since irradiating a certain

FOR OFFICIAL USE ONLY

## FOR OFFICIAL USE ONLY

section of a ground or water surface can be accomplished from any direction, it is essential for effective camouflage that the intensity of the additionally produced return is practically independent of the irradiation angles in the horizontal and vertical plane. This can be accomplished to some extent through the use of group corner reflectors, the structural design of which was treated above. Since the reflectivity of a portion of a water or ground surface is governed by the effective radar cross-section of the resolving area,  $\sigma_f$ , then for successful camouflaging of an object using corner reflectors, it is necessary to meet the condition  $\sigma_t \leq \sigma_f$ .

It is apparent that depending on the dimensions and configuration of the section being camouflaged and its reflecting properties, a various number of corner reflectors can be set up per unit area with a definite arrangement and dimensions of them.

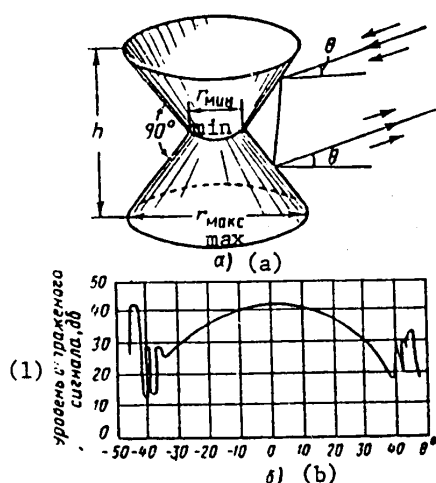


Figure 5.17. The structural configuration (a) and pattern of the returns (b) of a biconical reflector ( $r_{\min} = 5$  cm,  $r_{\max} = 43$  cm).

Key: 1. Reflected signal level, dB.

To produce decoy targets, the number of corner reflectors and their dimensions must be chosen so that the total effective radar cross-section is equal to the cross-section of the actual target. The spacings between the reflectors are chosen equal to or somewhat less than the resolving power of the radar.

Corner reflectors found widescale practical application for the first time during the Second World War. Thus, German submarines, in evading pursuit when running deep, using them to distract antisubmarine ships and aircraft in a false direction. The reflectors were thrown out in special buoys or were suspended from an air balloon.

In order to confuse the enemy about the true number of large submarines, as well as to disorient him relative to the direction of the main thrust, corner reflectors were installed on ships, launches or towed ships. Such

a method was used, for example, to disorient the enemy radar and distract the German attack aircraft from the main assault landing forces during the landing of the Allies in Europe at the end of the Second World War. Groups of small ships approached the French coast in the region of Boulogne from points which were widely separated from each other. The ships towed aerostats painted with aluminum paint and carried corner reflectors on themselves which simulate the returns from large battle and landing ships. Small groups of aircraft dumping packets of dipole reflectors and actively jamming German radars continuously flew over these ships. The demonstration continued for about four hours and the impression was created among the Germans that a large number of sea and air forces were approaching the

FOR OFFICIAL USE ONLY

egion of Boulogne. Trusting the reality of the decoy measures, the Germans sent their main forces to this region.

During the air attacks of the English and American bomber forces on Berlin, the numerous canals and lakes in the features of the city served as good landmarks during the bombing. To reduce the effectiveness of bombing strikes on the capitol, the Germans set up a large number of floating corner reflectors on the surface of the lake. They were constructed from two vertical, mutually perpendicular metal planes, installed on a floating wooden cross. The water surface served as the third reflecting plane. The reflectors were placed on anchors at spacings of 100 to 150 m. In the majority of cases, the water surfaces were not completely camouflaged, but were used only as partial antiradar camouflage and to break the lakes up into sections.

Because of such camouflage measures, numerous night air attacks of the English and American air forces proved to be unsuccessful. There was an instance where about 100 four-motor aircraft dumped their load on an accumulation of 100 corner reflectors, set up on one of the Berlin lakes.

Similar measures were taken to protect locks and dams in the port cities of the North Sea. The main purpose of these measures was to smooth out the contrast between the shore installations and the water surfaces on the screens of the radars.

Corner reflectors of rather large size were used in individual cases. Thus, for example, to "balance out" the radar image of air fields located in the vicinity of Berlin, corner reflectors with sides of 10 x 10 m were set up against the background of the terrain and structures of the city. In order to reduce the wind loads, the reflecting planes of the corners were fabricated from wire netting.

By the end of the war, the Germans had simulated the city of Kuestrin with corner reflectors; two cities were observed at a spacing of 80 km from each other on the screens of aircraft radar, something which naturally disoriented the radar operators.

Corner reflectors were also used to camouflage comparatively small ground facilities. It was reported in the West German press that a decoy target consisting of 50 large corner reflectors fully proved itself in action where the decoy was located close to a powerful electric power station. During poor visibility, this decoy target attracted the attention of radar operators in the English and American air forces, which dropped bombs on it.

Despite the design of such new effective radar reflectors as Luneber lenses, passive arrays and others, corner reflectors still remain in the arsenal of antiradar camouflage tools. Their major advantage as compared to other similar devices is the structural simplicity. When designing corner reflectors, the following major requirements are placed on them:

- Low weight;
- A minimum of assembly components;

FOR OFFICIAL USE ONLY

## FOR OFFICIAL USE ONLY

- Simplicity of the fabrication technology;
- The capability of being transported over various distances.

## 4. Luneberg Lenses

A structure made of several corner reflectors, as was shown above, nonetheless leads to a nonuniform secondary emission pattern. Another drawback to such designs is the fact that their effective radar cross-section, averaged over all possible directions, falls about 7 dB below the maximum effective radar cross-section of a corner reflector. Ideal omnidirectional reflectors are metal spheres, however, their effective cross-section is quite small.

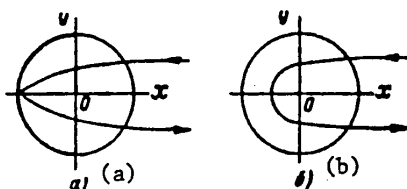


Figure 5.18. Trajectory of the rays in a Luneberg lens.

A quite effective, though still expensive reflector is the so-called Luneberg lens. Such a reflector makes it possible to obtain an effective radar cross-section pattern in a wider range of azimuths and elevation angles than any of the corner reflectors treated in the preceding section. The lens takes the form of a sphere made from a dielectric. One hemisphere of the sphere is metallized (Figure 5.18a). The dielectric permittivity  $\epsilon$  of the outer layer of such a reflector is close to the value of the dielectric permittivity of air and gradually increases with increasing thickness of the layer. Because of this, the lens focuses a parallel bundle of rays incident to it to a point on the metallized surface of the sphere and reflects this bundle in the opposite direction, parallel to the incident rays. When one hemisphere of the lens is metallized, it uniformly reflects the energy impinging on it within the limits of a spatial angle of 140 degrees.

The law governing the change in the dielectric permittivity  $\epsilon$  and the index of refraction  $n$  is determined by the following relationship:

$$\epsilon = n^2 = 2 - a^2,$$

where

$$a = r/r_0,$$

( $r_0$  is the radius of the sphere;  $r$  is the distance from the center of the sphere to the point on the sphere under consideration).

The effective back-scatter cross-section of a Luneberg lens is computed from the formula:



## FOR OFFICIAL USE ONLY

$$\sigma = \pi^3 d^4 / 4\lambda^2$$

where  $d$  is the lens diameter.

It has been reported in the press that a Luneberg lens mounted on a fighter increased the intensity of the radar return from it by a factor of 40 times.

It is possible in principle to design an omnidirectional lens reflector, the reflection factor of which is independent of the direction of the incident electromagnetic wave. If the incident ray, in bending inside the lens, approaches the OX axis at an angle of 90 degrees (Figure 5.18b), then by virtue of the spherical symmetry, it will be bent in the lower half of the lens through another 90 degrees and exit in parallel with the incident ray. In this case, there is no need of metallizing a portion of the sphere and we obtain a variant of the Luneberg lens, the so-called Eton Lippman reflector. There is yet another important difference between the Luneberg lens with a metallized shield and the omnidirectional reflector considered here. If they are both irradiated with a circularly polarized wave, then the former reflects the polarized wave with the opposite sign while the second reflects it with the same sign as the incident wave.

The law governing the change in  $\epsilon$  and  $n$  in such a reflector is determined by the expression:

$$\epsilon = n^2 = (2/a) - 1.$$

The index of refraction  $n$  in the center of the lens should tend to infinity, while at the exterior surface,  $n = 1$ .

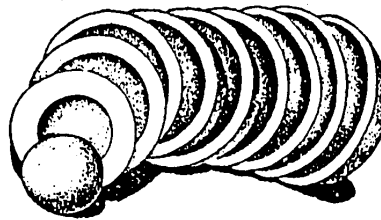


Figure 5.19. A Luneberg lens consisting of hemispherical shells, with discrete changes in the index of refraction.

It is very difficult in practice to realize a continuous change in the index of refraction from unity to infinity. Actual lens reflectors are composed of a large number of spherical shells, each of which has a constant index of refraction.

## FOR OFFICIAL USE ONLY

The discrete changes in the index of refraction approximate a continuous change in it. Thus, a practical problem in the fabrication of Luneberg lens type reflectors is the determination of the number of spherical shells and the amount of change in the dielectric permittivity in each of these shells.

Polystyrene foam, the index of refraction of which depends on its density, can serve as a material for the manufacture of such lenses.

A sample of a multilayer spherical Luneberg lens, manufactured in the U.S., is shown in Figure 5.19. The lens consists of concentric dielectric shells, arranged one inside the other. The dielectric permittivity of the individual shells varies in a range of 1.1 - 2, with increments of 0.1 each. The diameter of such a lens with a stepwise change in the index of refraction is about 46 cm, while the working frequency is in the 3 cm band.

A large number of the most diverse lens reflectors has been developed based on the Luneberg lens. Thus, a reflector which is omnidirectional in azimuth can be obtained by encircling a Luneberg sphere with a reflecting metal ring, as shown in Figure 5.20. The position of the ring relative to the equator of the sphere determines the position of the main lobe of the directional pattern with respect to the horizontal plane. If the ring is centered relative to the equator of the sphere, the maximum of the pattern falls in the horizontal plane; if the ring is shifted, the elevation angle will be greater. With an increase in the width of the ring, the width of the directional pattern in the elevation angle plane also increases, but in this case, the amplitude in the aperture of the reflector falls off.

The maximum value of the effective radar cross-section of such a reflector can be approximately determined from the expression:

$$\sigma_{\text{max}} = \frac{4\pi}{\lambda^2} (\pi r^2 - 2rL)^2,$$

where  $r$  is the radius of the sphere and

$L$  is the width of the ring.

A broad directional pattern in the vertical plane with a minimal reduction of the amplitude along the aperture can be obtained by means of so-called "helisphere", which is practically speaking, a modification of a reflecting shield, covering one of the hemispheres of a Luneberg lens. A helisphere can be obtained by replacing the solid metal ring with an array of parallel wires, wound at an angle of 45 degrees (Figure 5.21a, b).

If you look from the center of the sphere, the wires over the entire horizon will be arranged at an angle of 45 degrees. However, if you look at such a reflector from the outside, then behind the exterior surface wires, which are arranged at an angle of 45 degrees, there are the rear surface wires which are perpendicular to them and which have an inclination angle of 45 degrees to the horizontal. Thus, if a plane wave with polarization of 45 degrees reaches the front surface, passes through the wire grid without losses until it reaches the rear reflecting surface,

## FOR OFFICIAL USE ONLY

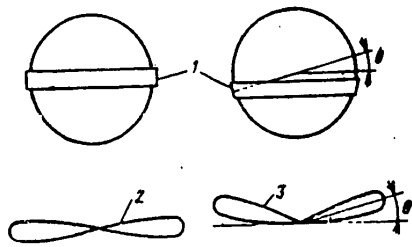


Figure 5.20. An omnidirectional Luneberg reflector (in the azimuthal plane) with a metallic ring.

Key: 1. Ring;  
2. Plane omnidirectional reflection pattern;  
3. Conical pattern.

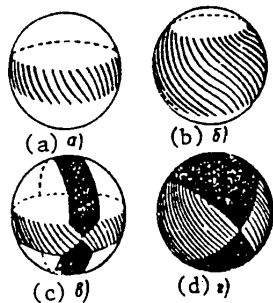


Figure 5.21. Various kinds of omnidirectional Luneberg lens reflectors.

and if the gaps between the wires of the "helisphere" has been chosen correctly, it is focused to a point located approximately half way on the radius of the sphere. The use of two orthogonal rings of wire arrays to obtain an isotropic pattern in the azimuth and elevation angle planes is shown in Figures 5.21c and d. The advantage of such reflectors is the fact that their effective radar cross-section remains approximately the same both for circular polarization and for horizontal or vertical polarization. The polarization losses with the double travel through the lens will amount to no more than 6 dB (as compared with 45 degrees polarization), and they can be compensated by a slight increase in the dimensions of the reflector.

At the present time, it is considered extremely expedient to use hollow spherical reflectors instead of heavy Luneberg lenses. In them, the dielectric sphere is replaced with a hollow helispherical array, within which a reflective metal ring is placed coaxially with the helisphere at a spacing equal to the focal distance, where this metal ring takes the form of a spherical segment having a diameter equal to approximately half of the diameter of the outer sphere (Figure 5.22).

The width of the reflecting ring,  $w$ , governs the width of the directional pattern of the reflector in the elevation plane. Consequently, when choosing the width of the ring, it is essential to achieve the optimal ratio between the width of the pattern in the elevation (vertical) plane and a permissible reduction in the amplitude over the aperture of the reflector.

The main requirements which the structural designs of hollow helispherical reflectors should meet are as follows: high fabrication precision for the spherical surface, high precision in the angular position of the array wires, minimal

## FOR OFFICIAL USE ONLY

## FOR OFFICIAL USE ONLY

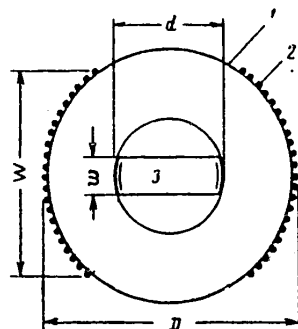


Figure 5.22. A hollow helisphere reflector.

- Key: 1. Hollow transparent sphere;  
 2. Array of parallel wires, wound at an angle of 45 degrees;  
 3. Metal ring with a diameter of  $d = 0.5D$ .

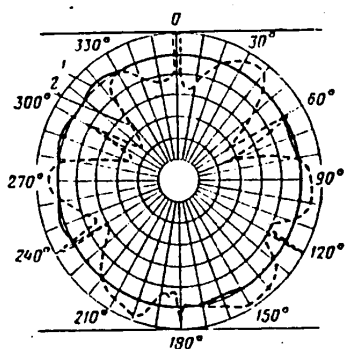


Figure 5.23. Patterns of the return in a horizontal plane from a hollow helisphere (1) and a corner reflector (2).

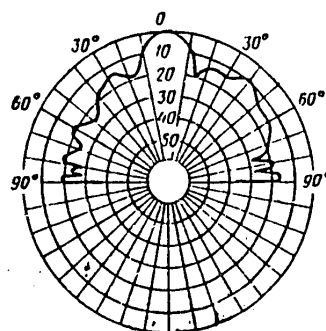


Figure 5.24. Diagram of the return in the vertical plane from a hollow helisphere.

dielectric losses, minimal internal impedance at microwave frequencies, high mechanical strength, low weight, low cost and stability with respect to climatic factors.

The reflection pattern of a hollow omnidirectional helispherical reflector with a diameter of 609 mm and a structure consisting of six corner reflectors, inscribed in a sphere with a diameter of 609 mm are shown in polar coordinates in Figure 5.23 for comparison. A grid of nichrome wires arranged parallel to each other with an angle of 45 degrees to the horizontal was used in the construction of the helispherical reflector. The wires were pressed into a fiberglass base; the spacing between the wires is 1.6 mm. The secondary emission pattern of the helisphere for a reflecting ring 76.2 mm wide is shown in Figure 5.24. It has been experimentally determined that the optimum diameter of the reflecting ring for the given helisphere should be 355.6 mm. The effective radar cross-section of the reflector when the ring diameter is reduced down to 304.8 mm is cut almost in half. The reflector weighs 3.175 kg. It can be seen from the graph of Figure 5.25 that the effective radar cross-section of a helisphere with a reflecting ring on the inside is

## FOR OFFICIAL USE ONLY

## FOR OFFICIAL USE ONLY

approximately 10 dB less than the effective cross-section of a Luneberg reflector with dimensions equal to it (curves 2 and 3). This is explained by the presence of spherical aberration in such reflectors in both the horizontal and vertical planes. Removal of the internal ring leads to an additional reduction in the effective radar cross-section by 5 dB.

Hollow helispheres, just as Luneberg lenses of various designs can find widescale applications as decoy targets for antiradar camouflage, primarily air and space objects. Such reflectors have also been proposed for installation on targets and on controlled decoy targets to increase their effective radar cross-sections.

## 5. Passive Antenna Arrays

A passive antenna array (a Van-Atta reflector) takes the form of a device consisting of several horizontal and vertical rows of half-wave dipoles, positioned in one plane at a spacing of  $\lambda/4$  from the reflecting screen (the reflector). A metal plate serves as the reflector. In this case, the dipole pairs which are arranged in mirror fashion relative to the center of the screen, are coupled together with coaxial cable sections.

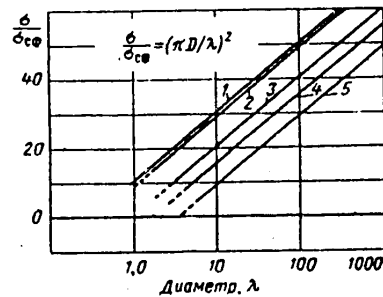


Figure 5.25. Values of the effective radar cross-sections of lens reflectors, referenced to the effective cross-section of a metal sphere of the same diameter.

- Key: 1. Circular disk;  
2. Luneberg reflector;  
3. Helisphere with a ring on the inside;  
4. Hollow helisphere (linear polarization);  
5. Hollow helisphere (circular polarization).

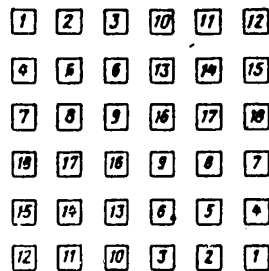


Figure 5.26. Schematic showing the connection of radiators in a plane antenna array.

The system used for connecting the 18 pairs of radiators by means of cable of the same length is shown in Figure 5.26. The coupled elements (indicated by identical numbers) are located in diagonally opposite quadrants of the plane of the array. When the electrical length of the lines connecting the radiators which are coupled in pairs is equal, the re-radiated wave front matches the incident wave front. In other words, the back-scattering of the electromagnetic energy by such a reflector occurs in the direction of the transmitting source.

## FOR OFFICIAL USE ONLY

Antenna arrays have the following major advantages over the reflectors treated earlier. 1) They have a wider return pattern as compared to corner reflectors. 2) They make it possible to modulate the reflected signal in accordance with any modulating law; 3) They can return the incident wave in directions other than the direction to the transmitter; 4) They provide for the selection of the requisite return polarization; 5) They make it possible to use signal amplifiers built into the connecting lines, by means of which one can obtain a significant boost in the effective radar cross-section of the reflector; 6) They open up the widescale possibility of fabricating high efficiency reflectors (false targets) using printed circuits and stripline technology.

The effective back-scatter cross-section of a passive plane antenna array is determined from the formula:

$$\sigma = \frac{G^2 \lambda^2}{4\pi},$$

where  $G = 4\pi S_e / \lambda^2$  is the directional gain of the array.

From this:

$$\sigma = S_e G,$$

where  $S_e$  is the effective geometric cross-section (aperture area) of the array.

The effective radar cross-section of an array composed of  $n$  half-wave dipoles, positioned at a spacing of  $\lambda/2$  from each other and at a distance of  $\lambda/4$  from the screen, is equal to:

$$\sigma = \frac{4\pi S_e^2}{\lambda^4} \left[ \sin \left( \frac{\pi}{2} \cos \theta \right) \right]^2,$$

where  $\theta$  is the angle of incidence; the factor  $\sin([\pi/2]\cos\theta)$  characterizes the dipole directional pattern in the plane of the magnetic field, taking the mirror image into account;  $S_e \approx n\lambda^2/4$  is the aperture area of the antenna.

The effective radar cross-section of an array will depend on the angle of incidence of the incoming electromagnetic wave, i.e., the back-scattering of a Van-Atta reflector is a of a directional nature. The return pattern of an antenna array of 16 coaxial dipoles in a plane perpendicular to the axes of the dipoles are shown in Figure 5.27. The return pattern of a flat screen is also shown for comparison in the same graph. The studies were carried out at a frequency of 2,850 MHz. It can be seen from the figure that in the case of normal incidence of the wave, the effective radar cross-section of the array is equal to the cross-section of a flat metal plate (shield) of the same size as the array, while in the case of incidence angles of  $\pm 35^\circ$  and  $\pm 55^\circ$ , it is 3 and 10 dB less than the maximum value. When a corner reflector is irradiated in a direction which deviates from the optimal by  $\pm 20$  to  $\pm 30$  degrees, its effective radar cross-section is reduced by 8 to

## FOR OFFICIAL USE ONLY

10 dB; the conclusion can be drawn from this that with identical maximum values of the effective radar cross-section, an antenna array has a wider return pattern than a corner reflector.

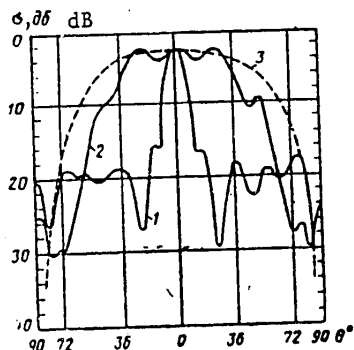


Figure 5.27. Pattern of the return of an antenna array of 16 dipoles in a plane perpendicular to their axis.

Key: 1. Metal plane;  
2. Antenna array (experimental data);  
3. Antenna array (calculated data).

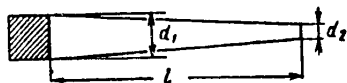


Figure 5.28. A dielectric rod reflector (the shaded portion is covered with conductive material).

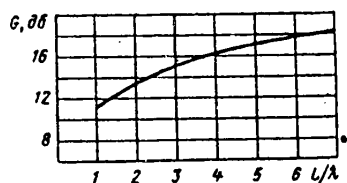


Figure 5.29. The gain of a dielectric antenna as a function of its length.

The major drawbacks to antenna arrays (as passive reflectors), composed of identical half-wave dipoles, is the narrow bandwidth and polarization selectivity. To eliminate these deficiencies, wideband radiators with circular polarization can be used as the radiating elements, for example, plane and conical spirals or dielectric rods.

Abroad it is recommended that dielectric rods be used as the main re-radiating elements of Van-Atta reflectors. Usually, a dielectric rod has a circular cross-section over its entire length, decreasing towards one of the ends. At the wide end of the rod, a volumetric resonator is created by means of coating the dielectric with a thin layer of copper. The length of the metallized portion is governed by structural design considerations.

The optimum values of the diameters of a cone shaped dielectric rod (Figure 5.28) depend on the radar wavelength as well as on the dielectric permittivity of the material from which the rod is fabricated:

## FOR OFFICIAL USE ONLY

## FOR OFFICIAL USE ONLY

$$d_1 = 0.564\lambda \sqrt{\epsilon - 1},$$

$$d_2 = \sqrt{0.4d_1}.$$

For a polystyrene rod ( $\epsilon = 2.55$ ), at a wavelength of  $\lambda = 3$  cm,  $d_1 = 12$  mm, while for the 6 cm band,  $d_1 = 25$  mm. When operating at comparatively low frequencies, it is expedient to use a material with a high dielectric permittivity, for example, low loss ceramics.

The effective radar cross-section of a dielectric rod is governed by the dielectric antenna gain,  $G$ , which is a function of the rod length:

$$\sigma = G^2 \lambda^2 / 4\pi.$$

The function  $G = f(l/\lambda)$  is plotted in Figure 5.29. Knowing  $G$  and the requisite value of the effective radar cross-section, the rod length  $l$  can be determined from this graph.

The effective bandwidth of a rod reflector is approximately  $\pm 15\%$  (with this frequency deviation from the center value, the effective radar cross-section of the reflector is cut in half).

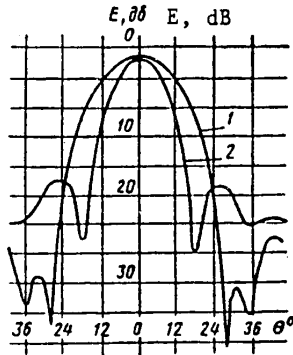


Figure 5.30. Patterns of the secondary emission of a dielectric rod (1) and an equivalent disk 63.5 mm in diameter (2) recorded in the 3 cm band.

It follows from a comparison of the results of measuring the effective back-scatter cross-sections of a dielectric rod with a gain of 16 dB and a flat disk equivalent to it (Figure 5.30), that the main lobe of the secondary emission pattern of the rod is considerably wider than that of the disk, and can be brought up to about 90 degrees, if the gain of the rod is substantially reduced. Naturally, by connecting several dielectric rods in an antenna array, a false target can be obtained using them which has a broad secondary emission pattern and a large effective radar cross-section.

An extremely simple two-element array can be obtained by means of connecting two U-shaped rods with a bracket. It has been demonstrated that the increase in the



## FOR OFFICIAL USE ONLY

intensity of the return and the width of the secondary emission directional pattern will depend on the spacing between the axes of rods. Thus, with a spacing between the rods of  $2.5\lambda$ , a return gain of 6 dB can be achieved above the gain of a single rod (with the identical directional pattern width).

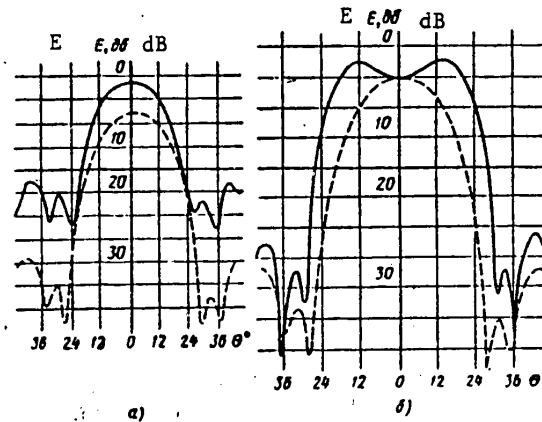


Figure 5.31. Secondary emission patterns for a U-shaped reflector with a spacing of  $2.5\lambda$  (a) and  $\lambda$  (b) between the axes of the rods; (the directional patterns of a single rod are shown with the dashed lines).

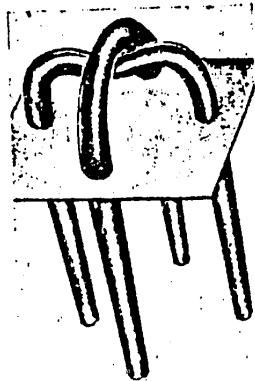


Figure 5.32. A four-element antenna array.

If the spacing between the rods is equal to the wavelength  $\lambda$ , then the advantage gained in the gain with respect to a single rod will amount to only 3 dB in all, but in this case, the width of the main lobe is almost doubled (Figure 5.31).

The combination of the two U-shaped sections, arranged at right angles to each other, takes the form of a four-element antenna array (Figure 5.32). For it, the intensity of the return increases by 12 dB as compared to the dual element array. Other combinations of U-shaped reflectors are possible which allow for even greater return intensity.

As studies have demonstrated, the reflective properties of a single dielectric rod are independent of the type of incident wave polarization. However, U-shaped reflectors provide for a maximum return only in the case where the polarization plane of the incident wave is normal to the plane of the bend of the reflector. If the polarization plane of the incident wave is parallel to the plane of the bend, then

FOR OFFICIAL USE ONLY

## FOR OFFICIAL USE ONLY

the effective radar cross-section is somewhat reduced, where the amount of this reduction depends on the spacing between the axes of the rods. With a spacing between the rods of  $2.5\lambda$ , this reduction is approximately 0.5 dB. Thus, when the reflector is irradiated with a circularly polarized wave, the reflected signal will be elliptically polarized and have the same direction as the incident wave.

Elementary reflectors (dipoles and rods) can be joined together not only in planar, but also in linear phased arrays in an appropriate manner.

The secondary emission pattern of a linear Van-Atta array of  $n$  radiators is determined by the expression:

$$F(\theta) = \left\{ \frac{\sin \left[ \frac{n\pi d}{\lambda} \left( \sin \theta + \frac{\phi}{2\pi d} \right) \right]}{\sin \left[ \frac{\pi d}{\lambda} \left( \sin \theta + \frac{\phi}{2\pi d} \right) \right]} \right\}^2,$$

where  $d$  is the spacing between the radiators;

$\phi$  is the phase shift between adjacent radiators.

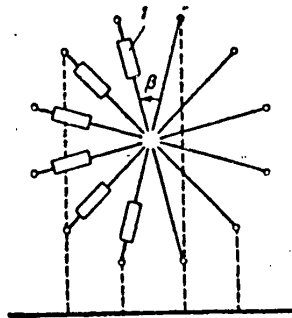


Figure 5.33. Schematic of a circular antenna array (l are delay lines).

A circular antenna array is shown in Figure 5.33. Here, diametrically opposite radiators are coupled together in pairs. For such a reflector, the expression for the secondary emission pattern has the form:

$$F(\theta) = J_0 \left( \frac{4\pi r}{\lambda} \sin \frac{\theta}{2} \right),$$

where  $J_0$  is a zero order Bessel function;  
 $r$  is the radius of the array.

The directional pattern of a circular array  $2\lambda$  in diameter and a linear array with a length of  $2\lambda$  are shown in Figure 5.34 for comparison.

The requirement that the return from the camouflaged object and the return from the

decoy target simulating this object be identical can be most completely met by means of Van-Atta reflectors (see §1, Chapter 5).

Thus, if phase shifters which are controlled by a specified program are inserted in the lines connecting the coupled elements of a passive antenna array, one can produce amplitude modulation of the reflected signal at the requisite frequency.

Let a plane electromagnetic wave impinge on a U-shaped array at an angle of  $\theta$ , where the array is made of two radiators positioned at a spacing of  $2d$  from each other and joined together by a feeder of length  $l$ .

## FOR OFFICIAL USE ONLY

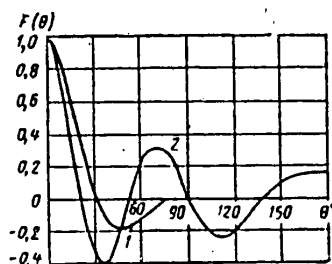


Figure 5.34. The secondary emission patterns of a linear array with a length of  $2\lambda$  (curve 1) and a circular array with a diameter of  $2\lambda$  (curve 2).

If a phase shifter is inserted in the connecting feed line which provides for a phase shift of  $e^{-jB}$ , then the amplitude of the return expressed as a function of the incident angle  $\theta$  will have the following form [16]:

$$E = \cos\left(\frac{B + kl}{2}\right) \cos(kd \sin \theta).$$

By changing the quantity  $B$  (when  $kl = \text{const.}$ ), one can vary the amplitude of the return field in a specified direction from the maximum value to zero. A similar result can also be obtained for a multielement array.

The use of amplifiers for the reflected signal designed around tunnel diodes or parametric amplifiers opens up broad possibilities for improving the design specifications of decoy targets. Such amplifiers not only make it possible to increase the effective radar cross-section of an antenna array by several times without increasing its dimensions, but also to produce a return with specified amplitude, phase or frequency modulation. Both one-way and two-way amplifiers can be inserted in the lines connecting the pairs of coupled elements. In the case of two-way amplifiers, strong feedback can occur between the elements of the array, something which limits the level of the reflected signal gain. As a result of this phenomenon, a tunnel diode circuit makes it possible to obtain a permissible gain not exceeding 15 to 20 dB.

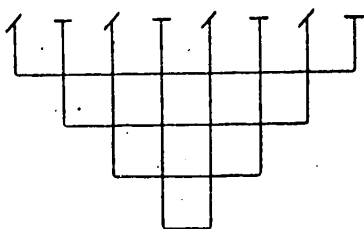


Figure 5.35.

Schematic showing the connection of radiators in a semiactive antenna array with polarization decoupling between the receiving and transmitting subarrays.

A structural design with two individual subarrays for reception and return is used to increase the decoupling between the radiating elements of a Van-Atta reflector. The subarrays are made from orthogonally polarized radiators arranged in checker-board fashion and connected by a feeder, as shown in Figure 5.35. In this case, one-way amplifiers are employed. For the structure shown in Figure 5.35, one can achieve an isolation between the receiving and adjacent radiators of more than 50 dB.

## FOR OFFICIAL USE ONLY

## FOR OFFICIAL USE ONLY

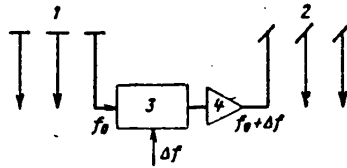


Figure 5.36. Schematic showing frequency modulation in an antenna array with amplification of the reflected signal.

Key: 1. Receiving elements;  
2. Transmitting elements;  
3. Mixer;  
4. Amplifier.

If frequency conversion such as shown in the circuit of Figure 5.36 is employed in the amplifiers built into the antenna arrays, then the reflected signal can be phase and frequency modulated. Here, a local oscillator is used for the modulation.

The results of tests of a model of such equipment are cited in the foreign press [16]. Tunnel diode amplifiers and mixers were used in the circuit. Mutually orthogonal dipoles, arranged on a reflecting screen in checkerboard order played the part of the radiators. The frequencies of the received (2,000

MHz) and transmitted (2,150 MHz) signals differed by 150 MHz with an amplifier passband of 120 MHz. The local oscillator made it possible to employ frequency and pulse modulation. The measured gain of the array amplifier was 14 dB. Such an antenna array can be used to simultaneously retransmit several signals at different frequencies, incoming from different directions.

#### 6. Guided Missiles - Decoy Targets

Special guided missile decoy targets are used to simulate air objects which have a high flight speed. As a rule, they are small aircraft, launched from bombers or missile carriers at a distance from the enemy radars greater than the detection range for the bomber or rocket carrier. This leads to false conclusions concerning the nature of the attack (instead of the real target, the enemy begins to pursue the missile), and also overloads the enemy data retrieval and processing system.

Corner reflectors, Luneberg lenses or other devices which increase the effective back-scatter cross-section of the missile can be installed on decoy missiles. However, it is difficult to generate radar returns commensurate in power with the returns from actual air targets by means of decoy missiles equipped only with passive reflectors.

It is well known that corner and lens radar reflectors produce a good effect in the case where the wavelength of the radar irradiating them is much less than the dimensions of the reflector, while the transmitter and receiver of the radar are located at a single point. When the transmitter and receiver are spaced a certain angle apart relative to the reflector, the effectiveness of the reflector falls off sharply with an increase in this angle. This is explained by the directional nature of the back-scattering pattern of such reflectors.

If the signal reflected from a false target is small for the simulation of a large object, it is necessary to amplify it. For this, a special amplifier is

FOR OFFICIAL USE ONLY

## FOR OFFICIAL USE ONLY

installed in the decoy missile which retransmits the echo signal impinging on the decoy target. A missile equipped with such an amplifier-transponder will simulate a large aircraft, even with a significant separation angle (relative to the target) between the radar transmitter and receiver. The device takes the form of a radar transponder, similar to a conventional radar beacon. In receiving the signals from the radar, it amplifies them by means of a klystron or traveling wave tube (TWT) amplifier and retransmits them in the direction of reception. The frequency of the return signal for a stationary target will always be equal to the frequency of the transmitting radar. If the trap simulates a moving target, then the frequency of the signal transmitted by it will have precisely the same doppler frequency shift as in the case of the motion of the actual object. When it is necessary to simulate a false signal of the same power as the signal return from a camouflaged target, it must be considered that the average pulse power of the transponder signal of the decoy target depends on the average effective radar cross-section of the object being simulated. On the other hand, the average return power is governed by the average incident power of the search radar and the transponder gain. Naturally, the transponder gain of the decoy target should be equivalent to the effective radar cross-section of the object being camouflaged. The following expression can be derived from the basic radar equation for the gain of a decoy target with an active return:

$$K = 10 \log(4\pi\sigma_t/\lambda^2 G_{\text{rec}} G_{\text{trans}}), \text{ dB.}$$

It follows from this that the gain of a decoy target transponder is governed by the effective radar cross-section of the object being camouflaged,  $\sigma_t$ , the wavelength of the radar,  $\lambda$ , as well as the directional gain of the transponder antennas ( $G_{\text{rec}}$ ,  $G_{\text{trans}}$ ). It is apparent that the average pulse power of the decoy target signal is proportional to the power of the transmitting radar; the nature of this power as a function of range should be the same as for the actual target.

The intensity of the returns from actual objects is always subject to considerable fluctuations, which have a definite spectral composition and corresponding probability distribution of the signal parameters with time. In order that the returns from a decoy target do not differ from the returns of the objects being simulated in terms of the nature of the fluctuations, the signal is modulated simultaneously with the amplification of the signal in the transponder circuitry. The envelope of the actual signal reflected by the corresponding simulated object is used as the modulating voltage.

Klystron amplifiers are comparatively narrow band devices: electronic frequency tuning of a klystron is possible in a range of 30 to 60 MHz, while the bandwidth of an oscillator or amplifier using a klystron is only 10 MHz. For this reason, a klystron amplifier-transponder, installed in a decoy missile, can simulate the target only for one particular radar or a group of radars operating in one frequency band.

## FOR OFFICIAL USE ONLY

## FOR OFFICIAL USE ONLY

Under actual conditions, several radars can work on an aircraft, bomber or missile vehicle simultaneously (detection, target acquisition, fire control, etc.), where each of the radars has its own working wavelength. The target being camouflaged can be simulated simultaneously for several radars by means of a decoy missile, on board which a TWT amplifier is installed. Such an amplifier has 100 to 100,000 times more gain than the usual klystron and can operate in a wide range of frequencies.

The American company of "Temco" has designed a TWT amplifier, which together with the power supply weighs 4.5 kg. The equipment is built with semiconductor devices and contained in a hermetically sealed housing. The antennas are chosen in accordance with the structure of the false target for which the device is intended. The power used by the amplifier at a DC supply voltage of 24 to 29 volts does not exceed 80 watts. The service life of the amplifier is 400 hours. When such an amplifier installed in a light pleasure aircraft was tested, the signals reradiated by it produced the same blips on the screens of radars as heavy four-engine bombers. Similar equipment is being manufactured by another American company: Lockheed Electronics. The equipment complement includes a TWT amplifier, a transistorized power supply and matched receiving and transmitting antennas. The frequency range is 5,000 to 11,000 MHz. The effective back-scatter cross-section of the simulated target is adjusted by an attenuator at the antenna output and can be increased up to 850 m<sup>2</sup>. The minimum output power is one watt, although over the majority of the range it reaches 3 watts. The signal gain varies in a range of 65 to 72 dB; the DC power consumption is 100 watts for a power supply voltage of 25 to 29 volts. The transponder can be used at a temperature of from -54 to +71 °C and at altitudes up to 21 km.

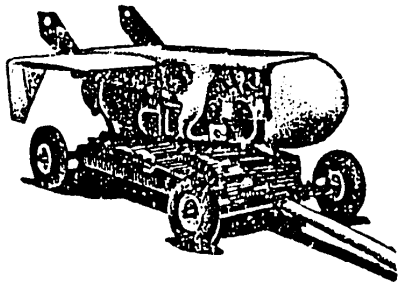


Figure 5.37. The "Green Quail" decoy target.

We shall cite the data on the American decoy missile, the GAM-72 "Green Quail" (Figure 5.37), as an example of decoy targets on which such transponders and amplifiers can be installed. This is a guided missile of the "air to ground" class. The basic function of the missile is to decoy the radars of the enemy air defense system to itself, thereby providing the long range bombers or missiles with nuclear warheads the opportunity to reach the set targets unimpeded. In its external appearance, the missile takes the form of a small aircraft, manufactured from armor plate, with a short fuselage and triangular wings. The length of the missile is about 4 m, the weight about 540 kg and the wingspan is 1.6 m. The missile has one jet engine which can develop a thrust of up to 1,100 kg, something which provides the missile with a speed close to that of sound. The range of the "Green Quail" missile is 360 km and its ceiling is 15,000 m. The missile is controlled by an autopilot with program control or by radio instructions; following the execution of the combat mission, it is destroyed by means of a self-destruction device. Special electronic equipment (of the type of amplifier-transponders

FOR OFFICIAL USE ONLY

considered above) is installed in the nose of the missile, where this equipment makes it possible to produce returns of the same levels as those from a B-52G bomber on the screens of enemy radars.

The B-52G strategic bomber of the U.S. Air Force, besides the major armaments, carries four "Green Decoys" on board. It should be noted, that other means of antiradar camouflage are provided on the B-52G bomber besides the decoy missiles. The "Green Quail" missile can be launched from any strategic bomber in the U.S. Air Force. When the missile is hung in the bomb compartment, its wings are folded and brought to the normal position immediately prior to releasing the missile from the aircraft.

The guided "Firebee-20" decoy, which can be launched from aircraft and ground installations, was developed by the American company "Ryan". The length of the "Firebee" missile is 7 m, the wingspan is 3.9 m and the maximum flight weight is 990 kg. The flight velocity is close to the speed of sound and the ceiling is 23 km. A Luneberg lens is installed in the tail portion of the missile while a TWT amplifier-transponder is mounted in the nose compartment. These devices make it possible to produce a return level from the missile comparable to the return from an aircraft.

Besides air decoys, it is also proposed that ground and water decoy targets be used, which take the form of high power electromagnetic wave retransmission or reflection sources. Such decoys, which are set up at a certain distance from the objects being protected, by reradiating or reflecting the electromagnetic energy will attract the guided missiles with the radar homing warheads to themselves.

It is thought that the widescale application of semi-active antenna arrays using tunnel diodes or parametric amplifiers as the amplifying elements will open up great prospects for the design of decoy targets. Using such devices, one can achieve the most complete matching of the parameters of the signal reflected from the real target and the signal from the simulator.

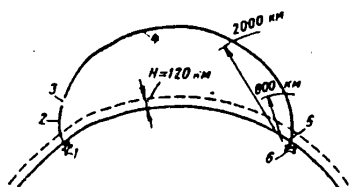
The effectiveness of all of the decoy targets treated in this chapter increases sharply if a set of measures is implemented for the object they are simulating to reduce its radar visibility.

#### 7. Anti-Radar Camouflage of Ballistic Missiles

Because of the continuous refinement of systems for the detection and interception of air and space attacks, which have a great range and enormous destructive power, extensive work is underway abroad to create means which facilitate the penetration of ballistic missiles through an antimissile defense system (PRO) [ABM systems]. For this purpose, various counter-measures for ABM systems are undergoing intense development in the U.S., which are intended for their equipping the "Atlas", "Titan" and "Minuteman" ICBM's, the "Polaris" long range ballistic missile and the "Pershing" intermediate range ballistic missile. According to data in the American press, about a billion dollars have already been expended for the creation of ABM system counter-measures. A significant portion of these funds is being spent on the design of antiradar camouflage.

## FOR OFFICIAL USE ONLY

Figure 5.38. Standard ballistic missile trajectory.



- Key: 1. Launch site;  
 2. Powered phase;  
 3. Rocket motor separation phase;  
 4. Central portion of the trajectory;  
 5. Maximum deceleration phase (50 g) at an altitude of 10 to 20 km;  
 6. Target.

We shall briefly examine how the means of antiradar camouflage make it difficult to intercept an ICBM at various points in its trajectory (Figure 5.38).

The problem of intercepting a ballistic missile in the general case consists in preventing its warhead from exploding in the region of the object being protected. In the case where a nuclear warhead is used, interception must be made at the rather high altitude and long range from the protected facility, otherwise, the explosion of such a device causes destruction over the protected territory.

Calculations performed in the U.S. show that an interceptor should be launched approximately 15 seconds after receiving the intercept command. The characteristics of existing engines and power sources, as well as the comparatively long time needed to cage gyroscopes make it very difficult to meet this requirement [24]. It follows from this that for the timely interception of an ICBM, it must be detected at the greatest possible range.

The utilization of tools which reduce the power of radar returns from ICBM's makes it possible to sharply reduce the range and detection probability of the missile by a radar. If the effective radar cross-section of a ballistic missile warhead is reduced by a factor of 20 using poorly reflecting forms and antiradar coatings, then as follows from formula (2.1), its radar detection range is more than cut in half. The target detection probability is reduced by no less than the same factor.

In this case, very little time remains for the interception of the ICBM. Reliable target interception can be accomplished only with a sharp increase in the speed of the interceptor.

The relationship between the velocity of the interceptor  $v_{\max}$  and the target detection range  $D$  for a protected zone radius of 185 km is shown in Figure 5.39. It can be seen from the graph that when the ultimate detection range of an ICBM is cut in half (the effective radar cross-section is reduced by a factor of 16), the

## FOR OFFICIAL USE ONLY



## FOR OFFICIAL USE ONLY

missile can be successfully intercepted on in the case where the speed of the interceptor is increased by approximately a factor of 1.5 times. When this condition is not met, the nuclear warhead will then explode over the territory being defended.

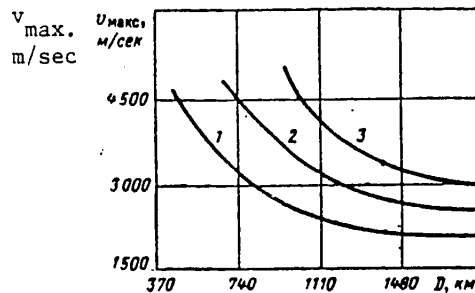


Figure 5.39. Interceptor speed as a function of target detection range.

- Key: 1. Target velocity of  
 $v_t = 6,000$  m/sec;  
 2.  $v_t = 9,000$  m/sec;  
 3.  $v_t = 12,000$  m/sec.

It is obvious that it is desirable to achieve a reduction in the effective back-scatter cross-section of a ballistic missile over all portions of its trajectory. However, in this case it must be kept in mind that despite the relatively simple geometric shape of the component structures of the missile, the value of its effective radar cross-section will change in different portions of the flight. This is due to the sequential separation of the rocket stages and the continuous change in the radius of the last stage (the warhead) relative to the radar station. Moreover, the effective radar cross-section can change because of back-scattering of the radio waves by the rocket engine flare, as well as because of inhomogeneities in the ionosphere, perturbed by the operating engine.

Despite the fact that the missile

is the most vulnerable in the powered phase of the trajectory, there is little probability of its detection in this phase by means of ground radar since in this case, their range will be limited by the curvature of the earth. The placement of long range missile acquisition and tracking radars on radar patrol aircraft for satellites as yet still involves considerable technical difficulties.

Having achieved the specified trajectory parameters, the rocket begins the middle phase of the flight outside the limits of the atmosphere with the engine shut down. In this phase of the flight, the warhead can be separated from the body of the rocket. The detection range and probability for a warhead in the central phase of a trajectory can be significantly decreased by means of special measures to decrease its effective radar cross-section, which reduce to the selection of the optimum shape of the rocket nose cone and the utilization of radio absorbent materials. In order that the sharp point of the warhead be directed towards the radar station of the air defense system at all times, for the purpose of maintaining the minimum effective radar cross-section of the warhead during its flight, it is necessary to stabilize the nose portion of the rocket over its flight path. The need for stabilizing gear arose because of the fact that the nose sections of missile which were not oriented towards the radar (for example, the "Mark-4" on the Atlas-8, Atlas-F and Titan-1 ICBM's) turn end over end in the

## FOR OFFICIAL USE ONLY

FOR OFFICIAL USE ONLY

central portion of the flight trajectory and represent large targets for the operators of enemy radars.

Various decoys can be used following the detection of the nose of the rocket to camouflage it, i.e., to disorient the enemy or completely saturate the carrying capacity of the detection and tracking system of the air defense complex.

The effectiveness of antiradar camouflage of ICBM's using decoy targets can be quite high in the central portion of a trajectory. Since the influence of the atmosphere is completely eliminated in this phase of the flight, light objects can be used as the decoy targets, for example, such as dipole reflectors or inflated balloons having the shape of the warhead or a sphere.

For example, successful tests in the U.S. of a set of such decoy targets ejected from a Titan long range ballistic missile were reported in the press. The rocket which was equipped with dummy nuclear charge flew 8,000 km and fell in the region of the south Atlantic Ocean.

After separating the spent stages, the missile warhead jettisoned six decoy targets. All of the decoys had balloons in the noses, where these balloons produced magnified blips on radar screens which camouflaged the true dimensions and position of the target and made radar observation difficult [7].

Following the ejection of decoys from the nose section of a missile, it is necessary to correct the position of its center of gravity which is shifted as a result of dumping the decoy targets.

Disorienting decoys can also be placed in the last stage of the rocket, and in this case, following the ejection of the decoy target and the separation of the last stage, it should be thrown off to the side from the warhead by means of braking motors or destroyed so that the trajectory of the missile warhead cannot be governed by the flight trajectory of the last stage.

Despite the fact that at first glance the destruction of an ICBM in the middle phase of the trajectory is the most advantageous, since it can be accomplished at a great distance from the defended facility, the problem of guiding the interceptor where decoy targets are used becomes so complex, that in the opinion of foreign specialists, there is little probability of an interception in this case and such an approach can be treated only as an auxiliary one.

The use of antiradar camouflage which reduces the effective back-scatter cross-section of an ICBM takes on especially great significance in the final flight phase of the missile. In this phase, the use of false radar target "decoys" can be less effective than during other phases of the trajectory, since because of the different dynamic conditions for the entry of the warhead and false targets into the atmosphere, the probability of selecting the warhead from among the decoys increases. The warhead, which has greater weight and lower frontal resistance begins to lose velocity at comparatively lower altitudes, while for metallized strip or inflated balloon type decoy targets, the reduction in speed becomes perceptible early on at high altitudes.

FOR OFFICIAL USE ONLY

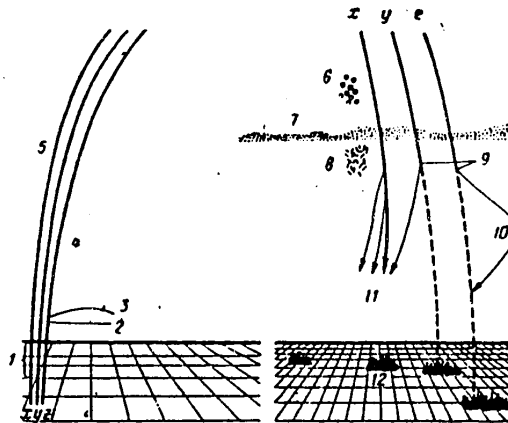


Figure 5.40. The use of antiradar camouflage in various phases of the flight trajectory (x, y, z) of a ballistic missile.

- Key :
1. Powered phase of the trajectories;
  2. Point of separation of the last stage;
  3. Destruction of the spent stage or the change in its trajectory;
  4. Passive jamming or decoy targets;
  5. Central portion of the trajectory;
  6. False targets in the form of air balloons;
  7. The region of entry into the dense layers of the atmosphere;
  8. Heavy reflectors (decoy targets);
  9. The point of trajectory change;
  10. Maneuvering nose cone;
  11. Missiles guided to the radars;
  12. Target.

The recognition of warheads when they enter the atmosphere can be made considerably more difficult if heavy objects are used as the false targets, the ballistic coefficients of which are equal to or close to the ballistic coefficients of the warhead.

The designers of false targets have been forced to increasingly deal with the refinement of air defense radars as regards the increase in the volume of information which can be extracted on air targets (their dimensions, fluctuations in the return, objects rotating end over end in space, etc.) by means of new techniques of analyzing the fine structure of the return. This in turn forces designers to make the structure of decoy targets increasingly complex, something which leads to

FOR OFFICIAL USE ONLY

FOR OFFICIAL USE ONLY

an increase in their overall dimensions and weight. However, with an increase in the weight of decoy targets, it is necessary to consider the fact that each kilogram of payload costs the same to deliver, regardless of the destructive power of the charge. In other words, increasing the weight of decoy targets unavoidably leads to a reduction in the weight of the missile payload.

A missile warhead, entering the dense layers of the atmosphere in the descending phase of the flight trajectory at supersonic speed, forms a strongly ionized or plasma sheath and a plasma trail of comparatively great extent. The plasma has the capability of reflecting radar signals, and for this reason the effective radar cross-section of the missile nose cone increases due to ionization. Since the decay time of the plasma trail is about two seconds, its length for a nose cone traveling at a speed of 600 m/sec [sic], will be approximately 12 km.

A reduction in the ionized sheath and the plasma trail can be achieved by means of changing the geometric shape of the nose cone as well as through the use of special ablation materials. Thus, for example, with a thin cone shape for the missile nose cone section, a less intense plasma sheath is produced, while a rounded-off base section of the nose cone promotes the suppression of a turbulent, strongly ionized (plasma) trail.

It is recommended that teflon be used, for example, as the special low temperature destructible coatings which are capable of absorbing the thermal radiation of nose cones when they enter the dense layers of the atmosphere or to neutralize the plasma by means of oppositely charged gas particles. Ways of reducing the ionized sheath by means of introducing special substances into it through holes in the missile nose cone are also being studied abroad.

The set of antiradar camouflage measures treated above makes it possible to significantly boost the reliability of penetrating and ABM system with ballistic missiles, and consequently, increase the efficiency of missiles while executing the combat missions assigned to them (Figure 5.40).

It is natural that antiradar camouflage measures for ballistic missiles should occupy a firm place in the set of ABM counter-measures. To evaluate the efficiency of such a complex of measures, one turns to games modeling of operations to overcome an enemy ABM system. The solution of such a problem proves to be extraordinarily complex, since in the opinion of American military specialists, there are about 20 critical parameters for an enemy ABM system and hundreds of less critical parameters. By means of individual and successive variations of these parameters in the course of the iterative game simulation process with a specified ballistic missile warhead power and a given combination of ABM counter-measures, an estimate can be derived for the probability of successfully breaking through an enemy ABM system.

FOR OFFICIAL USE ONLY

BIBLIOGRAPHY

1. Dulevich V.Ye., Korostelev A.A., Mel'nik Yu.A., et al., "Teoreticheskiye osnovy radiolokatsii" ["Radar Theory Fundamentals"], Sovetskoye Radio Publishers, 1964.
2. Saybel' A.G., "Osnovy radiolokatsii" ["Radar Fundamentals"], Sovetskoye Radio Publishers, 1964.
3. Skolnik M., "Vvedeniye v tekhniku radiolokatsionnykh sistem" ["Introduction to Radar Systems Engineering"], Mir Publishers, 1965.
4. Mentser J.R., "Diffraktsiya i rasseyaniye radiovoln" ["Radio Wave Diffraction and Scattering"], 1958.
5. Vaynshteyn L.A., "Elektromagnitnyye volny" ["Electromagnetic Waves"], Sovetskoye Radio Publishers, 1957.
6. Shchukin A.N., "Ugolkovyye otrazhateli" ["Corner Reflectors"], Moscow, 1949.
7. Stepanov Yu.G., "Maskirovka ot radioelektronnogo nablyudeniya" ["Camouflage against Radioelectronic Observation"], Voenizdat Publishers, 1963.
8. Mishchenko Yu.A., "Radiolokatsionnyye tseli" ["Radar Targets"], Voenizdat Publishers, 1966.
9. "Radiolokatsionnaya tekhnika" ["Radar Engineering"], Vol. 1, translated from the English, Sovetskoye Radio Publishers, 1949.
10. Peresada V.P., "Radiolokatsionnaya vidimost' morskikh ob'yektov" ["Radar Visibility of Sea Objects"], Sudpromgiz Publishers, 1961.
11. Sluchevskiy B.F., "Radiolokatsiya i yeye primeneniye" ["Radar and Its Application"], Voenizdat Publishers, 1962.
12. Vishin G.M., "Selektsiya dvizhushchikhsya tseley" ["Moving Target Indication"], Voenizdat Publishers, 1966.
13. "Porogovyye signaly" ["Threshold Signals"], Translated from the English, Sovetskoye Radio Publishers, 1952.
14. Paliy A.I., "Radiovoyna" ["Electronic Warfare"], 1963.
15. Shlesinger R., "Radioelektronnaya voyna" ["Radioelectronic Warfare"], Translated from the English, Voenizdat Publishers, 1963.
16. "Antennyye reshetki", "Obzor zarubezhnykh rabot" ["Antenna Arrays", "Review of Foreign Literature"], Sovetskoye Radio Publishers, 1966.
17. Arenberg A.G., "Rasprostraneniye detsimetrovykh i santimetrovykh voln" ["Propagation at Decimeter and Centimeter Wavelengths"], Sovetskoye Radio Publishers, 1957.
18. Proceedings of the National Electronics Conference, 1959, Vol. XV.

FOR OFFICIAL USE ONLY

19. Kanareykin D.B., et al., "Polyarizatsiya radiolokatsionnykh signalov" ["Radar Signal Polarization"], Sovetskoye Radio Publishers, 1966.
20. MICROWAVE JOURNAL, 1961, Vol 6, No. 3, p 4.
21. RADIOTEKHNIKA I RADIOELEKTRONIKA ZA RUBEZHOM [RADIO ENGINEERING AND RADIO ELECTRONICS ABROAD], 1959, Nos. 3 and 6.
22. AVIATION WEEK, 1963, Vol 79, No 9.
23. U.S. Patents Nos. 2,996,710; 2,801,411; 3,095,814; 3 443,965.
24. ASTRONAUTICS, 1960, Vol 5, No 10.
25. ANNALES DES TELECOMMUNICAT., 1961, Vol 16, Nos. 3, 4.
26. Fal'kovich S.Ye., "Vydeleniye sluchaynykh signalov na fone pomekh" ["The Discrimination of Random Signals against a Background of Interference"], Sovetskoye Radio Publishers, 1960.
27. Golev K.V., "Raschet dal'nosti deystviya radiolokatsionnykh stantsiy" ["Calculating the Range of Radars"], Sovetskoye Radio Publishers, 1962.
28. PROC. IEE, 1965, Vol 53, No 8.
29. SPACE AERONAUTICS, 1964, Vol 41, No 2.
30. L'ONDE ELECTRIQUE, 1958, Vol 38, No 381.
31. ELECTRONIC EQUIPMENT NEWS, 1963, Vol 4, No 10.
32. PLASTICS WORLD, 1963, Vol 21, No 2.
33. AVIATION WEEK AND SPACE TECHNOLOGY, 1964, Vol 80, No 3.
34. PHOTOGRAMM. ENG., 1960, Vol 26, No 4.
35. RADIO AND ELECTR. ENG., 1963, Vol 110, No 12.
36. Proceedings of the National Electronics Conference, 1963, Vol 19, Chicago.
37. NACHRICHTEN ZTSCHR. [COMMUNICATIONS JOURNAL], 1964, 17, No 5.
38. "Balkke Radarstrahlung - Radartarnung" "Balkke Radar Transmission - Radar Camouflage"], Vol 1, Dusseldorf Knoff. Sa, 1960 [sic].
39. Trofimovich A.D., Stepanov Yu.G., "Sredstva protivoradiolokatsionnoy zashchity v vooruzhennykh silakh SShA i Anglii" ["Antiradar Camouflage in the Armed Forces of the U.S. and England"], "Morskoy sbornik" ["Maritime Handbook"], 1961, No 10.

FOR OFFICIAL USE ONLY

FOR OFFICIAL USE ONLY

40. Demin I.D. "Radiolokatsionnoye obnaruzheniye nadvodnykh ob'yektov na fone passivnykh pomekh" ["Radar Detection of Water Surface Objects against a Background of Passive Interference"], "Informatsionnyy sbornik TsNII MF" ["Information Handbook of the Central Scientific Research Institute of the Maritime Fleet"], "Sudovozhdeniye i svyaz" ["Navigation and Communications"] Series, 1965, No 32.
41. Stepanenko V.D., "Vliyaniye atmosferykh osadkov na dal'nost radiolokatsionnogo obnaruzheniya tseley" ["The Impact of Atmospheric Precipitation on the Radar Detection Range of Targets"], "Voprosy Radioelektroniki" ["Questions in Radioelectronics"], Series XII, No 6, 1960.
42. Stepanov Yu.G., Levin D.Z., "Apparatura radioprotivodeystviya na samoletakh i kosmicheskikh korablyakh" ["Electronic Countermeasures Equipment in Aircraft and Space Vehicles"], VESTNIK PROTIVOVODZUSHNOY OBORONY [AIR DEFENSE JOURNAL], 1963, No 3.
43. ZARUBEZHNYAYA RADIOELEKTRONIKA [FOREIGN RADIO ELECTRONICS], 1965, No 4, 1966, No 1.
44. PROC. INST. ELECTR. ENGRS., 1963, Vol 110, No 12.
45. Stepanov Yu.G., "Zashchita samoletov i raket ot tekhnicheskikh sredstv nablyudeniya" ["Protecting Aircraft and Missiles against Technical Means of Observation"], VESTNIK PROTIVOVODZUSHNOY OBORONY, 1962, No 5.

COPYRIGHT: Izdatel'stvo "Sovetskoye radio", 1968

8225

CSO: 8144/1882

- END -

- 115 -

FOR OFFICIAL USE ONLY